FACULTY OF VETERINARY MEDICINE
accredited by EAEVE

Effect of equine herpesvirus type 1 infection on the expression of major histocompatibility complex 1 in respiratory epithelial cells

Word count: <27.398>

Dani Vaughan
Student number: 01306667

Supervisor: Prof. Dr. Hans Nauwynck
Supervisor: Prof. Dr. Herman Favoreel
Supervisor: Dr. Katrien Poelaert
Supervisor: Drs. Sarah Descamps

A dissertation submitted to Ghent University in partial fulfilment of the requirements for the degree of Master of Veterinary Medicine

Academic year: 2018–2019

GHENT UNIVERSITY

Preface

First, I would like to thank my promotors Prof. Dr. Hans Nauwynck, Prof. Dr. Herman Favoreel, Dr. Katrien Poelaert, Drs. Sarah Descamps, and the all-knowing lab technician Carine Boone, for all their time, patience, advice and knowledge. They introduced me to the world of research, for which I will always be grateful.

Next, I would like to show my gratitude to my friends, those that have stood by me since secondary school and even since nursery, and the friends I have made throughout my university experience. They have been a shoulder to cry on, a study buddy, a listening ear, and a coffee date during much needed breaks. Whoever said you need your friends the most when you have boy trouble, has not yet written a thesis. Special thanks to the person who got me through all those long nights, Marie-Laure. I think we may have broken the world record in longest skype sessions.

Finally, I would like to thank my beloved family, who have always been proud and never stopped believing in me. Mum, Dad and Marko, thank you for your unconditional support these past six years.

"Develop a passion for learning.

If you do, you will never cease to grow."

- Anthony J. D'Angelo

Table of Contents

I List of Abbreviations

A-5021	(1'S,2'R)-9-[[10,20-bis(hydroxymethyl) cycloprop-10-yl]methyl]guanine
ATP	Adenosine triphosphate
ATPase	Adenosine triphosphatase
B cell	B lymphocyte
BHV1	Bovine herpesvirus type 1
C	Cytosine
cDC	Conventional dendritic cells
CF	Complement-fixation test
CTL	Cytotoxic T lymphocyte
CPE	Cytopathic effect
DC	Dendritic cells
DMEM	Dulbecco's Modified Eagle Medium
DNA	Deoxyribonucleic acid
dUTPase	Deoxyuridine triphosphatase
EBMEC	Equine brain microvascular endothelial cells
EBV	Epstein-Barr virus
ED cells	Equine dermis cells
EGTA	ethylene glycol-bis(β-aminoethyl ether)-*N*,*N*,*N*',*N*'-tetraacetic acid
EHV1	Equine herpesvirus type 1
EHV4	Equine herpesvirus type 4
ELISA	enzyme-linked immunosorbent assay
ER	Endoplasmic reticulum
EREC	Equine respiratory epithelial cells
ERK pathway	Extracellular-signal-regulated-kinase pathway
FITC	Fluorescein isothiocyanate
FCS	Fetal calf serum
G	Guanine
Gp	Glycoprotein
HCMV	Human cytomegalovirus
Hpi	Hours post infection
HSV1	Herpes simplex virus type 1
IEP	Immediate early proteins
IFN	Interferon
Ig	Immunoglobulin
IL	Interleukin
ILTV	Infectious laryngotracheitis virus
IR	Inverted repeat
IRF1	Interferon regulatory factor 1
ISRE	Interferon-sensitive response element
Kbp	Kilobase pair
LT-α	Lymphotoxin-α
MAC	Membrane-attack complex
MALT	Mucosal associated lymphoid tissue
MAPK pathway	Mitogen activated protein kinase pathway
MASP	MBL-associated serine protease
MBL	Mannose-binding lectin
MHC1	Major histocompatibility complex class 1
MHC2	Major histocompatibility complex class 2
MOI	Multiplicity of infection
mRNA	Messenger ribonucleic acid
NaBut	Sodium butyrate

NF-κB	nuclear factor-kappa B
NK cells	Natural killer cells
NLR	NOD-like receptor
NOD	nucleotide-binding oligomerization domain
ORF	Open reading frame
PAMPs	Pathogen-associated molecular patterns
PBL	Peripheral blood leukocytes
PBMC	Peripheral blood mononuclear cell
PBS	Phosphate buffered saline
PCR	Polymerase chain reaction
PI(3)K	phosphoinositide 3-kinase
PRR	Pattern recognition receptor
PrV	Pseudorabies virus
RIG	Retinoic acid inducible gene
RK-13 cells	Rabbit kidney cells
RLR	RIG-like receptor
RNA	Ribonucleic acid
Rpm	Revolutions per minute
RPMI	Roswell Park Memorial Institute
RT-PCR	Reverse transcriptase polymerase chain reaction
SB	Sodium butyrate
SCFA	Short-chain fatty acids
sIgA	Secretory immunoglobulin A
SN	Serum-neutralization test
SNP	Single nucleotide polymorphism
S phase	Synthesis phase
SPr	Sodium propionate
TAP	Transporter associated with antigen processing
T cell	T lymphocyte
$TCID_{50}$	Median tissue culture infectious dose
TEER test	Transepithelial electrical resistance test
TK	Thymidine kinase
TLR	Toll-like receptor
TNF-α	Tumor necrosis factor α
TR	Terminal repeat
TR	Texas Red
TSA	Trichostatin
U_L, U_S	Long unique and short unique regions
VZV	Varicella zoster virus

II Summary

Equine herpesvirus type 1 (EHV1) infection causes abortions and neurological symptoms worldwide, with a majority resulting in life-long infections. EHV1's ability to overcome certain recognition by the immune system is related to its immune evasion strategies, which is why the production of a vaccine that is able to prevent viremia has been difficult. The cytotoxic T lymphocyte (CTL) mediated response is essential in eliminating intracellular virus, and studies have shown that various members of the genus *Varicellovirus* interfere with the major histocompatibility complex class 1 (MHC-1) antigen presenting pathway. Understanding EHV1-host cell interaction and its effect on MHC-1 can contribute to the development of vaccines that will elicit an effective cellular immune response.

Previous studies have demonstrated EHV1 induced MHC-1 downregulation using flow cytometry with non-target cells and equine respiratory epithelial cells (EREC). This thesis aims to demonstrate the MHC-1 expression patterns during infection with an abortigenic and neurovirulent strain through confocal microscopy, for the first time to our knowledge. Moreover, we mimicked the *in vivo* situation closely by using the *in vitro* EREC model, after which we used the complementary *ex vivo* explant model.

We saw that MHC-1 downregulation occurs in the viral plaques, which coincides with previous research. Moreover, a general upregulation of MHC-1 expression was seen in the areas surrounding the plaque of the inoculated EREC and explants, which could potentially be associated with the secretion of interferons. Although this prominent trend could be seen when comparing the MHC-1 expression of the region of interest (ROI) in the EREC model, statistically the differences were insignificant, which could be due to the software used to calculate the ROI, the signal-to-noise ratio and the highly variable MHC-1 expression. Finally, this trend was confirmed when comparing ROIs in the explant model, though statistics were not performed due to the high variability in MHC-1 expression.

Further research should focus on investigating the mechanism underlying virus-induced MHC-1 upregulation in non-infected cells and whether MHC-1 downregulation by EHV1 in infected cells effectively renders these cells more susceptible to natural killer (NK) cell mediated cell lysis.

II Samenvatting

Equine herpesvirus type 1 (EHV1) infectie veroorzaakt wereldwijd abortussen en neurologische symptomen, waarvan de meerderheid resulteert in levenslange infecties. EHV1's vermogen om bepaalde herkenning door het immuunsysteem te overwinnen is gerelateerd aan zijn immuno-evasie strategieën, waardoor het moeilijk is gebleken een vaccin te produceren dat in staat is viremie te voorkomen. De cytotoxische T lymfocyt (CTL) gemedieerde respons is essentieel bij het elimineren van het intracellulaire virus. Studies hebben aangetoond dat verschillende leden van het genus *Varicellovirus* interfereren met de major histocompatibility complex klasse 1 (MHC-1) antigeen presenterende route, welke belangrijk is om deze CTL gemdieerde respons te activeren. Inzicht in de EHV1-gastheercel interactie en het effect ervan op MHC-1 kan bijdragen tot de ontwikkeling van vaccins die een effectieve cellulaire immuunrespons teweeg zullen brengen.

Eerdere studies hebben EHV1 geïnduceerde MHC-1 downregulatie aangetoond met behulp van flow cytometrie met niet-doelwitcellen en equine respiratoire epitheliale cellen (EREC). In deze masterproef werd voor het eerst, bij onze kennis, de MHC-1 expressiepatronen tijdens infectie met een abortigene en neurovirulente stam aangetoond door middel van confocale microscopie. Bovendien werd de *in vivo* situatie zo goed mogelijk nagebootst door gebruik te maken van het *in vitro* EREC model, waarna we het complementaire *ex vivo* explantmodel hebben gebruikt.

In deze masterproef kon geconcludeerd worden dat MHC-1 downregulatie optreedt op de plaats van de plaque, wat samenvalt met eerder uitgevoerd onderzoek. Bovendien werd een algemene opregulatie van MHC-1 expressie waargenomen in de epitheelcellen rond de plaque van de geïnoculeerde EREC en explanten, die mogelijk geassocieerd kan worden met de secretie van interferonen. Hoewel deze opvallende trend kan worden waargenomen bij het vergelijken van de MHC-1 expressie van de region of interest (ROI) in het EREC-model, waren de verschillen statistisch gezien niet significant, wat te wijten kan zijn aan de gebruikte software voor de ROI berekening, de signaal-ruis verhouding en de zeer variabele MHC-1 expressie. Tot slot werd deze trend bevestigd bij de vergelijking van de ROI's in het explant model, hoewel er geen statistiek berekening werd gedaan vanwege de hoge variabiliteit van de MHC-1 expressie.

Verder onderzoek zou zich richten op het mechanisme dat ten grondslag ligt aan de virus-geïnduceerde MHC-1 upregulatie in niet geïnfecteerde cellen, en of MHC-1 downregulatie door EHV1 in geïnfecteerde cellen deze cellen effectief gevoeliger maakt voor natural killer (NK) cel gemedieerde cellyse.

III Introduction

1. Equine herpesvirus type 1

A. Herpesvirus

1.1. Introduction

Viruses are small, infectious, intracellular pathogens, minimally consisting of proteins and nucleic acids. They require the metabolic activities of a host cell to produce more virus by assembling the structural components produced in the host cell. Despite having a much simpler architecture than their host cell, they can do a considerable amount of damage. Thus, earning their name virus, the Latin word for poison (Voyles, 2002).

1.2. Taxonomy and Characteristics

Herpesviruses are highly successful pathogens that can infect both animals and humans. The family *Herpesviridae* contains the herpesviruses of mammals, birds and reptiles classified under the *Alphaherpesvirinae*, *Betaherpesvirinae* and *Gammaherpesvirinae*. Of these, the alphaherpesviruses are the most important in animal virology. *Herpesvirales* contain two other families, *Alloherpesviridae*, which incorporates the fish and frog viruses, and *Malacoherpesviridae,* which contains the bivalve virus (Davidson et al., 2009). The subfamilies of the *Herpesviridae* differ in genetic content rather than in morphology (Davidson et al., 2011).

Horses are the natural host of equine herpesvirus type 1 (EHV1), a member of the subfamily *Alphaherpesvirinae.* Characteristics shared by the alphaherpesviruses are the variable host range, the rapid spread in cell culture, short reproduction cycle, the efficient destruction of infected cells and the ability to establish latent infections in the trigeminal ganglia, lymphoid tissues and peripheral blood leukocytes (Roizman and Pellet, 2001; Gryspeerdt, 2011). Conversely, betaherpesviruses such as the human cytomegalovirus (HCMV) have a narrow host range and long replication cycle. Other characteristics are a slow spread in cell culture and latency in secretory glands as well as lymphoreticular cells (Davidson, 2008). The final subfamily, namely the gammaherpesviruses, include viruses such as the Epstein-Barr virus (EBV) and equine herpesvirus type 2. These viruses are oncogenic and associated with lymphoproliferative diseases. According to Ackermann (2005), gammaherpesviruses have a surprisingly wide host range. In contrast to the other two subfamilies, infection predominantly leads to latency in cells rather than in lytic infections. Latency is hereby established in lymphoid tissue.

1.3. Genome organisation and Relatedness

All members of the order *Herpesvirales* contain a relatively large, double stranded, linear DNA genome. There are three genes shared by all three herpes families. The first being the adenosine triphosphatase (ATPase) subunit (encoded by the T4 gene) in terminase, a complex that is responsible for packaging viral deoxyribonucleic acid (DNA) into the capsid. The T4 gene lacks a counterpart in the host cell. The two other encoded proteins are DNA polymerase and deoxyuridine triphosphatase (dUTPase), which do have cellular relatives (Davidson, 2007).

Herpesviruses have DNA molecules that range in size from about 125 to 240 kilobase pairs (kbp) and in nucleotide composition from 32 to 75% guanine (G) + cytosine (C), depending on the virus species (Honess, 1984). EHV1 fits in this range with a genome of 150,223 bp in size and a base composition of 56.7% G + C (Telford et al., 1992). In contrast to the *Alpha*- and *Betaherpesvirinae*, the genomes of most *Gammaherpesvirinae* are generally deficient in the G + C dinucleotide. According to Honess et al. (1989), this depletion is a sign of latency in dividing cell populations, where the latent genome is

obliged to replicate as host cells divide. We can see this depletion in EBV, which latently infects dividing B lymphocyte populations (Honess et al., 1989).

EHV1 has been fully sequenced and has a type D genome. This genome structure is also shared by other herpesviruses such as bovine herpes virus type 1 (BHV1), pseudorabies virus (PrV) and infectious laryngotracheitis virus in poultry (ILTV). It is characterized by two sets of unique sequences, covalently linked. These are long unique regions and short unique regions (U_L, U_S). The U_S component is flanked by a large inverted repeat sequence (inverted repeat, IR_S; terminal repeat, TR_S) and the U_L component by a small inverted repeat sequence (IR_L and TR_L) (Telford et al. 1992; Mettenleiter and Sobrino, 2008).

EHV1 contains 80 open reading frames (ORF). As mentioned previously, herpesvirus genomes are not solely simple lengths of unique DNA, but contain inverted or direct repeats. This explains why the genome is considered only to contain 76 distinct genes. Since four open reading frames are duplicated in the major inverted repeat, two open reading frames are probably expressed as spliced mRNA, and one may contain an internal transcriptional promoter. The explanation for the presence of repeats is presumably linked to the mode of DNA replication, rather than with any advantage gained by having multiple copies of certain genes, as herpesvirus genomes are thought to replicate by circularization. Four sizeable regions of the EHV1 genome appear not to encode proteins (Telford et al., 1992; Davidson, 2007).

1.4. Virion structure

The linear DNA genome is contained in a icosahedral protein capsid, which is 125-130 nm in diameter. EHV1's capsid consists of 162 protein capsomeres, of which 150 hexons, 12 pentons, and the portal. The hexons contain six copies, and the pentons five copies of the major capsid protein. Every copy of this major capsid protein occurring in the hexons is distinguished by an external protein. The portal consists of 12 copies of the portal proteins and forms the site through which DNA leaves and enters the capsid. The capsid is embedded (though not centrally) in a tegument, linking it to an envelope (see Figure 1 for an overview of the EHV1 virion). A degree of icosahedral symmetry exists in the region of the tegument closest to the capsid. It is made up of viral and cellular proteins, derived from the cytosol of infected cells. Many interactions occur between these proteins and with membrane glycoproteins. Coller et al. (2007) suggests these tegument proteins play a role in the production of virions by linking the capsid to envelopes in the infected cell. Other functions of the tegument include modulation of the host-cell environment and transport of virus capsids to the nucleus. The nucleocapsid is covered by an envelope, a lipid bilayer derived from the cell membrane of the infected cell, in which viral glycoproteins, lipoproteins and glycolipid proteins are incorporated. Twelve glycoproteins (gp) have been identified for equine herpesvirus, of which gB (gp14), gC (gp13), gD (gp18), gE, gG, gH, gI, gK, gL, gM and gN are conserved in comparison with those of other alphaherpesviruses. Glycoprotein 2 (gp2) is only encoded in equine alphaherpesviruses (Mahmoud et al., 2013). These envelope proteins are involved in virus attachment, penetration, egress and cell-to-cell spread (Lloyd et al., 1982; Baker et al., 1990; Roizman and Pellet, 2001; Davidson 2008; Owen et al., 2015).

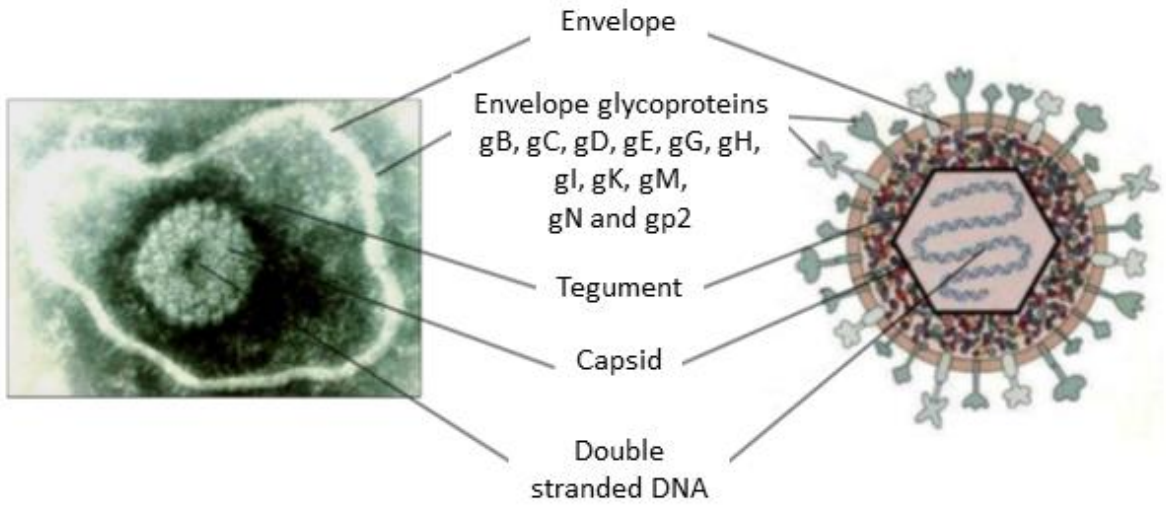

Figure 1. Electron microscopic photomicrograph (left), and schematic drawing (right) of an EHV1 virion (adapted from: Gryspeerdt, 2011; picture from: University of Wisconsin).

1.5. Replication cycle

Cell entry by herpesviruses occurs either through fusion with the plasma membrane or by receptor-mediated endocytosis. Prior to entry, a low affinity interaction between glycoproteins gB and gC and cellular heparin sulfate allows the virus to attach (Osterrieder, 1999). Osterrieder (1999) investigated this by creating a mutant EHV1 virus lacking the ORF for gC and inhibiting cellular glycans. Following this low affinity binding, more specific interactions mediate virus entry.

The entry mechanism can depend on the cell type. For EHV1 for example, the entry in equine endothelial cells occurs predominantly via fusion at the plasma membrane while in peripheral blood mononuclear cells (PBMC) this goes through endocytosis (Van de Walle et al., 2008). The basic fusion machinery in herpesviruses involves the conserved gB and gH-gL complex. The trigger for this fusion is the viral glycoprotein gD in the case of many alphaherpesviruses. Furthermore, during the fusion of EHV1, an uncharacterized cellular receptor is involved, disparate from previously described alphaherpesvirus receptors (Spear and Longnecker, 2003; Frampton et al., 2005).

In endocytosis, Van de Walle et al. (2008) have determined that in EHV1, gD is once again required, this time to interact with cellular integrins. Additionally, evidence was provided that EHV1 is able to use different cellular pathways during entry. Hassebe et al. (2009), investigated these endocytic pathways in primary cultured equine brain microvascular endothelial cells (EBMEC) and equine dermis (ED) cells using confocal immunofluorescence microscopy and cells expressing a dominant negative form of equine caveolin-1. This study suggests that EHV1 enters EBMEC via caveolar-mediated endocytosis. A significant reduction in EHV1 entry after adenosine triphosphate (ATP) depletion and treatments with lysosomotropic agents suggests that EHV1 enters ED cells via energy- and pH-dependent endocytosis. The results indicated that clathrin-dependent endocytosis plays only a minor role in EHV1 entry into EBMECs, thus confirming the use of multiple endocytic pathways by EHV1 in different cells.

Subsequent to penetration there is an introduction of the viral genome into the cellular compartment (in Figure 2, a schematic overview of EHV1 replication is shown). The manner of uncoating depends on the entry mechanism. In the case of fusion with the cell membrane, the nucleocapsid is directly conveyed into the cytoplasm, whereas virions entering through endocytosis uncoat by fusing with the endosome bilipid membrane after the pH drop caused by proton pumps (Voyles, 2002). Once the nucleocapsid is delivered into the cytoplasm, it is transported along microtubules to the nuclear pore of the cell, where the introduction of nucleic acid ensues (Gryspeerdt, 2011). Following circularization and replication of the viral DNA, transcription may commence once the viral genome has entered the nucleus, with the aid of cellular ribonucleic acid (RNA) polymerase II and several consecutive viral components. Herpesvirus genes can be divided roughly into immediate-early (α), early (ß) and late (γ) categories. Transcription of the immediate early genes occurs first, consequently providing a manner of regulation for all three gene categories. Hereafter, the expression of the three gene groups is temporally regulated through a series of feedback loops. Early genes primarily encode non-structural proteins involved in DNA replication and nucleotide metabolism such as DNA polymerase, whilst late gene products include many virion proteins, such as virion tegument proteins, capsid and envelope proteins. The onset of viral DNA synthesis occurs during late viral transcription, despite the host cells not all being in synthesis phase (S phase), as the virus provides its own replicative machinery (Gray et al., 1986; Voyles, 2002; Mettenleiter and Sobrino, 2008). Other herpesviruses like HCMV and EBV require special strategies for generating their numerous proteins, e.g. alternative splicing of transcripts (Voyles, 2002).

New virus arises from self-assemblage of viral components, comprising of newly synthesized DNA copies in the nucleus and capsid proteins formed after translation in the cytoplasm. This process, encapsidation, takes place in the nucleus (Voyles, 2002). According to Mettenleiter et al. (2009), capsid proteins first autocatalytically assemble with and around a scaffold consisting of pUL26 and its carboxyterminal half pUL26.5, after which the viral DNA gets built in.

Final maturation of nucleocapsids occurs in the cytoplasm. Three hypotheses have been proposed for this transport out of the nucleus. The most likely one involves an envelopment and de-envelopment process. Following primary envelopment through fusion with the intranuclear membrane, the nucleocapsid gets translocated to the cytoplasm by fusion of the primary envelope with the outer nuclear membrane. The movement towards the inner nuclear membrane prior to envelopment is dependent on actin. To avoid the production of inoperative virus particles a preference is exhibited in wild type virus infections. Namely, a preference towards the primary envelopment of capsids containing viral DNA rather than immature capsids lacking viral DNA (Mettenleiter et al., 2006). Mettenleiter et al. (2006) developed alphaherpesvirus mutants that lack pUS3 and observed an accumulation of primary enveloped virions in the lumen of the perinuclear cleft, concluding that phosphorylation of a component of primary enveloped virions by pUS3, which is present in the immature virions itself, might be the trigger for the de-envelopment. The second theory, lumenal nuclear egress, also entails a budding process at the inner nuclear membrane. However, it proposes transit of the enveloped virion through the secretory pathway, and therefore retaining the structural integrity of the primary enveloped virion. This maintenance of integrity between primary and mature virions is opposed by Mettenleiter et al. (2008) by indicating that two conserved herpes proteins (pUL31 and pUL34) required for nuclear egress, are both part of primary virions but absent from mature virus particles. The third model, the ‘nuclear pore’ nuclear egress pathway, suggests that nucleocapsids leave the nucleus via widely dilated nuclear pores. This model is controversial due to apparent integrity of nuclear pore assemblies until very late in the virus infection (Mettenleiter et al., 2006).

After nuclear egress tegumentation ensues, which can be initiated at two sites; the capsid and the future envelope. The capsid proximal tegument contains pUL36 and pUL37, which appear to be the only tegument proteins that are conserved within all herpes subfamilies. These mediate the transport of nucleocapsids to the envelopment site, where in addition to envelope glycoproteins, the remainder of the tegument awaits them. Tegumentation is the result of complex protein-protein interactions. The trans-Golgi network is the final envelopment site, where glycoproteins are gathered together with the remainder tegument proteins. Interactions amongst tegument proteins, between tegument proteins and the nucleocapsid, as well as with the cytoplasmic tails of several glycoproteins, result in the formation of a mature herpes virion, within a cellular vesicle. Subsequently, these are transported to the cellular membrane, where fusion between the cellular membrane and vesicle occurs, releasing the mature virion (Mettenleiter, 2002; Mettenleiter, 2004; Mettenleiter et al., 2008; Mettenleiter et al., 2009; Mettenleiter et al., 2012).

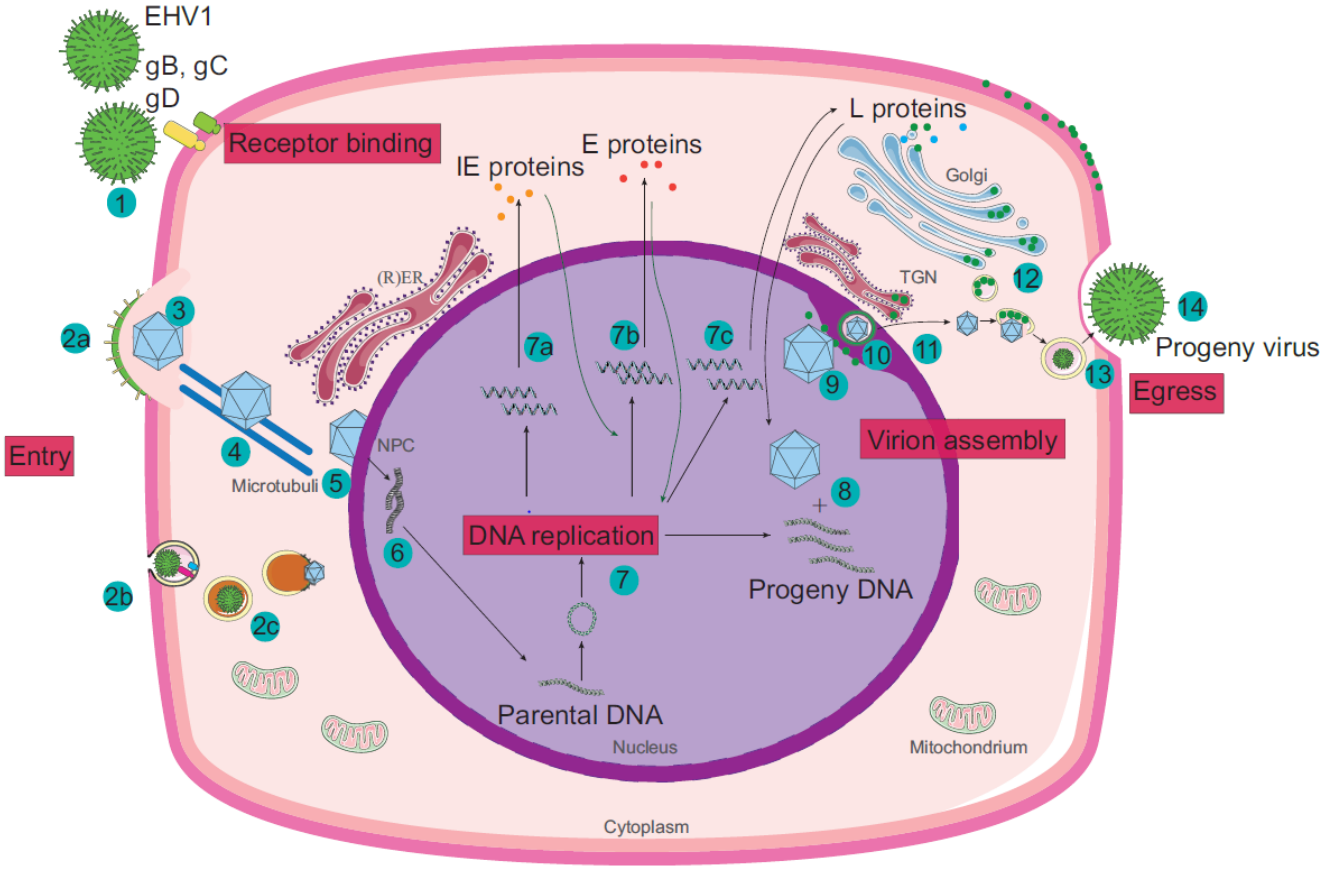

Figure 2. The EHV1 replication cycle (1) Attachment of free virions to cell surface (2a) Fusion with the plasma membrane or (2b) Endocytosis (2c) Fusion with the bilipid of the endosome (3) Release of nucleocapsid into cytoplasm 4) Transport along microtubules into nucleus 5) Transfer through nuclear pore (6) Circularization of DNA (7) Replication (7a,b,c) Transcription and translation into proteins (8,9) Encapsidation (10) Budding of the nucleocapsid through inner leaflet of the nuclear membrane (11) Fusion of nucleocapsid with outer leaflet of nuclear membrane, resulting in entry of naked nucleocapsids into cytoplasm (12) Envelopment through budding into the trans-Golgi network (TGN) (13) Transport to cell surface (14) Vesicle-mediated exocytosis ((R)ER: (rough) endoplasmic reticulum) (from: PhD thesis Poelaert, 2019b).

B. *Equine herpesvirus type 1*

1.6. Epidemiology

EHV1 is endemic worldwide, with most horses being infected during their first year of life. Reinfections occur throughout their whole life, though disease becomes less severe. Horses of any breed, year or sex can be infected, even after being vaccinated. There are two infection routes: the first being exogenously introduced, through virus shed in nasal mucus or less commonly through contact with an EHV1 infected aborted fetus. Aside from transmission through direct contact, aerosol transmission cannot be excluded (van Maanen, 2002; Gryspeerdt, 2011). The second route is endogenous, by reactivating latent infections following weaning, castration, relocation and terminal illness. Stress plays an important role in reactivation (Burrows et al., 1984; Patel and Heldens, 2005). Sucking foals can get infected from the age of 30 days, suggesting that latently infected mares are primarily responsible for this transmission (Gilkerson et al., 1997; Gilkerson et al., 1999). From their clinical study, Wang et al. (2007) concluded that the presence of EHV1 is uncommon in healthy horses, suggesting that spread of EHV1 is typically accompanied with clinical signs and that subclinical infections are less probable, although the clinical signs can be very mild (Gryspeerdt et al., 2011).

1.7. Pathogenesis

1.7.1. Introduction

The viral infection can lead to two clinical manifestations. Next to respiratory symptoms, the virus can either cause abortions, or neurological symptoms, depending on the virus strain. The abortigenic and neurovirulent strain can be distinguished by a single nucleotide polymorphism (SNP) in the DNA polymerase gene, which is present in ORF 30, and leads to a change in amino acids and consequently phenotype (Nugent et al., 2006). Cases with horses showing neurological symptoms are on the rise. Moreover, EHV1 is the most important cause of infectious abortion worldwide (van der Meulen et al., 2003a). The virus causes huge economic and emotional losses all over the world. Therefore, it is important to understand the pathogenesis, so that more effective vaccines can be developed (see Figure 4 for a schematic overview of the pathogenesis of EHV1). The production of effective vaccines has been difficult, due to the immune evasion strategies developed by EHV1. These will be discussed more in depth further on, as this dissertation aims to clarify one of the protective measures of the immune system.

1.7.2. Primary Replication

EHV1 primarily replicates in the epithelial cells of the nasal cavities, pharynx, trachea and bronchi(oli), followed by a replication in the local lymph nodes. The infection in the airway is predominantly lytic, causing various respiratory symptoms like nasal and ocular discharge, fever and anorexia (Patel and Heldens, 2005). In uncomplicated clinical cases, clinical signs can persist for two to seven days. The development of distinct herpetic lesions (plaques) in mucosal membranes can occur in all parts of the upper respiratory tract. In addition to necrosis, intranuclear inclusion bodies can be observed microscopically (van Maanen, 2002).

Gryspeerdt et al. (2010) investigated the difference in replication between neurovirulent and abortigenic strains in the upper respiratory tract, *in vivo,* and came to the conclusion that both strains replicated in a similar plaque-wise manner in epithelium of the nasal mucosa, but replication in epithelium of the nasopharynx was largely limited to abortigenic EHV1. Similar results were obtained in *in vitro* studies on explants. Vandekerckhove et al. (2010) detected significantly larger plaque sizes with the abortigenic strain in comparison to the virulent strain, at 48 - and 72 hours post infection (hpi). In addition, a second experiment, in which inter-horse variability was eliminated, demonstrated a higher number of viral plaques for the abortigenic strain at 48 hpi. Finally, Poelaert et al. (2018) also

observed larger plaques and a higher number of plaques in the upper respiratory tract for the abortigenic strain in comparison to the neurovirulent strain, although the results were not significant. Furthermore, virus titration showed similar levels of virus. No difference in replication between strains was observed in the equine respiratory epithelial cell (EREC) model, implying tissue specific replication (Poelaert et al., 2018).

A second observation made by Vandekerckhove et al. (2010) was that these viral plaques never crossed the basement membrane, in contrast to the closely related alphaherpesvirus PrV, suggesting the virus causes a viremia in an alternative way. Despite the inability of plaques to cross the basement membrane, individual infected cells in the connective tissue below the basement membrane were observed. Scott et al. (1983), demonstrated that T lymphocytes (T cells), B lymphocytes (B cells) and monocytes are all able to harbour virus. In other words, EHV1 seems to hijack these PBMCs to cause a viremia.

Vandekerckhove et al. (2010) discovered that neurovirulent strains crossed the basement membrane via single infected cells at an earlier time point than abortigenic strains, namely 24 hpi in contrast to 36 hpi. Gryspeerdt et al. (2010) established that the total number of infected individual cells in underlying connective tissue was three to seven times lower in horses infected with abortigenic strains than those infected with neurovirulent strains. These results suggest that both strains have different invasion kinetics. Vandekerckhove et al. (2010) suggested that neurovirulent strains are superior at infecting immune cells, whilst abortigenic strains are more apt to infect epithelial cells, since abortigenic strains induce larger plaques and have a slower migration to underlying tissues.

Furthermore, disrupted epithelium leads to an enhanced invasion of the deeper tissues in the respiratory tract, whereby EHV1 preferentially binds to epithelial cells basolaterally and infection of leucocytes occurs (Van Cleemput et al., 2017).

1.7.3. Viremia

After primary replication in epithelial cells, mononuclear cells become infected. These infected mononuclear cells that enter the bloodstream cause a cell-associated viremia that can be detected as early as one day post infection and can persist for at least 14 days. This viremia is more robust with neurovirulent strains than with abortigenic strains (Gryspeerdt, 2010). The PBMC subpopulations that are hijacked by EHV1 varies between studies (Scott et al., 1983; Gryspeerdt et al., 2010; Vanderkerckhove et al., 2010; Wilsterman et al., 2011; Poelaert et al., 2019a). This could be due to the use of different viral strains, different methods for the isolation of PBMCs, inter-animal variability, and to the different number of animals used to generate data

Scott et al. (1983) identified the T cell population as the primary PBMC subpopulation infected with EHV1 during viremia in an *in vivo* study. A more recent *in vivo* study used PCR techniques to identify viral DNA, and found that $CD8^+$ T cells, followed by B cells, are most frequently infected during a viremia (Wilsterman et al., 2011). In contrast, Gryspeerdt et al. (2010) found that $CD172a^+$ cells and $CD5^+$ T cells were important targets for both strains, the former being the most frequently infected cells, despite a more substantial amount of infected $CD5^+$ cells with the abortigenic strains. Furthermore, B cells were an important target in lymph nodes, irrespective of the strain. Similar results were obtained by Vandekerckhove et al. (2010), whose nasal explant system showed mainly and equally infected $CD5^+$ cells and $CD172a^+$ monocytic cells in the case of the abortigenic strain, whereas for neurovirulent strains, the majority of infected cells were $CD172a^+$. Further research on $CD5^+$ T cells, demonstrated that it was mainly $CD4^+$ cells that were infected, although $CD8^+$ T cells were also susceptible. Similar results were obtained by Poelaert et al. (2019a), whose research also demonstrated that the abortigenic strain was more efficient in infecting $CD4^+$ cells than the neurovirulent strain. Furthermore, B cells were rarely infected by both strains (Vandekerckhove et al., 2010). An *in vitro* study with the

abortigenic strain, confirmed that in fresh, unstimulated PBMC, monocytes are the most important cell fraction in which EHV1 replicates. Furthermore, this research showed an increased replication in mitogen stimulated lymphocytes (van der Meulen et al., 2000).

Poelaert et al. (2019a), demonstrated that EHV1 is able to directly infect blood- and lymph nodal-derived T cells, with both strains showing similar replication kinetics in both T cell populations. However, significantly more T cells were infected at 9 hpi with the abortigenic strain, once more suggesting a difference in T cell tropism of both strains. Finally, following viral replication in respiratory epithelial and/or $CD172a^{+}$ monocytic cells, EHV1 is able to transfer virus to T cells through cell-cell contact (Poelaert et al., 2019a).

In conjunction with reaching the bloodstream through PBMCs, EHV1 has been detected in submandibular, retropharyngeal and bronchial lymph nodes. Consequently, EHV1 can also reach the blood circulation via efferent lymph vessels (Kydd et al., 1994). Cell-associated viremia in immune cells cleverly permits the dissociation of virus to its target organs, where secondary replication in endothelial cells may commence.

1.7.4. Secondary replication

Once in the blood circulation, infected leukocytes are able to transfer EHV1 to endothelial cells lining the vasculature of target organs, namely the pregnant uterus, central nervous system and the eyes, through cell-to-cell contacts (see Figure 4 for a schematic overview of the pathogenesis of EHV1). Moreover, studies have shown that release of viral progeny from T cells only occurs after contact with endothelial cells (Poelaert et al., 2019a). This cell-to-cell, direct spread is an efficient immune evasion technique, which will be discussed further on. Poelaert (2019b) has suggested two explanations for EHV1's three secondary replication sites; the first explanation is linked to the expression of specific adhesion molecules, which will be addressed further on. The second explanation is linked to a similarity in the anatomical microvasculature structure of those organs, namely a low blood velocity due to the small blood vessel diameter.

Following viremia, EHV1 infection proceeds through leukocyte extravasation, a process in which leukocytes migrate out of the bloodstream, through the endothelium and into tissues. This process involves the interaction of leukocyte and endothelial adhesion molecules (a schematic overview of leukocyte recruitment is given in Figure 3). Leukocyte extravasation includes leukocyte rolling, adhesion and trans-endothelial migration. Rolling is mediated by the weak binding between selectins and their carbohydrate ligands. This binding is then transformed into a high affinity integrin-mediated adhesion by activating signals derived from chemokines. These leukocyte integrins interact with their endothelial counter-receptors of the immunoglobulin superfamily. Subsequently, leukocytes move over the endothelial cell surfaces using integrins. Ultimately, leukocytes are able to transmigrate (Chavakis et al., 2009).

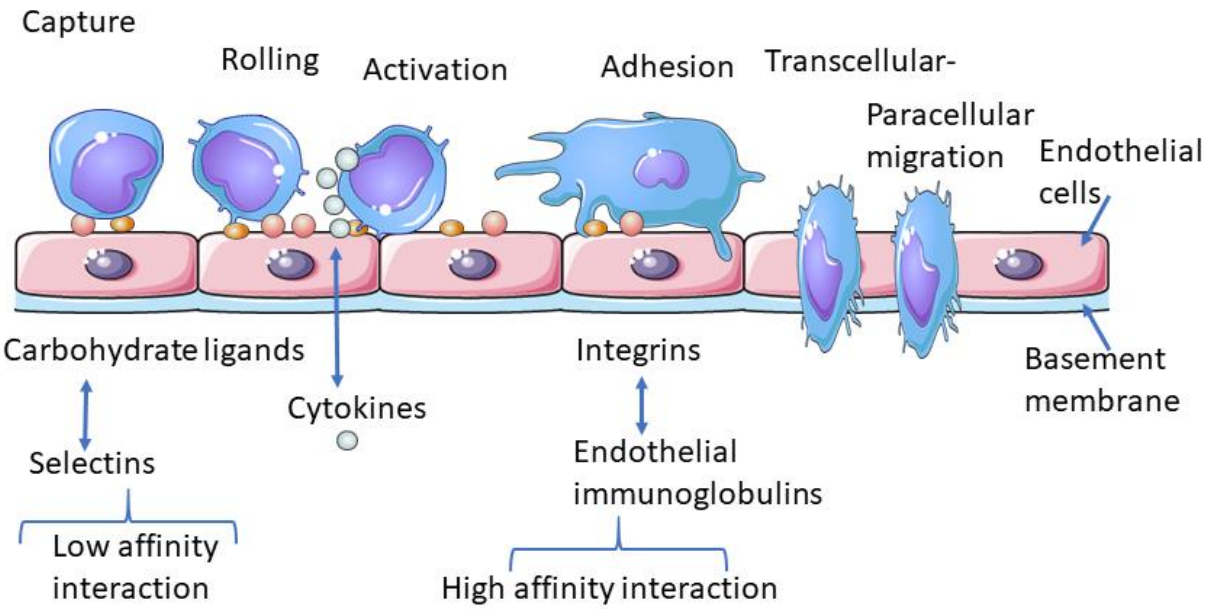

Figure 3. The multistep process of leukocyte recruitment to the endothelium.

Generally, adhesion molecules are expressed as a consequence of virus infection of endothelial cells, enabling the adhesion of leukocytes to the endothelial site of viral replication, as has been described for HSV1 and HCMV. However, EHV1's transfer to endothelial cells is dependent on expression of adhesion molecules associated with leukocyte adhesion, prior to endothelial infection. This may clarify the restricted replication in target tissues expressing these adhesion molecules. Furthermore, it is apparent that these adhesion molecules do not function as a receptor, as is the case with human rhinovirus 1, considering both infected as virus negative leukocytes adhere to the endothelial cells expressing adhesion molecules (Smith et al., 2002). Laval et al. (2015a) performed antibody-blocking experiments and discovered that α4β1, αLβ2 and αVβ3 integrins mediated adhesion of infected $CD172a^{+}$ cells to endothelial cells.

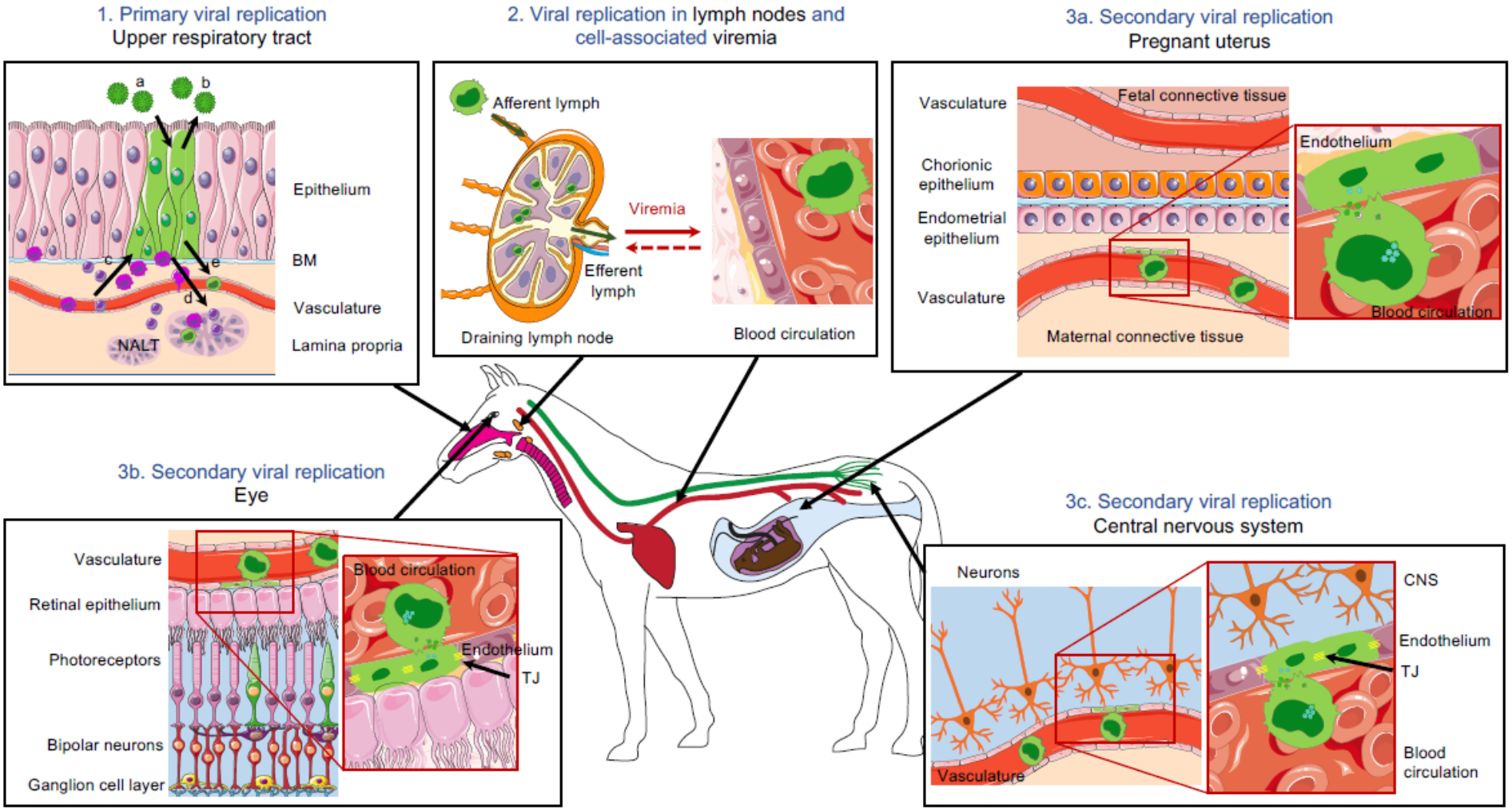

Figure 4. Schematic overview of the pathogenesis of EHV1. (1) Primary replication occurs in epithelial cells in the upper respiratory tract, during which PBMC are recruited and subsequently infected. These can enter the bloodstream directly or migrate to lymph nodes. (2) Viral replication occurs in lymph nodes, after which virus can enter lymphatic vessels and bloodstream by hijacking PBMC. (3) Secondary replication occurs in endothelial cells of the (3a) pregnant uterus, (3b) eye, (3c) and central nervous system (from: Poelaert, 2019b).

1.7.5. Clinical signs

Respiratory infections are usually mild or subclinical, though as previously mentioned, EHV1 can cause symptoms such as rhinopharyngitis, tracheobronchitis, nasal and ocular discharge, fever and anorexia. Additionally, an EHV1 infection can lead to abortion, neonatal syndrome, and neurological symptoms, due to its tropism for endothelial cells of these target organs (see photos with clinical signs in Figure 5) (Patel and Heldens, 2005).

Replication in the pregnant uterus can cause vasculitis and multifocal thrombosis. This leads to necrosis and edema of the uterus, possibly resulting in detachment of fetal membranes and thus abortion of an EHV1 negative fetus. If the virus disseminates in the fetus, presumably through the umbilical cord, this could result in abortion of an EHV1 positive fetus (Smiths at al., 1992; Smiths et al., 1993; Smiths et al., 1996). A third scenario can occur at a late stage of gestation, where the transplacental infection could result in the birth of a live infected foal, that could still die a few days later (Laval, 2016). 95% of abortions due to EHV1 occur in the last third of pregnancy (Patel and Heldens, 2005).

Neurovirulent strains of EHV1 can affect all parts of the central nervous system. Unlike several other alphaherpesviruses, that replicate in neurons, EHV1 causes myeloencephalitis due to its endotheliotropism, rather than a neurotropism, as is the case with HSV1, BHV1 and PrV. This secondary replication can cause vasculitis, with or without hemorrhages, and necrosis (Wilson, 1997). Equine herpes myeloencephalopathy develops due to a lack of nutrients and oxygen, resulting in varying clinical signs such as mild ataxia, swaying, stumbling and falling, to complete paralysis (van Maanen et al., 2001; Stierstorfer et al., 2002). Generally, the hind limbs are most affected. The period between infection and neurological disorders differs from six to eight days (Mumford et al., 1994). Finally, EHV1 can also induce ocular disease, due to secondary replication in the vasculature of the eye. Despite the presence of multifocal chorioretinal lesions, these were not associated with a loss of vision or any clinical ocular signs in an *in vivo* study (Hussey at al., 2013).

Figure 5. Clinical signs associated with EHV1, (A) Neurological disease with ataxia (McAuliffe, 2013) (B) Abortion (from:[1]ExtensionHorses) (C) Respiratory disorders with serous nasal discharge (from: [2]The Horse).

1.8. Diagnosis

For optimal management strategies, rapid diagnostic tests are essential (see Table 1 for a summary of diagnostic techniques). Currently, the golden standard is virus isolation and culture, which can allow a positive identification in three days. Viral culture can be unsuccessful in cases where the peak of viral shedding has already passed and where antibodies have already interfered (van Maanen et al., 2001). In other cases, a positive virus isolation is characterized by cytopathic effects (CPE), though it is not possible to differentiate between EHV1 and equine herpes virus type 4 (EHV4) solely based on the CPE, so immunofluorescence is performed with type-specific monoclonal antibodies for positive identification (see Figure 6 for positive identification of the abortigenic EHV1 strain). Immunofluorescent approaches can be very useful in rapid diagnosis. For isolation, nasal and pharyngeal swabs can be collected, as well as heparinized blood samples, considering viremia often coincides with clinical signs of respiratory and neurological disease, and abortion. Furthermore, thymus, spleen and lungs can be collected from aborted foals (Lunn et al., 2009).

[1]ExtensionHorses, viewed on 13 May 2019, https://www.flickr.com/photos/64081615@N06/5842373370/

[2]The Horse, viewed on 12 May 2019, https://thehorse.com/163682/the-nose-knows-what-equine-nasal-discharge-tells-us/

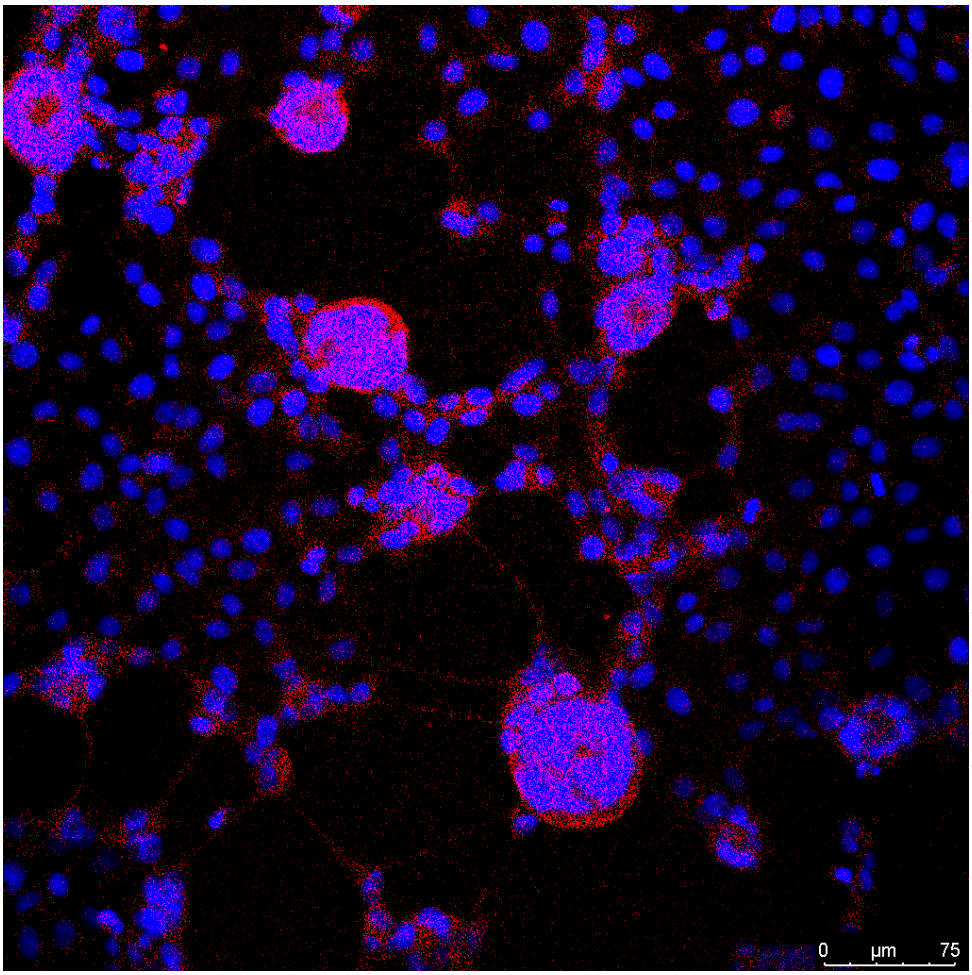

Figure 6. Cytopathic effect in rabbit kidney cells (RK-13 cells) inoculated with the EHV1 abortigenic strain. Nuclei were labeled with the molecular probe Hoechst (blue) and immediate early viral proteins were labeled with Texas Red (red).

Polymerase chain reaction (PCR) assays are widely used and are both rapid and sensitive. Real-time PCR assays have been developed, that allow quantification of viral load, and can distinguish between neurovirulent and abortigenic strains (Pusterla et al., 2009). Several other techniques have been described, based on enzyme-linked immunosorbent assay (ELISA) or nucleic acid hybridization probes, though their use is often restricted to specialized laboratories ([3]OEI Terrestrial Manual, 2017).

Serological diagnosis is based on a four-fold or greater increase in antibody titers through serum-neutralization tests (SN), ELISA or complement-fixation (CF) tests on paired sera; taken during acute illness and two to three weeks later (Kydd et al., 2006). However, these tests cannot distinguish between EHV1 and EHV4 due to cross-reactivity. Therefore, a specific ELISA test based on the C-terminal portion of glycoprotein G of both viruses has been developed (Crabb et al., 1995).

Table 1. Test methods available for diagnosis of equine rhinopneumonitis and their purpose.

Method	Purpose					
	Population freedom from infection	Individual animal freedom from infection prior to movement	Contribution to eradication policies	Confirmation of clinical cases	Prevalence of infection - surveillance	Immune status in individual animals or populations post-vaccination
Agent identification[1]						
Virus isolation	–	+++	–	+++	–	–
PCR	–	+++	–	+++	–	–
Detection of immune response						
VN	+	+	+	+++	+++	+++
ELISA	+	+	+	++	+++	+
CFT	–	–	–	+++	–	–

Key: +++ = recommended method; ++ = suitable method; + = may be used in some situations, but cost, reliability, or other factors severely limits its application; – = not appropriate for this purpose. Although not all of the tests listed as category +++ or ++ have undergone formal validation, their routine nature and the fact that they have been used widely without dubious results, makes them acceptable. PCR = polymerase chain reaction; VN = virus neutralisation; ELISA = enzyme-linked immunosorbent assay; CFT = complement fixation test (from: OEI [3]Terrestrial Manual, 2017).

1.9. Control and Treatment

1.9.1. Treatment

There are three major priorities when a clinical case occurs; early diagnosis, prevention of further spread, and treatment and management of the patient. Currently, there are no treatments available with a proven efficacy, therefore, treatment is limited to the use of standard antiherpetic drugs and supportive therapy. The use of acyclovir and its derivative have conflicting results. Garré et al. (2009) saw no effect on clinical signs, viral shedding and viremia of infected ponies, except for the peak body temperature two days post infection, where treated ponies had a lower temperature. In an outbreak at a university equestrian center, prophylactical treatment, or treatment within 24 hours of the onset of neurological disease gave promising results (Henninger et al., 2007). Furthermore, acyclovir has a poor oral bioavailability, necessitating high dosages, thus being costly. Its derivative, valacyclovir has a better bioavailability (Garré et al., 2009).

An alternative treatment is the development of small interference RNA molecules against envelope glycoprotein B and the origin-binding protein kinase. Research has shown that the severity of clinical disease, the number of infected animals and the magnitude of nasal shedding can be reduced (Fulton et al., 2009). In another study, no significant difference in viremia and viral shedding was shown. However, the cases that required euthanasia after infection were significantly reduced after treatment with siRNA (Brosnahan et al., 2009). Finally, it has been reported that (1'S,2'R)-9-[[10,20-bis(hydroxymethyl) cycloprop-10-yl]methyl]guanine (A-5021), is able to completely inhibit viral plaque

[3]OEI Terrestrial Manual, 2017, viewed on 20 March 2019, http://www.oie.int/fileadmin/Home/eng/Health_standards/tahm/2.05.09_EQUINE_RHINO.pdf

formation in equine nasal mucosal explants (Glorieux et al., 2012). The efficacy of A-5021 still needs to be evaluated in the horse.

Supportive therapy includes the use of broad-spectrum antibiotics to prevent secondary complications, despite the generally self-limiting character of respiratory disease. Fever can be treated with antipyretics. It has been recommended to treat horses suffering from neurological symptoms with corticosteroids or anti-inflammatory drugs for a short period to decrease inflammation associated with vasculitis. However, this must be given responsibly as it could increase virus spread and provoke secondary complications due to its immunosuppressive mode of action. Animals with severe ataxia could be supported with a sling (Figure 7 shows a horse suffering from neurological disease in a sling), and lateral recumbent animals must be rotated every few hours. In addition, food and water must be easily accessible. Antibiotics is advisable due to a higher risk for aspiration pneumonia and decubital ulcers. Generally, abortions are not associated with complications, though it has been advised to disinfect the mare's tail and hind quarters to prevent further viral contamination of other horses. In the case of birth of infected foals, intensive treatment should consist of warmth, oxygen, cardiovascular and nutritional support (Goehring and Sloet van Oldruitenborgh-Oosterbaan, 2001; van Maanen, 2002).

Figure 7. Horse suffering with neurological symptoms supported by a sling (from: [4]Tuesday's Horse).

[4]Tuesdays horse, viewed on 25 April 2019, https://tuesdayshorse.wordpress.com/tag/horses-canada/

1.9.2. Management

Preventive management is aimed at avoiding stressful circumstances such as weaning, transport and mixing horses from different origins, considering epizootics are often associated with the assembly of horses in stressful circumstances. In addition, a quarantine period of at least three weeks should be implemented to avoid import from an outside source. Division of animals into age groups, as well as keeping pregnant mares separate from not pregnant mares, could also help prevention. Following an outbreak of respiratory disease, abortions or neurological symptoms, affected animals should be isolated, material and bedding should be sprayed with disinfectant along with other hygienic procedures, and there should be a clinical monitoring of the horses (Van Maanen, 2002).

1.9.3. Vaccination

Current vaccines are able to reduce nasal virus titers (minimizing the shedding of the virus) and therefore reducing the severity of the respiratory symptoms (Mumford and Bates, 1984; Heldens et al., 2001; Goodman et al., 2006). The problem we face combatting this virus is that the vaccines that are on the market cannot offer 100% protection. None of them are able to prevent a viremia (or are limited in doing so), meaning the occurrence of the systemic symptoms mentioned above is variable (van der Meulen et al., 2007). When creating a vaccine, it is important to stimulate both the humoral and the cellular immunity. Neutralizing antibodies will capture free virus particles at primary and secondary replication sites, reducing viral shedding and interrupting the virus' cycle. Unfortunately, the mucosal antibodies are short-lived and they will not offer protection once the virus replicates intracellularly, demonstrating the importance of cellular immunity. Current vaccines are mainly inactivated EHV1 vaccines, ensuring a high antibody titer. However, they do not induce a cytotoxic T lymphocyte (CTL) mediated response and consequently do not eliminate the cell-associated viremia. Focusing on cellular immunity and using live virus vaccines could be the answer to this problem, but still poses the risk of reversion to virulence (Breatnach et al., 2001; Kydd et al., 2003; Kydd et al., 2006).

Despite the incomplete protection vaccination offers, a vaccination program combined with optimal management is the most cost-effective approach. The main goal of vaccination is to reduce viral replication, viral shedding, viremia, and ultimately preventing the development of severe secondary symptoms. It is recommended[5] to vaccinate horses two times, with a four to six-week interval. Following this primary vaccination, horses should be vaccinated every three to six months, considering the short-term protection. In addition, current advice suggests pregnant mares should be vaccinated during fifth, seventh and ninth month of gestation.

Inactivated virus vaccines generally consist of inactivated whole virus or glycoproteins (subunit vaccines). Though responses to inactivated vaccines in the field are variable, the current commercially available vaccine in Belgium is the inactivated whole virus vaccine marketed as Equip 1,4 (Zoetis). In the US, Pneumabort-K vaccine (Zoetis) is the commercialized inactivated whole virus vaccine, which has been shown to reduce adverse clinical signs, viral shedding and viremia (Goehring, 2010). Studies on the combination inactivated virus vaccine, Fluvac Innovator 6 (Zoetis, US) demonstrated poor results regarding clinical signs and viral nasal shedding, and insignificant differences when compared with the modified live vaccine, Rhinomune (Boehringer Ingelheim Vetmedica). However, it must be taken into consideration that Fluvac Innovator 6 has a relatively low immunogenicity (Goodman et al., 2006). Studies on another inactivated whole virus vaccine, Duvaxyn $EHV_{1,4}$ (Zoetis, Australia), established a clear reduction in clinical signs, in the duration of virus shedding and in the quantity of virus shed (Heldens et al., 2002).

[5] FAGG, medicinal product database, viewed on 25 June 2019, https://geneesmiddelendatabank.fagg-afmps.be/#/query/veterinary/

Despite the risk of reversion to virulence, attenuated live virus vaccines offer the advantages of inducing a CTL mediated response, a mucosal response and prolonged protection. Prevaccinol (Merck MSD-Intervet, Munich, Germany), is a commercial live-attenuated vaccine based on the RacH strain, in Europe (Kydd et al., 2006). After further passages of this live virus in rabbit kidney cells and equine epidermal cells, it has been licensed as Rhinomune (Boehringer Ingelheim Vetmedica) in the US, and causes a significant reduction in clinical signs and in viral shedding, though not in viremia (Goodman et al., 2006; Goehring et al., 2010).

Alternative vaccines such as DNA vaccines, live-vectored vaccines and gene deletion mutants are being designed and tested, though are not commercially available yet. Van de Walle et al. (2010) described a significant reduction in clinical signs, nasal shedding and viremia levels in horses vaccinated with a recombinant modified live EHV1 vaccine based on the abortigenic strain, NY03. Combinations of plasmids encoding the gB, gC, and gD glycoproteins or plasmids encoding the immediate early (IE) and early proteins (UL5) of EHV1 were tested. This DNA vaccine induced limited immune responses and protection, though the authors suggested that future vaccination strategies should focus on inducing stronger CTL responses (Soboll et al., 2006). A recombinant canarypox-based vaccine (ALVAC) expressing EHV1 gB, gC, and gD genes distinctly reduced virus shedding but failed to protect against cell-associated viremia (Minke et al., 2006). An immune stimulating complex (ISCOM) vaccine was developed early on from a purified virion, containing all major EHV1 glycoproteins. This EHV1 ISCOM vaccine generated fully protective responses in hamsters challenged with an otherwise lethal dose of the hamster-adapted EHV1 strain RacH (Cook et al., 1990).

More recently, inoculation of EHV1 gD and gB produced by a recombinant baculovirus and presented by the adjuvant Iscomatrix, similar to ISCOM, resulted in reduced viral shedding (Foote et al., 2006). A thymidine kinase (TK)-deficient deletion mutant virus that is still able to replicate but is markedly less pathogenic, is able to induce partial protection with reduced clinical symptoms, though it is not able to prevent viremia after challenge (Slater et al., 1993). Another deletion mutant, lacking glycoprotein E, was evaluated more recently. Following a wild type EHV1 challenge infection, vaccinated foals showed milder clinical symptoms. In addition, viral nasal shedding and viremia were reduced (Tsujimura, 2009).

It is apparent that the development of novel vaccines is necessary. Certainly recombinant ones, that are able to replicate in the respiratory epithelium, providing local protection and therefore preventing viremia. Although these should not be too virulent, so that replication in immune cells is not possible, otherwise this would lead to cell-associated viremia.

2. Immunity

2.1. Introduction

Our immunity encompasses two major systems, namely, innate immunity and adaptive immunity. Together, they provide remarkable protection from infectious agents, such as viruses. The innate response is a rapid, non-specific, first-line defense against pathogens, which is strengthened by an adaptive response if it is unable to eliminate the threat. This secondary response is developed during the lifetime of an individual as an adaptation to infection with a certain pathogen. In summary, recognition occurs of specific pathogens due to highly specialized antigen receptors. Moreover, this latter response leads to a lasting immunity, offering protection against reinfection with the same pathogen.

The immune system comprises white blood cells or leukocytes, which originate from pluripotent hematopoietic stem cells in bone marrow. These leukocytes can be divided into two main categories, the lymphoid and myeloid lineages (see Figure 8 for a schematic overview of the immune cells). The common myeloid progenitor is the precursor of mast cells and phagocytes of the innate immune system, as well as red blood cells and megakaryocytes. There are three types of phagocytes, namely, the macrophages and dendritic cells, which have differentiated from monocytes; and granulocytes, which is the collective term for neutrophils, eosinophils and basophils. The common lymphoid progenitor gives rise to lymphocytes of the adaptive immune system and the natural killer (NK) cells of the innate immunity (Murphy, 2012a).

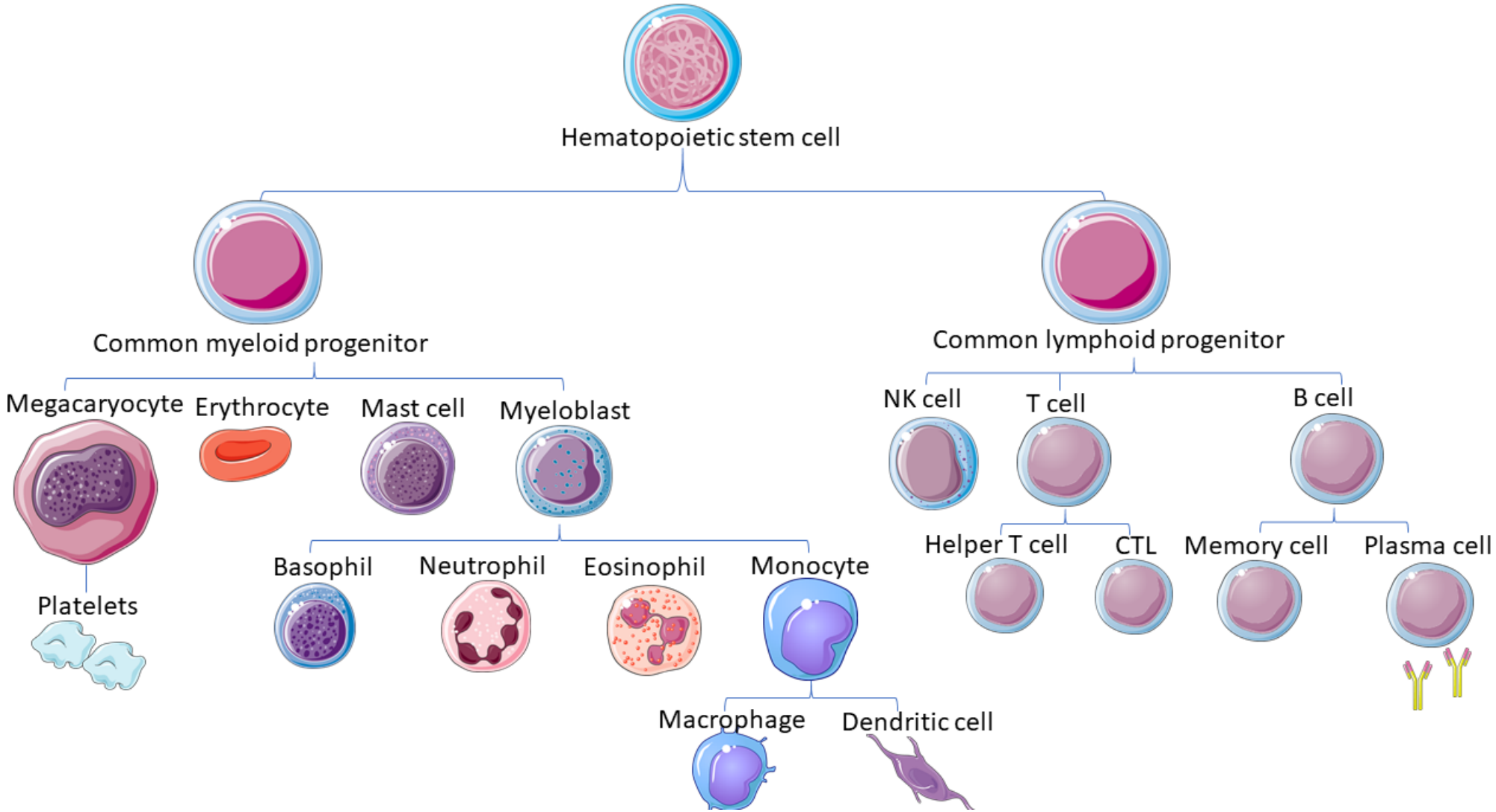

Figure 8. Schematic overview of the immune cells

2.2. Innate Immunity

2.2.1. First line defense

The initial defense against infection is the physical barrier, consisting of the mucus layer, which entraps pathogens and consequently expels them by cilia, and epithelial cells. Van Cleemput et al. (2017) has demonstrated that the firm intercellular connections in the epithelium are essential in restriction of EHV1 replication.

The epithelial cells express signaling receptors, that recognize respiratory viruses in extracellular spaces by their pathogen-associated molecular patterns (PAMPs). Of these signaling receptors, Toll-like receptors (TLRs) represent an evolutionary ancient host defense system (Murphy, 2012a). Three TLRs are particularly important in herpesvirus infections. TLR2 is known to interact with viral envelope proteins of HSV1 (Leoni et al., 2012). TLR9 and 3, are able to recognize double-stranded DNA and sense viral RNA, respectively (Lund et al., 2003; Zhang et al., 2007). These TLRs are responsible for signaling cascades that ultimately result in an antiviral innate immune response with the production of cytokines and chemokines (Kawai and Akira, 2007). This corresponds with *in vitro* studies that demonstrated an increased expression of TLR3-and 9, as well as inflammatory cytokines (interleukin 1 (IL-1), tumor necrosis factor α (TNF-α), type 1 interferon (IFN) and IL-6) and chemokines (IL-8 and monocyte chemoattractant protein-1) (Hussey et al., 2014a). A second important pattern recognition receptor (PRR) is the cytoplasmic nucleotide-binding oligomerization domain (NOD)-like receptor (NLR) which is known to control major histocompatibility complex class 1 (MHC-1) expression (Jacobs and Damania, 2012; Neerincx et al., 2012). During herpesvirus infections, this production of broad range of molecules can also be induced by triggering intracellular viral sensors such as the retinoic acid inducible gene (RIG)-like receptors (RLRs), which are triggered by viral messenger ribonucleic acid (mRNA) produced during virus replication (Takeuchi and Akira, 2010).

Following stimulation of signaling receptors, cytokines affect the behavior of nearby cells bearing appropriate receptors and initiate the acute-phase response; whereas chemokines act as chemoattractants, attracting cells such as neutrophils and monocytes (Murphy, 2012a). This inflammation process leads to an increased flow of lymph carrying pathogens and antigen-presenting cells to nearby lymphoid tissue, where they activate lymphocytes and trigger the adaptive immune response. Therefore, this innate response is not only acting as a first-line defense, but also as an inducer for the secondary adaptive immune response (Murphy, 2012a).

The interferon cytokines are essential in coordinating the innate response to herpesvirus infections. The production of type 1 IFN was directly associated with EHV1 infection and the duration of nasal shedding (Gryspeerdt et al., 2010). Type 1 and 3 IFN inhibit virus replication by inducing an antiviral state in cells, whereas type 2 IFN is an important mediator of the adaptive immune response (Fensterl and Sen, 2009).

Other antiviral substances produced by airway epithelial cells include the iron-binding glycoprotein lactoferrin, which is able to block cellular receptors or directly bind to virus particles, thus inhibiting herpesvirus replication (van der Strate et al., 2001). Furthermore, antiviral cysteine-rich cationic peptides ß-defensin 3 has been shown to inhibit HSV infection by preventing binding and entry. In addition, they may act as chemokines and upregulate the innate immune response (Hazrati et al., 2006). Finally, Poelaert et al. (2019c) has demonstrated that physiological concentrations of the short-chain fatty acids (SCFA), sodium butyrate (SB) and sodium propionate (SPr) are able to reduce the plaque size in equine respiratory epithelium *ex vivo*. Moreover, the presence of SCFA led to a significant reduction in the number of EHV1 plaques in endothelial cells, suggesting SCFA play a protective role in the pathogenesis of EHV1 infections.

2.2.2. Complement system

The next major component of the innate immune response is the complement system, which entails multiple pathways. It is composed of at least 30 soluble plasma proteins, that typically circulate in their inactivated state, which is maintained by inhibitors. Lectin pathway, classical pathway and alternative pathway are the three major pathways, which all result in destruction of the pathogen either directly, or by facilitating its phagocytosis, and in the induction of an inflammatory response. All three pathways converge at the central point at which C3 convertase is activated. Pathway complement components are essentially cleaved forming a main effector molecule, a larger serine protease which stays on the pathogen surface, and a peptide that is released that helps induce inflammation. C3b, the larger effector molecule, binds to the pathogen surface and acts as an opsonin, enhancing phagocytosis. C3b can also bind to C3 convertases formed by the classical and lectin pathways, forming C5 convertase. This cleaves C5 which results in anaphylaxis involving pro-inflammatory and chemotactic signals due to C5a, and in initiation of membrane-attack complex (MAC) formation. This ultimately creates a pore in the virus-infected cell membrane that leads to cell lysis (Murphy, 2012a). In this process, C5b associates with C6, C7 and C8, subsequently triggering C9 polymerization finalizing the MAC (see Figure 9 for a schematic overview of MAC formation) (Bayly-Jones et al., 2017).

Elimination of viruses by complement can be achieved by direct neutralization of extracellular virus, lysis of virus-infected cells, induction of an antiviral state, and boosting of virus-specific immune response through recognition of complement in combination with viral antigens by immune cells (Agrawal et al., 2017).

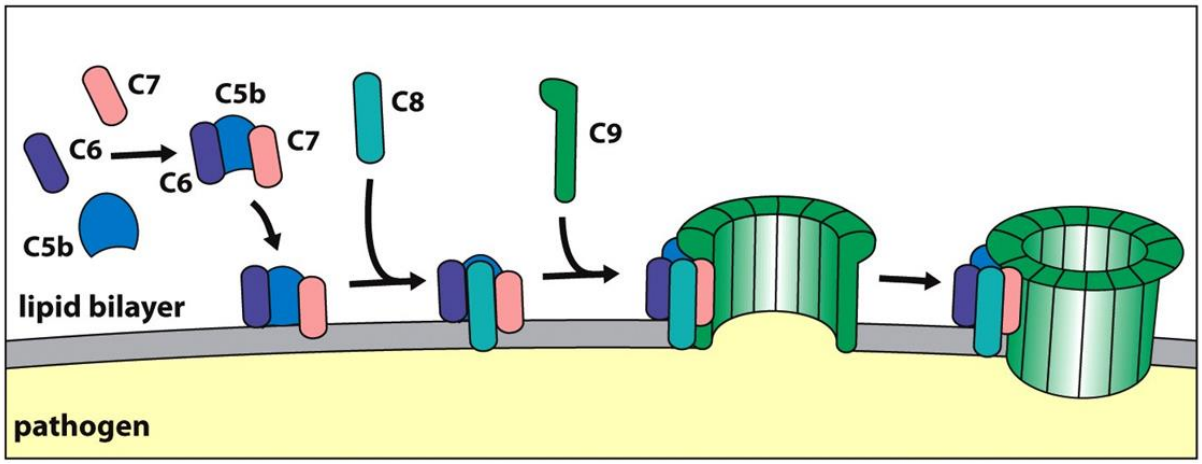

Figure 9. Schematic overview of MAC formation. C5b, C6, C7 and C8 aggregate together, with triggering of C9 polymerization (from: Garland Science, 2009).

The lectin pathway can be triggered by the interaction between carbohydrates on microbial surfaces and four different PRR, namely mannose-binding lectin (MBL) and ficolins (see Figure 10 for a schematic overview of the lectin pathway). MBL is bound to two MBL-associated serine proteases (MASP) in plasma, namely MASP-1 and MASP-2, that cleave C4 producing C4a and C4b. C4b, bound by the antigen, binds C2, allowing it to be cleaved by C1 into C2a and C2b, which results in the formation of C4b2a, the C3 convertase (Murphy, 2012a; [6]Bio-Rad Antibodies, 2015).

[6]Bio-rad Antibodies (2015), viewed on 10 April, https://www.bio-rad-antibodies.com/complement-system-minireview.html.

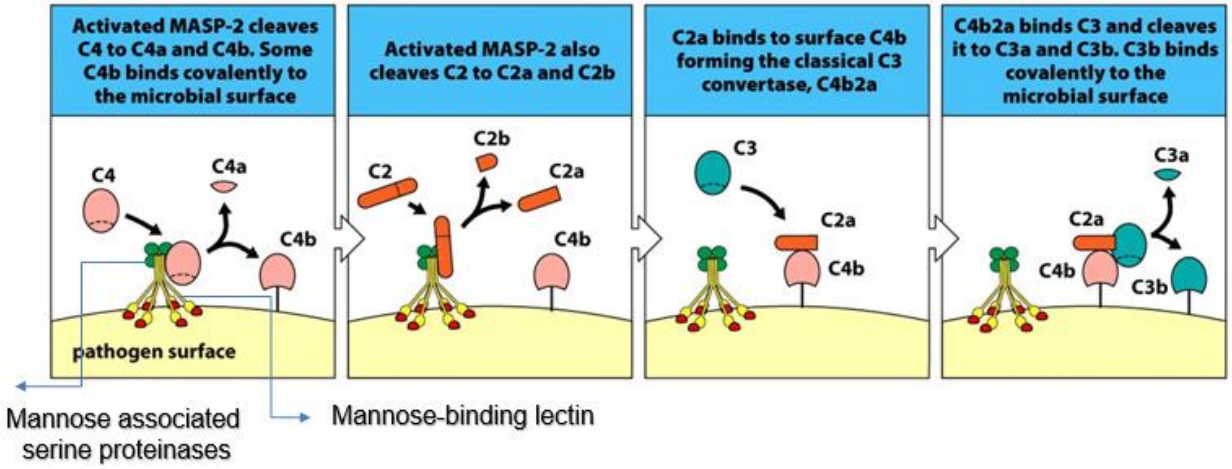

Figure 10. Schematic overview of the lectin pathway, initiated by sugar residues and mannose (adapted from: Garland Science, 2009).

The classical pathway is similar to the lectin pathway (see Figure 11 for a schematic overview of the classical pathway). Initiation occurs when C1 either recognizes a microbial surface directly or binds to the Fc region of an antibody-antigen complex during the adaptive immune response. Following activation, the C1 enzyme cleaves C4, resulting in an outcome homologous to the lectin pathway (Murphy, 2012a; [5]Bio-rad Antibodies, 2015). Da costa et al. (1999) demonstrated that activation of the classical pathway plays a key role in regulating the antibody response to HSV1, as C3-deficient mice had significantly diminished IgG responses.

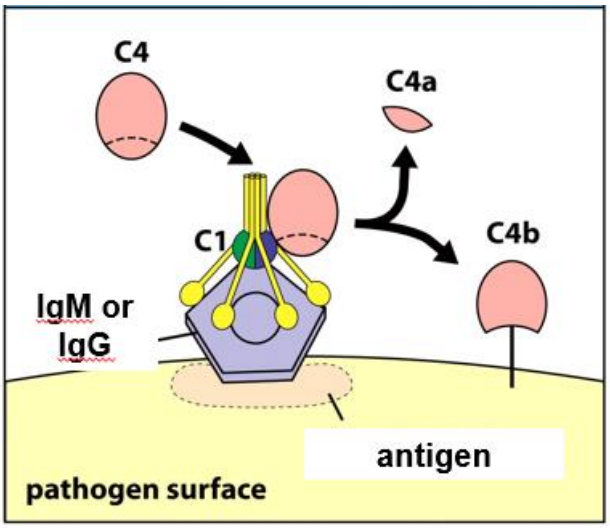

Figure 11: Schematic overview of the classical pathway initiated by an antibody-antigen complex (adapted from: Garland Science, 2009).

Finally, the alternative pathway is initiated by spontaneous hydrolysis and surface activation of the complement component C3, which then binds to factor B (see Figure 12 for a schematic overview of the alternative pathway). This complex subsequently gets cleaved by factor D, which results in the formation of complex C3(H20)Bb. Thereupon, this complex cleaves C3 into C3a and C3b, enabling C3b to directly bind to microbial surfaces (Murphy, 2012a; [5]Bio-Rad Antibodies, 2015).

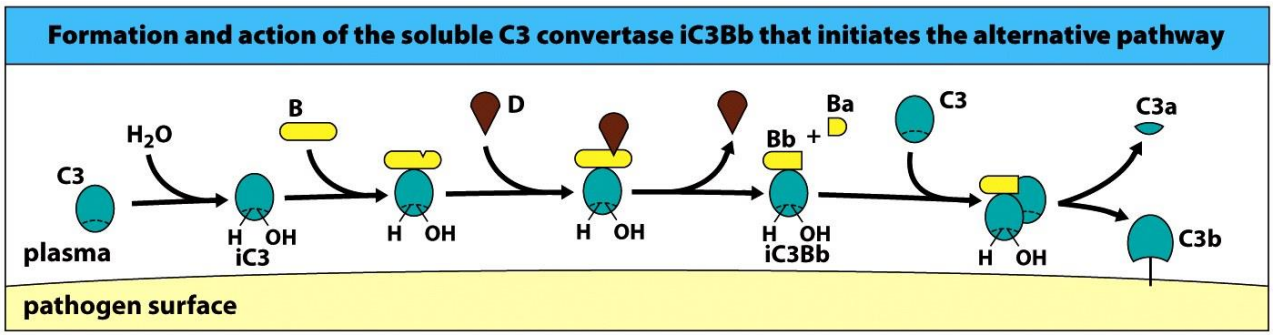

Figure 12. Schematic overview of the alternative pathway, initiated by hydrolysis or pathogen surface activation (from: Garland Science, 2009).

2.2.3. Innate cellular response

Besides pathogen recognizing proteins in the form of secreted molecules, as is the case in the complement system, these can also occur in the form of pattern recognition receptors on macrophages, neutrophils and dendritic cells and signal for a cellular innate immune response (Murphy, 2012a). These cellular receptors include membrane phagocytic receptors, that stimulate ingestion of the pathogen and subsequent internal degradation, but also membrane-bound signaling receptors such as TLRs and cytoplasmic signaling receptors such as RLRs, that stimulate the release of cytokines and chemokines (Murphy, 2012a).

All phagocytic cells internalize pathogens by a process called endocytosis, in which the bound pathogen is surrounded by the phagocyte's plasma membrane and then internalized in an endocytic vesicle referred to as a phagosome. Subsequently, the phagosome becomes acidified and fuses with lysosomes to generate a phagolysosome. Most pathogens are killed either by the acid environment or by hydrolysis by lysosomal contents. Furthermore, pathogens can be internalized through receptor-mediated endocytosis, a process that is not restricted to phagocytes. Macropinocytosis is a non-specific process for uptake of extracellular fluid and its content. Macrophages in the submucosal tissues are generally the first phagocytes to encounter pathogens and play an essential role by internalizing and processing viruses. These are however soon reinforced by neutrophils, which also produce lactoferrins and defensins to combat viral infections (Murphy, 2012a).

The primary function of dendritic cells is not the front-line large scale killing of microbes, and depends on the type of dendritic cell. There are two distinguishable types of dendritic cells. Plasmacytoid dendritic cells (DC), which are major producers of the antiviral type 1 IFN, and conventional dendritic cells (cDC). The latter cells digest virus particles and generate peptides that can activate T cells (Murphy, 2012a). Following activation of cDCs, there is an increase in expression of their chemokine receptor CCR7, which enables them to migrate to lymphoid tissue to present antigen. During this transit, dendritic cells undergo a maturation, that results in upregulation of co-stimulatory molecules and a translocation of major histocompatibility complex class 2 (MHC-2) molecules to the cell surface. Consequently, they will be able to present antigens to naïve T cells and induce their differentiation through appropriate cytokine release (Iwasaki, 2007).

Finally, NK cells are an essential component of the innate immune response against viruses and other intracellular pathogens (see Figure 13 for a schematic overview of NK cells). NK cells possess cytoplasmic granules containing cytotoxic granzymes and the protein perforin. These can be released onto the surface of a virus-infected cell, after which their contents induce the formation of pores in the membrane, resulting in programmed cell death. NK cells are activated in response to interferons or other macrophage-derived cytokines. In addition, NK cells can be stimulated by IL-12 and IL-18 to

secrete type 2 IFN (IFN-y). IFN-y has several functions, including the direct inhibition of viral replication, and the induction of increased expression of MHC-1 molecules on infected cells, therefore increasing the chance for recognition by cytotoxic T cells. Furthermore, it activates macrophages, recruiting them to sites of infection (Murphy, 2012a).

The specificity of NK cells for target cells is determined by a range of stimulatory receptors such as members of the immunoglobulin-like and the C-type lectin families, and inhibitory receptors. The latter receptors prevent the NK cells from destroying normal host cells. Some of these inhibitory receptors specifically bind to various MHC-1 molecules. Therefore, cells bearing high levels of MHC-1 molecules are better protected against destruction by NK cells. Nevertheless, NK cells are able to express several families of MHC-1 receptors, including some that act stimulatory. Activation of NK cells occurs due to a combination of changes in cell surface glycoprotein composition, and changes in the expression of MHC-1 molecules. The behavior of NK cells is ultimately determined by a balance between stimulatory and inhibitory signals (Raulet and Vance, 2006).

Virus-infected cells can be killed by NK cells following virus induced inhibition of all protein synthesis in their host cells, leading to an inhibition of MHC-1 proteins and consequently a decrease in inhibitory signals. Secondly, herpesviruses prevent the export of MHC-1 molecules, or downregulate the expression of MHC-1 molecules on the cell surface, in order to evade recognition by cytotoxic T cells. This potentially makes them more susceptible to NK cells (Murphy, 2012a).

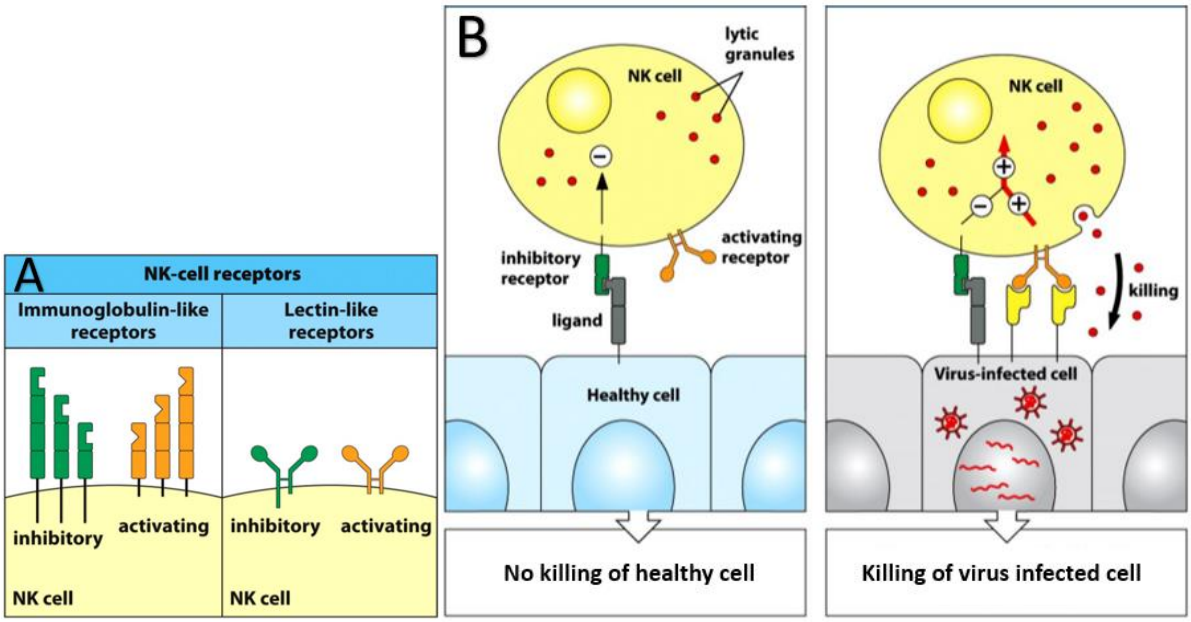

Figure 13. (A) NK cells expressing stimulatory - and inhibitory ligands. (B) The balance between stimulatory - and inhibitory signals determines whether a cell is destroyed (adapted from: Garland Science, 2009).

2.3. Adaptive immunity

2.3.1. Introduction

Adaptive immunity can be subdivided into two responses, namely the humoral response, characterized by antibodies, and a cellular immune response, in which $CD8^+$ CTLs are considered to be an essential defense mechanism against EHV1 infection. Adaptive immune responses are likely to be initiated in local lymphoid organs such as mucosal associated lymphoid tissue (MALT), after induction by the non-specific, innate immune response when the latter has been overwhelmed.

2.3.2. Humoral immune response

B cells are the dominant cell type of the humoral immune response. They recognize specific antigens through their B cell receptor, a membrane-bound immunoglobulin. Before activating B cells, naïve T cells interact with dendritic cells presenting relevant peptides. Consequently, these helper T cells are able to recognize peptide-MHC-2 complex on the B cell surface and secrete cytokines. This stimulates B cell proliferation which subsequently differentiate into plasma cells and memory cells. Not all B cells require activation by helper T cells ($CD4^+$) but can be activated directly by certain microbial antigens. Furthermore, helper T cells secrete cytokines that regulate which antibody isotypes are produced (Murphy, 2012a).

After differentiation into plasma cells, antibodies, also known as immunoglobulins (Ig), of the same antigen specificity are secreted in large quantities. Antibodies are composed of two distinct regions. Namely, a variable region which determines the antigen-binding specificity of the antibody; and the constant region, which will determine how the antibody will interact with various immune cells and therefore its effector function (see Figure 14 for a schematic drawing of an antibody). Furthermore, each antibody is composed of two identical heavy - and light chains, which each have variable and constant regions (Murphy, 2012a).

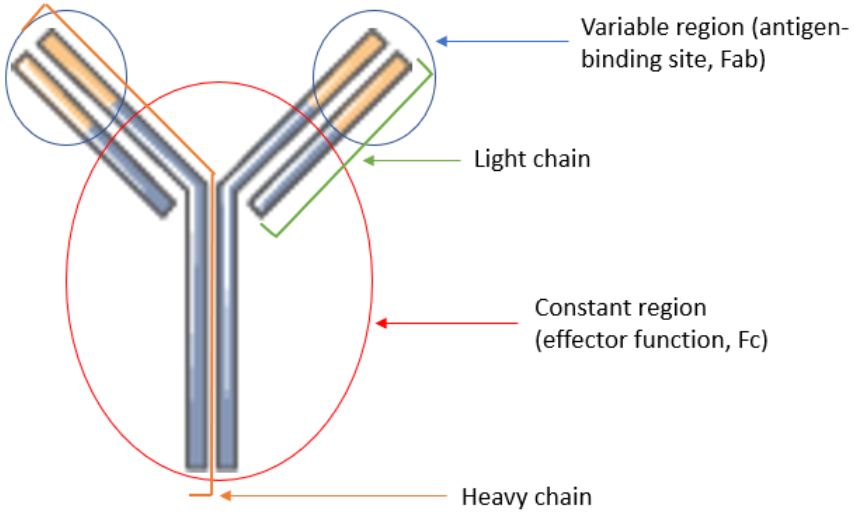

Figure 14. Schematic drawing of an antibody.

Antibodies have three strategies to eliminate pathogens. The strategy mainly used to target intracellular viruses, is through inhibiting their entry into cells by blocking the receptors used to bind to these cells, a process called neutralization (see Figure 15 for a schematic overview the neutralization strategy). The other strategies protect against extracellular pathogens through opsonization and activation of the classical pathway of the complement system. After activation, B cells also promote the T cells' continued activation through signals, for example by B7-family molecules (Murphy, 2012b).

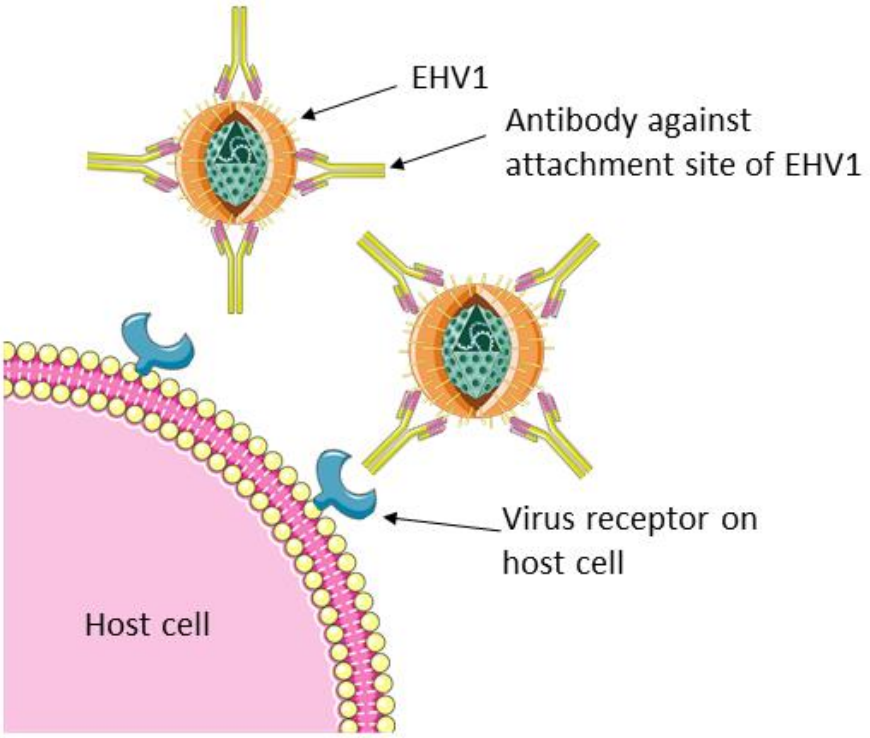

Figure 15. Schematic drawing of the neutralization strategy used by antibodies.

A second phase of the humoral response consists of the formation of germinal centers within primary lymphoid follicles in secondary lymphoid organs (see Figure 16 for a histological image of a secondary lymphoid follicle). The primary response results in the secretion of mainly IgM antibodies, as they can be expressed without class-switching, which provide immediate protection. The germinal center reaction provides for a more effective humoral response in the case that a pathogen establishes a chronic infection. Activated B cells migrate into a primary lymphoid follicle together with their associated T cells, where they organize into germinal centers, forming secondary lymphoid follicles. Herein, B cells proliferate, differentiate and achieve higher affinity for their specific antigen, by means of somatic hypermutation. Furthermore, it is the location where antibodies are able to switch their class, in order to secrete antibodies with the appropriate effector function (Murphy, 2012b). When precursor B cells move into a primary follicle, they push the IgM and IgD producing B cells aside, subsequently creating the mantle zone. The germinal center consists of a dark zone, with proliferating activated B cells called centroblasts, and a light zone, with centrocytes derived from centroblasts following somatic hypermutation, T cells, macrophages and follicular dendritic cells ([7]Virtual Pathology at the University of Leeds).

[7] Virtual Pathology at the University of Leeds, viewed on 26 April 2019, http://www.elearning.virtualpathology.leeds.ac.uk/store/87_Germinal_centre_tutorial/87/pdfs/The%20Germinal%20Centre.pdf

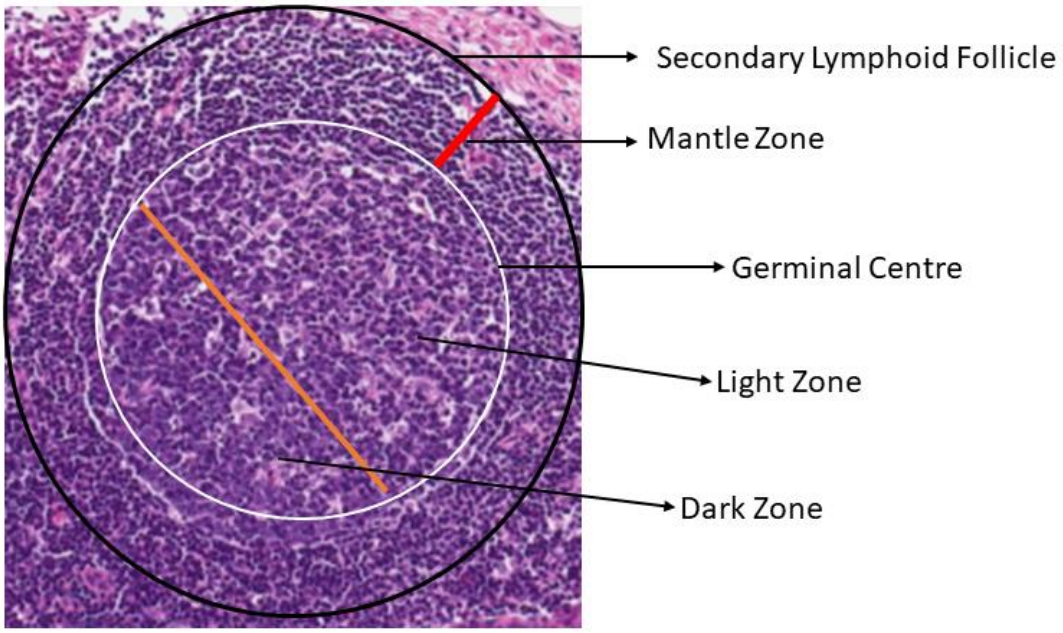

Figure 16. Histological image of a secondary lymphoid follicle (adapted from: [8]Virtual Pathology at the University of Leeds).

Next to IgM, other classes include IgG, which is the principle antibody present in blood and extracellular fluid and efficiently facilitates phagocytosis. IgA is the most important antibody present in the mucosa of the respiratory tract and acts chiefly as a neutralizing antibody. Finally, IgE is mainly produced in the case of parasitic infections and is generally bound by receptors on mast cells. These contain basophil granules, and release histamine during inflammatory and allergic reactions. For the elimination of viruses, IgA and IgG antibodies are particularly important (Murphy, 2012b). Complement fixation antibodies against EHV1 do not last longer than three months, whereas virus neutralizing antibodies can last longer than a year (O'Neill et al*.,* 1999). A study demonstrated that IgA dominated the mucosal antibody response during EHV1 infection in weanlings. Moreover, these antibodies were detectable up to 13 weeks after the first challenge, though persisted at until at least 26 weeks with subsequent infections (Breatnach et al., 2001).

2.3.3. Adaptive cellular response

A cellular response starts with dendritic cells that take up viral antigens in the infected tissues. Following activation, dendritic cells increase their synthesis of MHC-2 molecules and begin expressing co-stimulatory molecules such as B7 molecules on their surface. After migration into lymphoid tissues, dendritic cells present their antigen and MHC-2 complex to naïve T cells (Murphy, 2012b). The full activation of naïve T cells takes four to five days (Murphy, 2012b). In many cases, $CD4^+$ T cell help is required to allow for a dendritic stimulation of a $CD8^+$ T cell (cytotoxic T cell) response, which is called licensing of the antigen-presenting cell. Subsequently, T cells are activated and after several days of clonal expansion, they re-enter the circulation, where they migrate to the site of infection due to changes in vascular walls induced by inflammation. Expression of particular adhesion molecules can direct the lymphocytes to specific sites (Murphy, 2012b).

[8]Virtual Pathology at the University of Leeds, viewed on 26 April 2019, http://www.elearning.virtualpathology.leeds.ac.uk/store/87_Germinal_centre_tutorial/87/pdfs/The%20Germinal%20Centre.pdf

T cells play a key role in antiviral immunity, in which the response can be divided into $CD4^+$ T cells and $CD8^+$ T cells. Airway epithelial cells that are infected with virus produce chemokines that recruit T cells. Naïve $CD4^+$ T cells differentiate into distinct classes of $CD4^+$ effector T cells under the influence of cytokines. Viruses tend to induce T_H1 cell responses, which are generally involved in helping activation of $CD8^+$ T cells (see Figure 17 for a schematic overview of activation of macrophages, NK cells and T cells). Furthermore, T_H1 cells induce the production of subclasses of IgG antibodies, which neutralize virus particles (Murphy, 2012b). Effector $CD8^+$ T cells can, in addition to their cytotoxic function, secrete cytokines typically secreted by T_H1 or T_H2 cells, such as antiviral IFN-γ (Murphy, 2012b).

During priming, naïve T cells only recognize peptide antigens presented by MHC molecules. As a result, all effector T cells only act on other host cells displaying an antigen peptides-MHC-1 complex, and not on the pathogen itself. This explains why CTLs are essential in defense against intracellular pathogens, such as viruses. Moreover, EHV1 specific CTLs remain detectable for more than a year after infection (Allen et al., 1995).

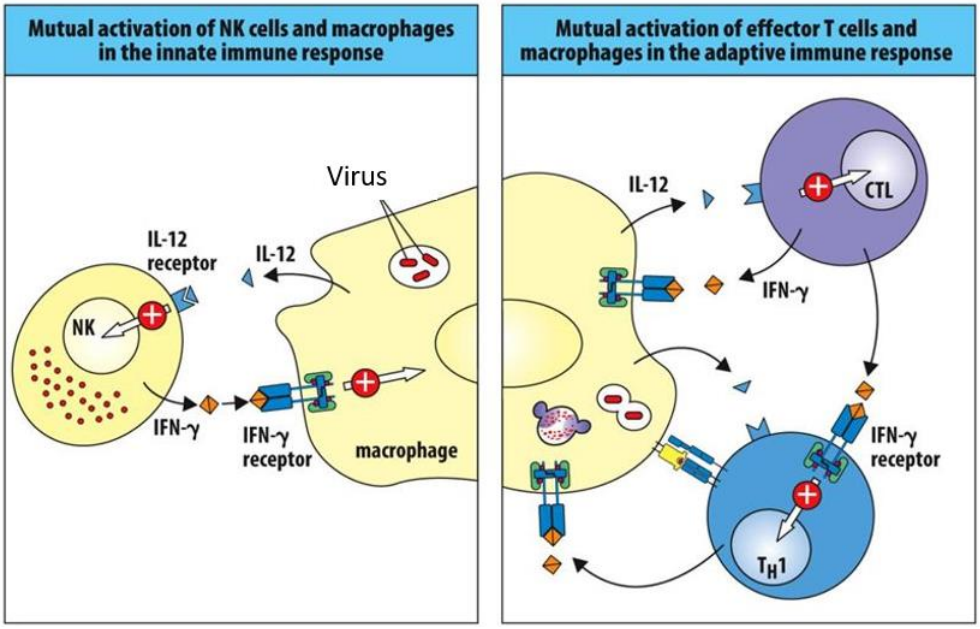

Figure 17. Schematic overview of mutual activation of NK cells and macrophages, and mutual activation of macrophages and T cells (adapted from: Garland Science, 2015).

CTLs kill their target cells by inducing apoptosis, also called programmed cell death; in which the cell degrades itself, inhibiting the virus' escape (Murphy, 2012b). This mechanism is based on the calcium-dependent release of cytotoxic granules, which are modified lysosomes containing cytotoxic proteins, synthesized during the first encounter of a naïve cytotoxic precursor T cell with its specific antigen. Three main cytotoxic proteins include perforin, which target cell membranes; granzymes, which are serine proteases that activate caspases; and finally, granulysin which has an antimicrobial activity. In addition, CTLs also act by releasing cytokines such as antiviral IFN-γ, TNF-α and lymphotoxin-α (LT-α) (Murphy, 2012b).

CTLs will only destroy a cell after recognition of an antigen-peptides-MHC-1 complex. MHC-1 glycoproteins are expressed on the cell surface of all nucleated cells and platelets in jawed vertebrates, where their primary function is to display foreign peptide fragments of proteins from within the cell to CTLs. MHC-1 consists of a heterodimer made up of two polypeptide chains, α and β2-microglobulin. The α-chain of MHC-1 is expressed in the endoplasmic reticulum (ER), where it is stabilized by the ß2-microglobulin (Murphy, 2012b).

When a cell becomes infected with a virus, some of the newly produced viral proteins are degraded into peptides via the cellular proteasome. A fraction of these viral peptides then reach the ER through the transporter associated with antigen processing (TAP), which translocates the peptides under consumption of ATP. Subsequently, particular peptides associate with MHC-1 molecules in the ER after which the MHC-1 undergoes posttranslational modifications. Proteins besides TAP protein involved in their assembly with peptides are tapasin, ERp57 and calreticulin, all together called the peptide loading complex. Ultimately, the MHC-1-peptide complex reaches the cell surface though a secretory pathway (see Figure 18 for a schematic overview of MHC-1 secretory pathway). Finally, this stable antigen-loaded MHC-1 complex is transported to the cell surface, where it may be recognized by CTL (via their T cell receptor), triggering cell lysis. The generation of peptides, transport of the peptides to the ER and loading of the peptides on MHC-1, all may be targets for viral interference with MHC-1 presentation of antigens. Furthermore, transport of MHC-1 from the ER to the cell surface is a possible target for viral interference, which may also consist of direct virus-mediated killing of CTLs (Williams et al., 2002; Hewitt, 2003; Peterson et al., 2003; van der Meulen et al., 2006a).

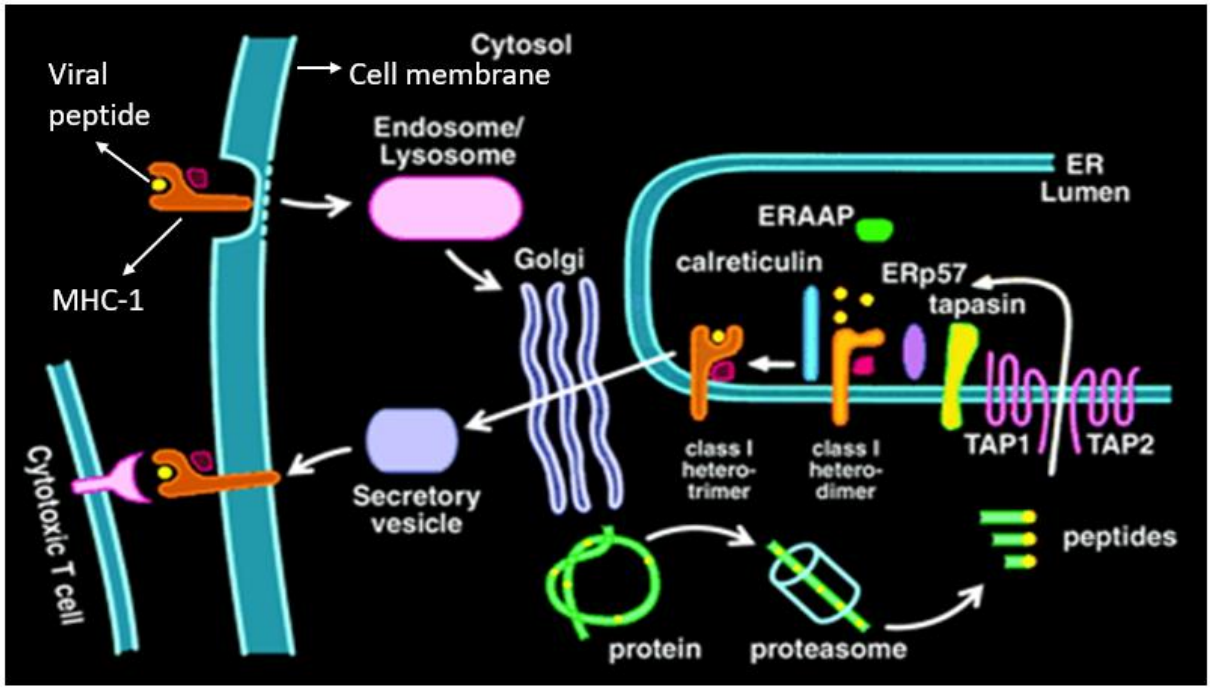

Figure 18. Schematic overview of the MHC-1 secretory pathway (adapted from: Peterson et al., 2003).

In summary, both the innate and adaptive immunity, as well as their interaction, are essential to eliminate viral infections. NK cells and interferon production are specifically important for viral infections, as NK cells are able to destroy cells infected with intracellular pathogens, and interferon directly interferes with virus replication, in addition to acting as a signaling molecule. In the adaptive immunity, antibody response is crucial for extracellular virus particles, whereas CTLs are responsible for the elimination of intracellular virus.

2.4. Immune evasion of herpesviruses

2.4.1. Introduction

There has been a clear evolution between EHV1 and the horse's immunity. Despite the complexity of the immune system, EHV1 has developed various strategies to evade virus elimination, which can result in life-long infections.

The presence of virus specific antibodies and CTL precursors do not prevent viremia in EHV1 infection, suggesting this virus uses immune evasion strategies to persist in its host (Gleeson and Coggins, 1980; O'Neill et al*.,* 1999). EHV1's tropism for immune cells, that are typically important for virus elimination, has been an important evolution in the aspect of immune evasion. Particularly their use of these immune cells as a 'Trojan horse', and subsequent cell-to-cell spread, as well as their ability to establish latency, are marvelous adaptations that allow EHV1 to establish life-long infections. The prevalence of latency is currently not well known, though it is presumed that EHV1 establishes latency in more than 50% of infected horses (Gulati et al., 2015). *Alphaherpesvirinae* establish latency in the trigeminal ganglia, lymphoid tissues and peripheral blood leukocytes (PBL), with $CD8^+$ T cells being a predominant site of infection, by restricting the expression of viral genes (Chesters et al., 1997; Ma et al., 2013).

As discussed previously, there are three major mechanism for virus elimination, thus virus interference can also occur at these three levels, namely antibody dependent lysis, the MHC-1 dependent lysis and the NK cell-mediated lysis. Furthermore, EHV1 is able to influence cytokine secretion. A fluorescent bead-based system was used to measure IFN-γ produced in supernatant EREC, and a reduction was observed (Hussey et al., 2014b). Poelaert et al. (2018) demonstrated the importance of IFN-α as an antiviral defense *in vitro* and *ex vivo*, where replication of both EHV1 strains was suppressed by recombinant equine INF-α. Their results additionally suggest that the abortigenic strain has developed an anti-IFN strategy that may be absent or is less pronounced with neurovirulent strains. *In vitro* studies have also demonstrated that EHV1 is able to bind to certain chemokines with its envelope protein gG, blocking the interaction of chemokines with their cellular receptors (Bryant et al., 2003).

2.4.2. Interference with antibody-dependent lysis

Firstly, EHV1 can avoid recognition by antibodies by not displaying viral antigens on the surface of infected cells. *In vitro* studies revealed that 68.6% of EHV1 infected PBMCs lacked surface expression of viral antigens (van der Meulen et al., 2003b). This research was reinforced by *in vivo* studies, in which not only surface viral envelope antigens were undetectable, but also intracellular viral envelope proteins, suggesting that EHV1 restricts its replication during migration in PBMCs, until they are triggered by activation signals (van der Meulen et al., 2006b). Laval et al. (2015b) compared EHV1 replication in $CD172a^+$ monocytic cells and in rabbit kidney cells (RK-13 cells). Results showed that replication of an abortigenic EHV1 strain was restricted to 4% of $CD172a^+$ cells, compared to 100% in RK-13 cells. This research also demonstrated that virus production was significantly lower in $CD172a^+$ cells than in RK-13 cells. Furthermore, the results showed that the silencing of abortigenic EHV1 gene expression is associated with histone deacetylases. This was determined by treating $CD172a^+$ cells with deacetylase inhibitors trichostatin (TSA) and sodium butyrate (NaBut). EHV1 proteins were expressed earlier in treated CD172a+ cells than in untreated cells. After migrating unrecognized, EHV1 cleverly induces adhesion of $CD172a^+$ cells to endothelial cells, which in turn enhances EHV1 replication (Laval et al., 2015a).

Finally, Poelaert et al. (2019a) also conducted research regarding this immune evasion strategy on T cells. Once more, results demonstrated a restricted expression of abortigenic and neurovirulent EHV1 viral glycoproteins on the T cell's surface, as well as a hampered release of progeny virus. Interestingly, efficient virus replication occurs, with membrane expression of viral glycoproteins. However, these

glycoproteins cluster at the cell membrane, indicating sequestration of the membrane-bound viral proteins, resulting in infected T cells with no visually detectable surface expression of viral proteins. This research suggests that EHV1 uses an alternative immune evasion strategy in T cells compared to monocytes, which is more prominent in the neurovirulent strains than in abortigenic strains. Moreover, this research demonstrates that T cells are able to transmit virus to adjacent cells such as RK-13 cells, monocytes, endothelial cells and respiratory epithelial cells through cell-cell contact (Poelaert et al., 2019a). In conclusion, the restriction of replication allows for longer survival of carrier cells, and allows EHV1 to disseminate throughout the body unnoticed, protected from antibody dependent lysis.

An alternate method used by herpesviruses to avoid antibody-dependent lysis involves the removal of antigen-antibody complexes from the cell surface, either by shedding or internalization. Favoreel et al. (1999), demonstrated *in vitro* that PrV induces endocytosis of antibody-antigen complexes in monocytes, which was confirmed to be an antibody-dependent process. In addition, experiments with deletion virus mutants were conducted, and demonstrated that gB and gD play an essential role in said endocytosis. Another strategy used by PrV entails shedding of antibody-antigen complexes. This was described by Favoreel et al. (1997) in swine kidney cells, in which gE plays a prominent role.

Some members of the herpes-and coronavirus families induce expression of a viral Fc-receptor on the cell surface, mimicking an antibody receptor ordinarily located on the membrane of certain immune cells. This results in sterically hindered access for virus specific antibodies, due to binding of non-immune IgG (Dowler and Veltri, 1984). Furthermore, this viral Fc receptor can bind the Fc receptor of specific virus antibodies, whilst the antigen-specific Fab domain of the antibody is simultaneously bound to the respective viral protein, making the Fc domain of the virus specific antibody no longer available for interaction with C1q of the complement system, or with the Fc receptor of NK cells and phagocytes. This process is called antibody bipolar bridging (Frank and Friedman, 1989). Using virus deletion mutants, it has been shown that gI and gE are responsible for inducing expression of viral Fc receptors at the cell surface in HSV and PrV (Dubin et al., 1990; Favoreel et al., 1997).

Members of the *gammaherpesvirinae* subfamily are able to avoid complement-dependent lysis through mimicry of cellular complement regulators. These show functional and genetic similarities with complement control proteins, thus inhibiting the complement cascade system (Favoreel et al., 2003). EHV1, EHV4, HSV, PrV and BHV1, which are all alphaherpesviruses, induce expression of virus complement-interfering proteins without genetic similarities to cellular complement regulators. These gC orthologues are known to bind C3b of the complement cascade, potentially interfering with further events in the cascade (Huemer et al., 1995; Favoreel, 2003).

2.4.3. Interference with CTL-mediated cell lysis

Interference with MHC-1 expression at the cell surface can result in decreased recognition and destruction by cytotoxic T cells. Various alphaherpesviruses have evolved mechanisms that target the MHC-1 antigen presentation pathway. These include inhibition of peptide translocation by the viral protein US12 in HSV, US6 in HCMV, ORF66 kinase in varicella zoster virus (VZV) and the viral protein UL49.5 in PrV and BHV1 (Früh et al., 1995; Ahn et al., 1997; Koppers-Lalic et al., 2005; Eisfeld et al., 2007). Other strategies used by herpesviruses include the non-specific co-internalization of MHC-1 with the viral glycoproteins in PrV infected monocytes (Favoreel et al., 1999). A non-specific downregulation of MHC-1 is also seen in BHV1, via its UL41 protein, which causes a general down-regulation of mRNA expression (Hinkley et al., 2000; Koppers-Lalic et al., 2001).

In vitro studies on non-target cells have shown that EHV1 induces downregulation of MHC-1 molecules from the cell surface (Rappocciolo et al., 2003; Ma et al., 2012). In addition, Hussey et al. (2014a; 2014b), observed MHC-1 downregulation In EHV1 infected EREC using flow cytometer analysis. Further research has proven that EHV1 virus is able to use more than one mechanism to accomplish downregulation. The first mechanism consists of increased dynamin-mediated endocytosis of MHC-1, induced by the early viral protein pUL56. *In vitro* studies were performed on RK-13 and human HeLa cells (Huang et al., 2014). Hussey et al. (2014b) confirmed this pUL56-dependent downregulation by using pUL56 negative mutants, which were unable to cause MHC-1 downregulation.

Huang et al. (2015) have pointed out a second viral protein that is required for downregulation. *In vitro* studies were performed on non-target cells. The pUL56-encoded protein requires the functional pUL43 protein to induce downregulation of MHC-1 expression in the context of virus infection, indicating that these two viral proteins cooperate during this process.

Besides downregulation of MHC-1 through endocytosis, research demonstrated a second mechanism used by EHV1 to interfere with MHC-1-mediated antigen presentation, which involves blocking the transport of peptides into the ER. An *in vitro* transport assay was used to directly assess the transport activity of TAP (Ambagala et al., 2004). These authors concluded that an EHV1 early protein is responsible for TAP inhibition. It was also mentioned that the inhibition of TAP activity could be due to the inhibition of synthesis of TAP proteins, but this was assumed to be highly unlikely as EHV1 does not show any early shut-off of protein synthesis (Feng et al., 1996). Indeed, Koppers-Lalic et al. (2008) have shown that the viral protein UL49.5 (commonly known as glycoprotein N, gN) is responsible for the inhibition of TAP, which is the same viral protein responsible for inhibition of TAP activity for PrV and BHV1 (Ambagala et al., 2000; Koppers-lalic et al., 2005).

An *in vivo* study presented similar expression of MHC-1 on the surface of PBMCs in EHV1 infected ponies (80-100%) and in non-infected ponies (83-100%). This discrepancy could be explained due to the fact that in this *in vivo* study, the absolute percentage of MHC-1 positive PBMCs was determined rather than the amount of MHC-1 per cell. It was also concluded that most EHV1-infected PBMCs lack viral antigen expression on their cell surface during viremia, which could explain inhibition of CTL-mediated cell lysis (van der Meulen et al., 2003b).

2.4.4. Interference with natural killer cell-mediated lysis

It can be speculated that EHV1 infected cells are more susceptible to NK cell-mediated lysis if down-regulation of MHC-1 occurs. As discussed previously, NK cells act according to a balance of inhibitory- and stimulatory signals. Various alpha-,beta- and gammaherpesviruses have developed strategies to disrupt this balance. For example, EHV1 may be able to avoid detection by causing the down-regulation of some MHC-1 molecules, but not all, suggesting EHV1 affects the expression of MHC-1 molecules in an allele specific manner, as has been demonstrated for PrV (Rappociolo et al., 2003). The glycoprotein gD of PrV and HSV2 causes downregulation of a ligand on the cell surface that is stimulatory for NK cells (Grauwet et al., 2014). In addition, US3 protein kinase of PrV increases the binding of a ligand that acts as an inhibitory signal for NK cell-mediated lysis. An alternative strategy used by HCMV in PBMCs involves the expression of a decoy, namely an MHC-1 inhibitor ligand orthologue, gpUL18. This can bind to inhibitory receptors of NK cells, potentially inhibiting NK-cell-mediated lysis (Cosman et al., 1999). In conclusion, herpesviruses have developed a wide array of strategies, based on suppressing NK cell-activating signals and increasing NK cell inhibitory signals (De Pelsmaeker et al., 2018).

IV Aims of the thesis

Equine herpesvirus type 1 (EHV1) infection causes abortions and neurological symptoms worldwide, with a majority resulting in life-long infections. EHV1's ability to overcome certain recognition by the immune system is related to its immune evasion strategies, which is why the production of a vaccine that is able to prevent viremia has been difficult, resulting in economic and emotional losses. One of these immune evasion strategies potentially impedes CTL from destroying virus infected cells. Understanding EHV1-host cell interaction and its effect on MHC-1 can contribute to the development of vaccines that will elicit an effective cellular immune response.

Downregulation of the peptide presenting molecule MHC-1 has been described by various researchers. These experiments, however, were largely limited to non-target cells, therefore, these are not representative of the actual situation. A small number of experiments was performed on EREC, and downregulation was ascertained by flow cytometry. Despite flow cytometry being an excellent quantitative research tool, visualisation of MHC-1 is not possible. Therefore, we will compare the MHC-1 expression patterns on the EHV1- and mock-inoculated cells by immunofluorescence assays and confocal laser microscopy. Herein, we will use *in vitro* and *in ex vivo* models, allowing us to take into account disadvantages and advantages of both models. The models share the feature of establishing an air-liquid interphase, thus we will closely mimic *in vivo* conditions.

We will fix the explants at different time points, in order to see how MHC-1 expression progresses with infection. Furthermore, in these EHV1-inoculated respiratory mucosa explants, MHC-1 immunofluorescence labeling will be performed in the absence or presence of the chelating agent EGTA, considering that the intercellular connections may prevent viral replication. In EREC, we will make a distinction between surface MHC-1 expression and total (surface and cytoplasmic) MHC-1 expression. In addition, EREC will be inoculated basolaterally, mimicking reactivation of virus after having been in a state of latency. Finally, the neurovirulent and abortigenic strains will be included in both experiments. There seems to be a difference in leukocyte tropism and immune evasion strategies between both strains, thus it is worthwhile to further characterize the cellular immune response against both EHV1 phenotypes.

In addition to a visual analysis, we will do a ROI analysis and subsequently use SPSS to analyze the ROIs in the EREC and explant model, to determine whether there are significant differences in MHC-1 expression between; mock, abortigenic and neurovirulent strains; the different time points post infection; the total and surface MHC-1 molecules in EREC; ethylene glycol-bis(β-aminoethyl ether)-*N*,*N*,*N*',*N*'-tetraacetic acid (EGTA) treated and untreated explants; and finally between the zone of the plaque and the surrounding zone in the EREC and explant model.

In this dissertation, we aim to clarify the effect of EHV1 infection on MHC-1 expression patterns in respiratory epithelial cells. Based on this, it will be possible to research the consequences and mechanisms of downregulation by the virus more accurately.

V Materials and Methods

1. Virus

Two EHV1 strains were included in this study. The abortigenic strain, 97P70, was isolated from lungs of an aborted fetus in 1997, and the neurovirulent strain, 03P37, was isolated in 2003 from the blood of a paralytic horse (Van der Meulen et al., 2000; Poelaert et al., 2018). Virus stocks used for inoculation were at the 6th passage for both strains, of which five were in equine embryonic lung tissues and the ultimate passage in RK-13 cells. A $10^{6.5}$ $TCID_{50}$/ml was maintained in these experiments.

2. Donor horses

In total, six tracheas were taken from healthy horses at the slaughterhouse. Three tracheas were used for the cultivation of EREC, and three were used for the production of explants. These were placed for transport to the lab into plastic bags on ice, in a transport medium consisting of Dulbecco's Phosphate-Buffered Saline with calcium and magnesium (DPBS, Gibco, Paisley, UK), supplemented with 1% gentamycin (Gibco), 1% kanamycin (Sigma-Aldrich, St. Louis, MO), 1% penicillin-streptomycin (Gibco), which are antibiotics to prevent bacterial contamination, and 0.1% amphotericin B (Bristol-Myers Squibb, New York, United States), which is an antifungal agent.

3.In vitro cell culture model (EREC)

3.1. Isolation and cultivation of equine respiratory epithelial cells (EREC)

3.1.1. Tissue dissociation

Isolation and cultivation of EREC was performed as described by Quintana et al. (2011). Tracheas were rinsed with transport medium, and fat and connective tissues were removed with a scalpel. The proximal part of the trachea was cut longitudinally and divided into parts of 2 tracheal rings, which were placed in a beaker containing DPBS (Gibco) and stirred gently to remove blood clots. Subsequently, the tracheal rings were placed into conical tubes containing DPBS for a second wash, and transferred into other conical tubes containing DPBS for 1 hour at 4°C. Finally, the tissues were treated with DNase/pronase solution for 48 hours for tissue dissociation, whilst turning the tubes every 24 hours. The enzyme solution included DPBS with 0.1% Dnase I (Sigma-Aldrich) and 1.4% pronase (Sigma-Aldrich), supplemented with 0.45% D(+)-Glucose (Merck & Co, New Jersey, United States), 1% sodium pyruvate (100 mM, Gibco), 1% penicillin-streptomycin (Gibco) and 0.1% amphotericin B (Bristol-Myers Squibb). This was filtered using a 500 ml bottle top filter (VWR Chemicals, Leicester, UK; poresize 0.2 µm) for sterility (see Figure 19).

Figure 19. Tracheal rings removed after tissue dissociation

3.1.2. Cell count

After enzymatic digestion, tissues were transferred to conical tubes containing 50% Dulbecco's Modified Eagle Medium (DMEM, Gibco) and 50% F12 (Gibco) and shaken softly. Following removal of the tissues, 10% fetal calf serum (FCS, heat inactivated, Gibco) was added to the conical tubes to stop enzymatic digestion, as FCS contains protease inhibitors. The purpose of heat treatment is to inactivate any components of the complement system, which are able to destroy mammal cells. Heat inactivation occurs through incubation for half an hour at 56°C. The conical tubes were then centrifuged for 10 minutes at 1200 rpm and 4°C (see Figure 20). Supernatant was discarded and the cell pellet was resuspended in complete medium containing 50% DMEM (Gibco) and 50% F12 (Gibco), supplemented with 1% MEM non-essential amino-acids (Minimal Essential Media, Gibco), 1% penicillin-streptomycin (Gibco), 0.12% insulin (Sigma-Aldrich) and 0.1% amphotericin B (Bristol-Myers Squibb). Fibroblasts were separated from epithelial cells by transferring the cells to an uncoated P100 plate (ThermoFisher Scientific, Geel, Belgium) which was placed into the incubator for 2 hours at 37°C and 5% CO_2. This separation occurs due to the high affinity of fibroblasts for plastic surfaces.

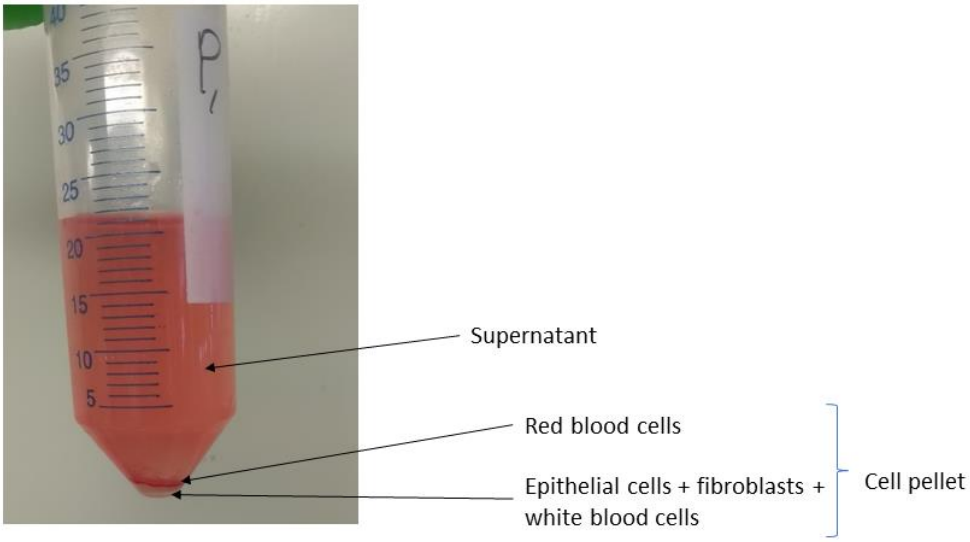

Figure 20. Cell pellet after centrifugation of cell suspension

Following incubation, the P100 wells (ThermoFisher Scientific) were rinsed and the cells were collected in conical tubes, which were centrifuged for 10 minutes at 1200 revolutions per minute (rpm, 300 g) and 4°C. The cell pellet was then resuspended in Afi 1 medium and subsequently counted using a Bürker Turk counting chamber at a dilution of 1:100 in Türk's solution (see Figure 21). Türk's solution is a hematological stain in acetic acid and distilled water. It is used because it stains nuclei and simultaneously causes lysis of red blood cells. Therefore, only white blood cells, epithelial cells and the remainder of fibroblasts will be visible for counting.

Afi 1 medium contains 50% DMEM (Gibco) and 50% F12 (Gibco), supplemented with 1% MEM non-essential amino-acids (Gibco), 1% penicillin-streptomycin (Gibco), 0.5% amphotericin B (Bristol-Myers Squibb) and 5% FCS (Gibco), which contains growth factors and calcium and magnesium ions. These will be important for respectively cell growth and attachment to the plates. The FCS is heat inactivated to maintain the fibrin for a superior attachment of cells.

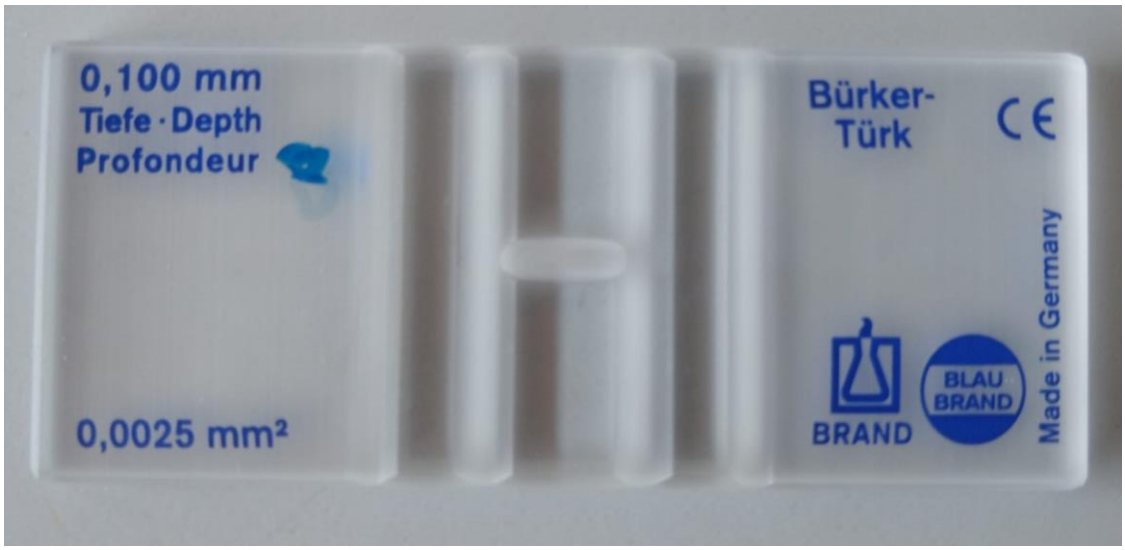

Figure 21. Bürker Turk counting chamber

3.1.3. Cell storage

Cells were frozen and stored in liquid nitrogen at -152°C for further use. This low temperature slows down the cell's metabolism, making preservation of intact, living cells possible. For this, cell suspension was transferred to a 15 ml tube and complete medium was added before centrifuging it for 10 minutes at 1200 rpm and 4°C. The cells were then resuspended in serum-free Bronchial Epithelial Cell Growth Medium (BEGM) which contains 69% DMEM (Gibco), 30% FCS (Gibco) and 1% penicillin-streptomycin (Gibco), and subsequently, dimethylsulfoxide (DMSO) solution which contains 49% DMEM (Gibco), 20% DMSO (Sigma), 30% FCS (Gibco) and 1% penicillin-streptomycin (Gibco) was added to the cryo-vials, after which the vials were rapidly placed in a freezing machine for 50 minutes, and ultimately stored in a nitrogen tank (see Figure 22). 50% of each solution was used. DMSO is an intracellular cryoprotectant, which penetrates inside the cells, preventing ice crystal formation and membrane rupture. This was done rapidly due to DMSO's cellular toxicity at room temperature (Lara et al., 2012).

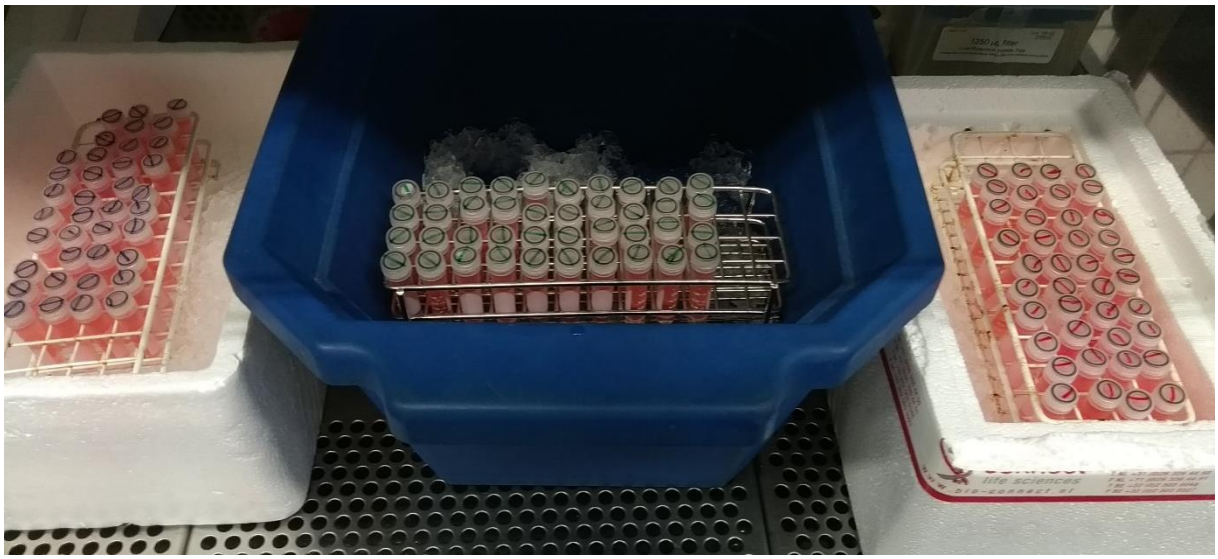

Figure 22. Vials containing EREC for storage in nitrogen tank

3.1.4. Cell plating

12-well transwells (Costar, Corning, Fisher Scientific, Fair Lawn, NJ) were coated with collagen type IV of human placenta (Sigma-Aldrich) 3-5 days before cell plating and wrapped in parafilm at room temperature to avoid contamination. Collagen type IV is used because it is a major component of basement membranes, it forms a network by interacting with cells, growth factors and other basement membrane components (Sand et al., 2016). These transwells were then washed and allowed to dry. Enough aliquots were retrieved to seed $2x10^6$ cells per well. They were thawed in a warm water bath after which the cell suspensions were transferred into one 50 ml conical tube to which DMEM/F12 (Gibco) was added. Subsequently, the cells were centrifuged for 10 minutes at 1200 rpm at 4°C and supernatant containing the toxic DMSO was discarded. The cells were resuspended in Afi 1.

Afi 1 medium was added to the lower compartment and the cell suspension was added to the upper compartment of the transwells. This was then incubated at 37°C and 5% CO_2. The following day, the inserts were gently rinsed with a DMEM/F12 solution (Gibco), after which Afi 2 was added into the lower compartment, and the upper compartment was kept empty. Afi 2 consists of 50% DMEM and 50% F12, supplemented with 1% penicillin-streptomycin (Gibco), 0.5% amphotericin B (Bristol-Myers Squibb) and 2% Ultroser G (Pall Life Sciences, Pall Corp., Cergy, France), which is a synthetic serum substitute, thus decreasing the risk of toxicity, infectious agents and interfering components. The medium from both compartments of the transwells was removed multiple times a day to maintain the air-liquid interphase, and Afi 2 was added to the lower compartment until a monolayer was formed (see Figure 23). Subsequently, the medium was changed every two to three days, so that the cells could acclimate to the cell culture conditions.

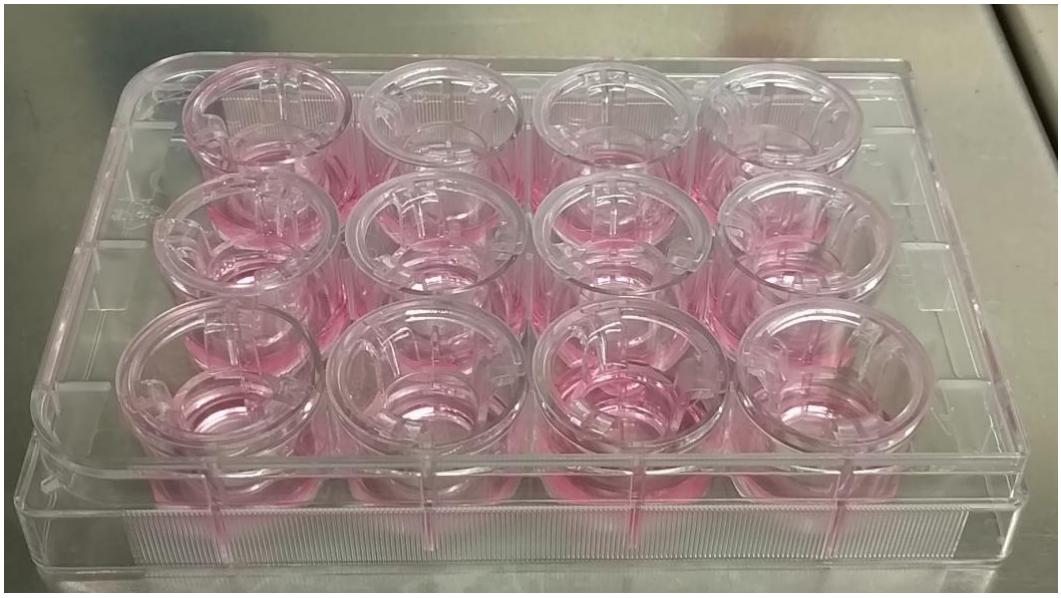

Figure 23. 12-well transwell

EREC is an *in vitro* model, in which the air-liquid interface is essential to mimic the *in vivo* situation. Respiratory epithelial cells form a monolayer on a porous polyester membrane, which allows for the situation in which medium is only located on the basal side of the cells. Ultimately, this will result in a polarization of the cells, with the formation of cilia at the apical side of the cells (see Figure 24 for a schematic overview of both culture models used in this thesis).

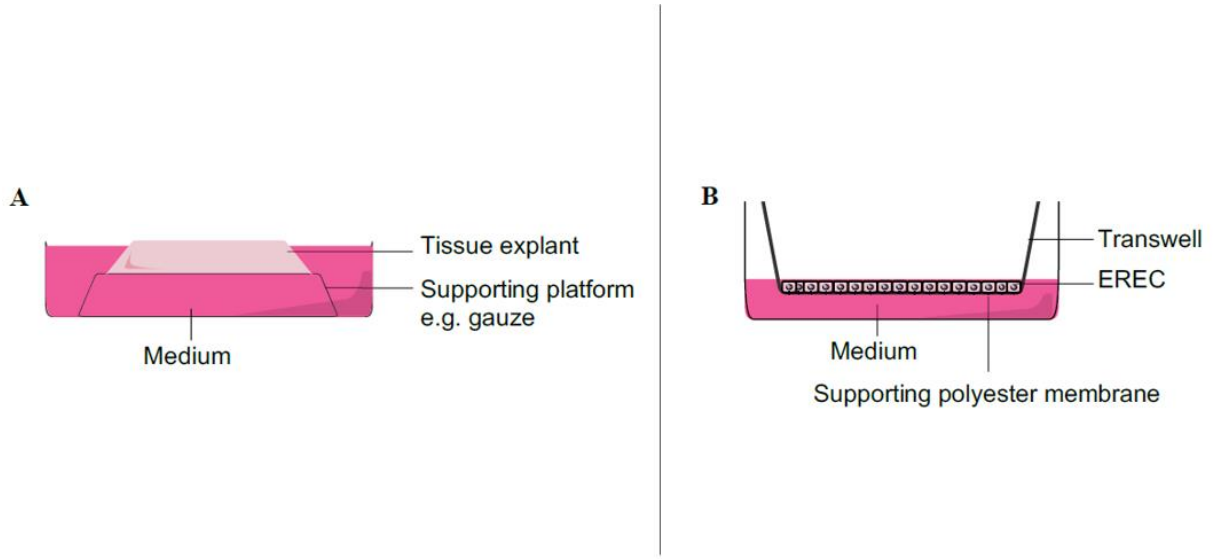

Figure 24. Schematic view of (A) explant model (B) EREC model (from: Poelaert, 2019b).

3.1.5. Transepithelial electrical resistance test (TEER test)

To measure the integrity of tight junctions in the EREC cultures, as a control for the respiratory epithelial monolayer, the transepithelial electrical resistance (TEER) was measured with a voltmeter (Millipore corporation, Bedford, MA, USA) (see Figure 25). For this, DMEM/F12 (Gibco) was added to the cells in the top and bottom compartment, and the electrode was sterilized in ethanol, and cleaned in DPBS (Gibco) and DMEM/12 in between transwells. The machine was set on 2000 Ω. TEER reflects the ionic conductance between the cells in the epithelial monolayer (Srinivasan et al., 2015). The higher the TEER, the better the connection is between the epithelial cells.

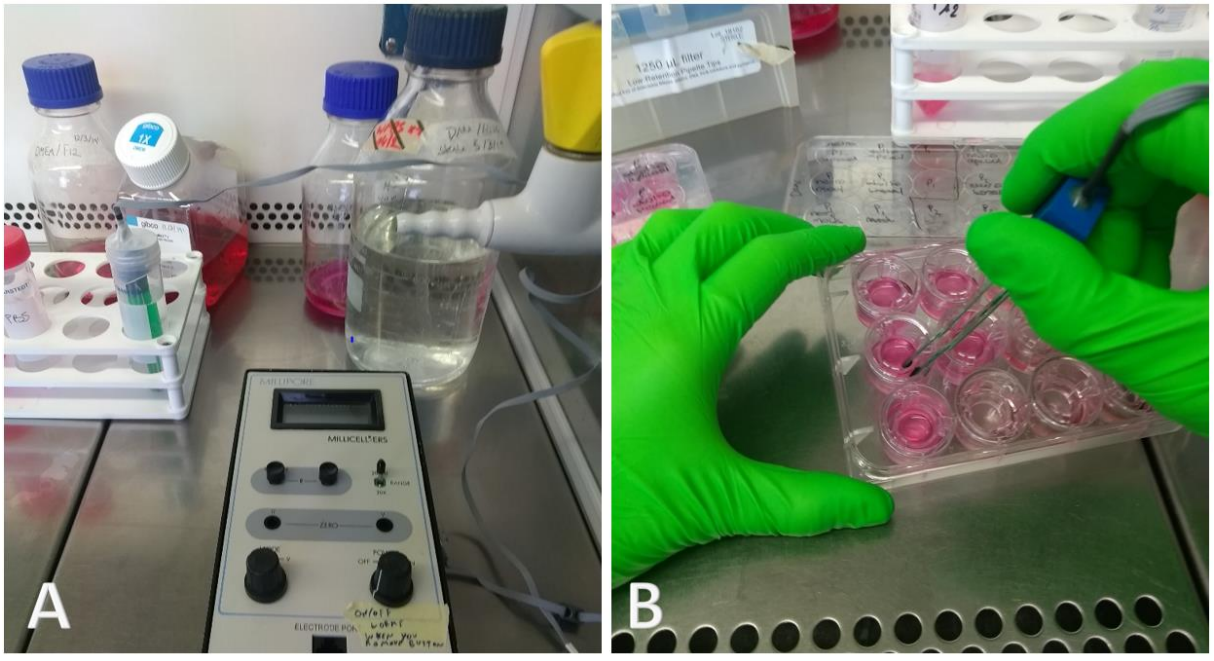

Figure 25. (A) Voltmeter (B) TEER test

3.2. Virus inoculation of EREC and fixation

Once a monolayer was formed, EREC were inoculated basolaterally, by starting with a wash step of the upper compartment and removing medium from both compartments. Medium was not replaced the night before inoculation, to allow for acclimatization of the cells in order for them to differentiate and polarize. The inserts were placed upside down in a large, sterile petri dish, under a laminar flow, after which the inoculum with a multiplicity of infection (MOI) of 0.1 was brought onto the inserts after a short vortex period (see Figure 26). The MOI is the ratio of the number of virus particles to the number of target cells present in a defined space. Subsequently, cells were incubated at 37°C and 5% CO_2, for 30 minutes. After incubation, the inoculum was removed and the inserts were brought back into their original transwells. Two wells were inoculated for each strain, and two mocks were included that were treated similarly. Afi 2 was added to the lower compartment after which the transwells were placed into the incubator for 5 minutes at 37°C and 5% CO_2, this was repeated two more times to wash away free viral particles. Finally, Afi 2 was added to the lower compartment and EREC were incubated at 37°C and 5% CO_2 until fixation of the cells.

The cells were fixed at 18 hpi by adding 1% paraformaldehyde (BDH chemicals VWR, Radnor, Pennsylvania, USA) to the lower compartments of the transwells, for 10 minutes, at 4°C. Formaldehyde is an aldehyde-based fixative, these aldehydes cross-link cellular proteins, stabilizing the sample. Alternative fixatives are organic solvents such as ethanol (70%) and methanol (100%), that dehydrate cells instantly and act by precipitating proteins. Aldehyde fixation results in relatively minimal changes to the cell structure, compared to organic solvents. A disadvantage using aldehydes entails the formation of adducts, these covalent modifications could prevent antibodies from binding to intracellular antigens. Furthermore, organic solvents do not require subsequent permeabilization, in contrast to aldehyde fixatives, as they remove lipids from the cell surface (Hobro and Smith, 2017).

Both compartments of the transwells were washed with DPBS supplemented with calcium and magnesium (Gibco), after which the DPBS was left in the upper compartment of the transwell for storage in 4°C until staining.

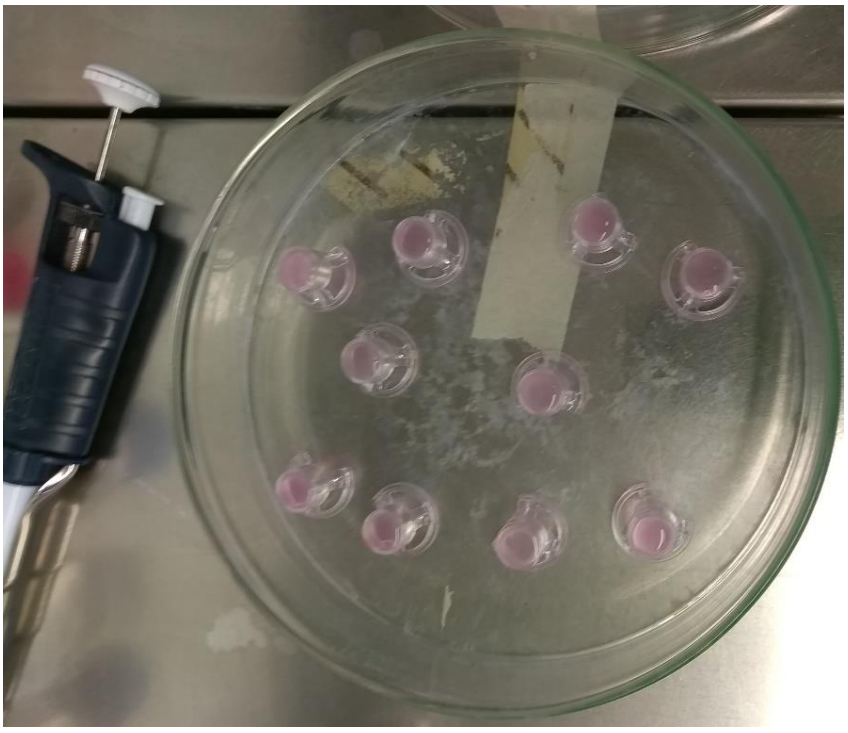

Figure 26. Inserts placed upside down in a petri-dish with inoculum on the basolateral side of EREC.

3.3. Indirect double immunofluorescence staining of EREC

A distinction was made between MHC-1 expressed at the surface of the cells and total (surface and cytoplasmic) MHC-1 molecules by permeabilizing the cells at two different time points (see Figure 27). Some transwells were labeled with monoclonal antibodies made in mice against bovine MHC-1 (1:100 in PBS, Kingfisher Biotech, Saint Paul, Minnesota), prior to permeabilization, which were incubated for 1 hour at 37°C. Other transwells were labeled with this primary antibody after permeabilization with Triton X-100 (0.1%, Sigma-Aldrich), to label intracellular MHC-1. Following permeabilization, immediate early proteins (IEP) were labeled with rabbit polyclonal antibody anti-IEP (1:1000 in PBS, kindly provided by Shreveport, LA, USA), and cells were incubated for 1 hour at 37°C. Negative goat serum (Invitrogen, ThermoFisher Scientific, Waltham, Massachusetts, USA) was used at a concentration of 1:10 in PBS (Gibco), which is necessary to prevent non-specific antibody binding. This serum carries antibodies that bind to reactive sites of the secondary antibody, so it must originate from the same source species as the secondary antibody.

Subsequent to a wash to remove unbound antibodies, secondary goat anti-mouse IgG Fluorescein Isothiocyanate (FITC, 1:100 in PBS, Molecular Probes, Eugene, OR) and goat anti-rabbit IgG Texas Red (TR, 1:100 in PBS, Invitrogen) were added and cells were incubated for 50 minutes at 37°C. Finally, Hoechst 33342 (1:50 in PBS with a final dilution of 1:100, Invitrogen) was added and cells were incubated for 10 minutes at 37°C. Mock inoculated EREC staining was carried out in parallel. EREC were washed with PBS (Gibco) supplemented with calcium and magnesium, and submerged in ultra-purified water (Gibco), after which the transwell membrane from the culture inserts could be excised and mounted on glass slides using glycerol (VWR Chemicals)-DABCO (1,4-diazabicyclo(2,2,2)octane 9.7%, Acros Organics, ThermoFisher) which were covered with a coverslip. DABCO is an anti-fading agent that prevents rapid photobleaching of fluorochromes attached to secondary antibodies. It is presumed that fading occurs due to interactions of the excited fluorochrome with oxygen radicals, or other excited fluorochromes. DABCO is able to react with oxygen radicals, making them no longer available to fluorochromes ([9]Favoreel, 2018).

Two positive controls for abortigenic (97P70) and neurovirulent (03P37) strains, were also carried out in parallel, on RK-13 cells. Furthermore, two isotype controls which were stained with and without permeabilization were included in this experiment on EREC. For these isotype controls, the supernatant of an anti-porcine circovirus type 2 hybridoma isotype IgG2B was used (12E12, Ugent).

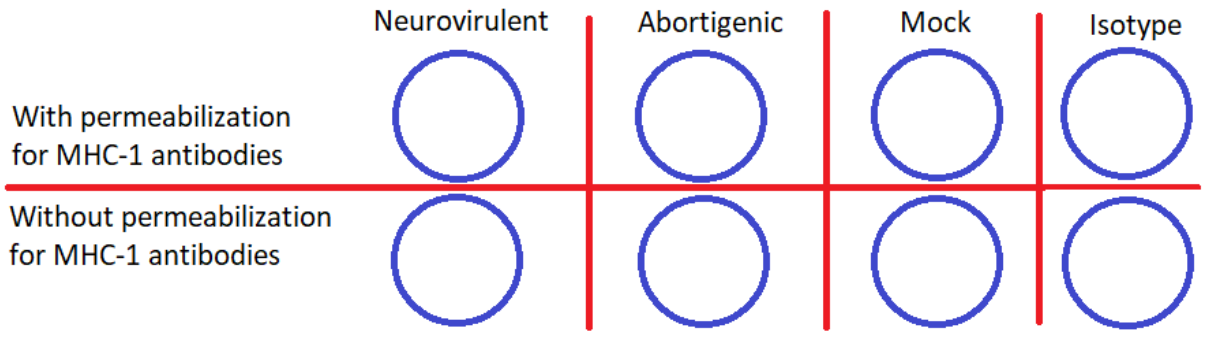

Figure 27. Schematic overview of inoculated EREC from one horse.

[9] Favoreel, H., Celbiologische en Moleculaire Technieken voor Biomedich Onderzoek, Ugent, p 63

4. Ex vivo explant model

4.1. Isolation and cultivation of respiratory mucosa explants

Isolation and cultivation were performed as previously described by Vandekerckhove et al. (2009). Briefly, tracheas were rinsed with transport medium, and the proximal mucosa was stripped from the cartilage and divided into equal parts of 0.5 cm^2 (see Figure 28B). These explants were then placed epithelium upwards on fine-meshed gauzes in 6-well plates, with only a thin film of medium covering the explants, thus mimicking *in vivo* respiratory tract conditions (see Figure 28A). Serum-free medium was used because the use of FCS results in enlarged epithelial cells, loss of cell-cell contacts and loosened epithelium (Glorieux et al., 2007). This culture medium consisted of 50% Roswell Park Memorial Institute (RPMI 1640, Gibco) medium and 50% DMEM (Gibco), supplemented with 1% gentamycin (Gibco), 1% penicillin-streptomycin (Gibco) and 0.1% amphotericin B (Bristol-Myers Squibb). Subsequently, the explants were cultured at air-liquid interface at 37°C and 5% carbon dioxide (CO_2) until inoculation the next day. To evaluate the effect of further manipulations on MHC-1 expression, two explants from two tracheas were fixed in methylcellulose (Methocel MC, Sigma-Aldrich) immediately after isolation.

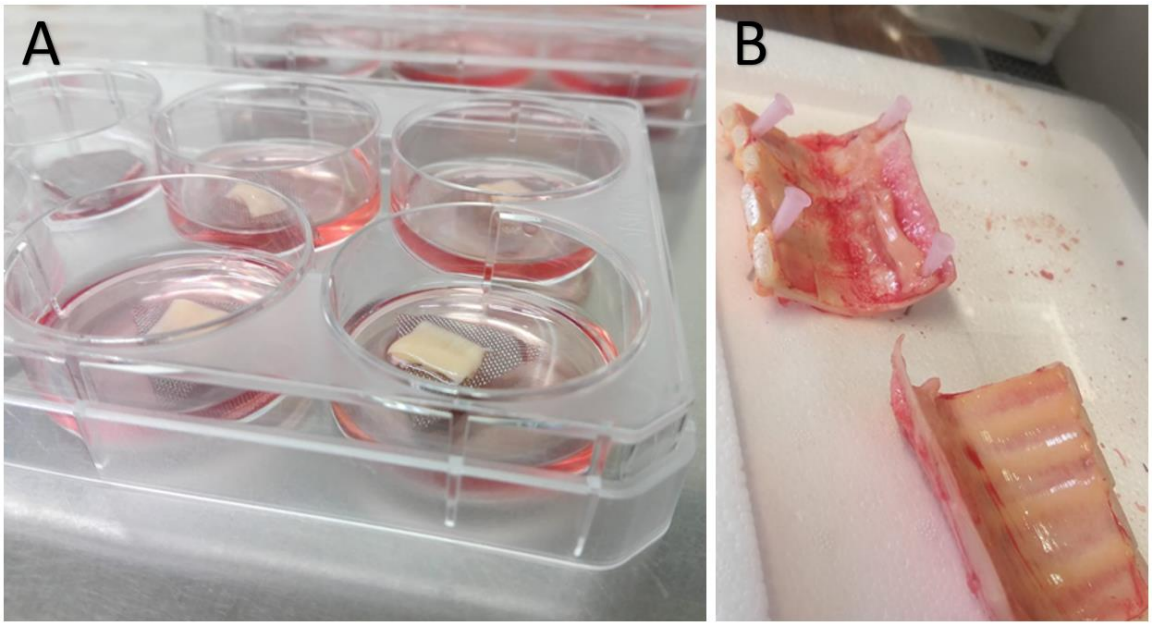

Figure 28. (A) Explants on fine-meshed gauzes in 6-well plates. (B) Proximal trachea cut longitudinally.

4.2. Virus inoculation and fixation of explants

For each inoculated virus strain, explants were fixed at three time points, namely, 12, 24 and 48 hpi. In addition, half of the explants were pre-treated with 8 mM EGTA (Sigma-Aldrich), a chelating agent that causes disruption of intercellular junctions by binding calcium ions in particular, to ensure viral infection (Van Cleemput et al., 2017). The other half was treated with DPBS (Gibco). EGTA solution was prepared by dissolving EGTA in DPBS and sodium hydroxide 10N (Merck KGaA, Darmstadt), followed by the addition of hydrochloric acid (HCL, BHD chemicals VWR) until a pH of 7.4 was achieved. This was subsequently filtered using Filtropur S (pore size: 0.2 µM, Sarstedt, Nümbrecht, Germany). Mock inoculated explants were included in this study as a negative control and were treated in the same manner as virus infected explants (see Figure 29). Medium was always placed in a water bath at 37°C throughout this experiment to avoid adverse effects on the viability of cells.

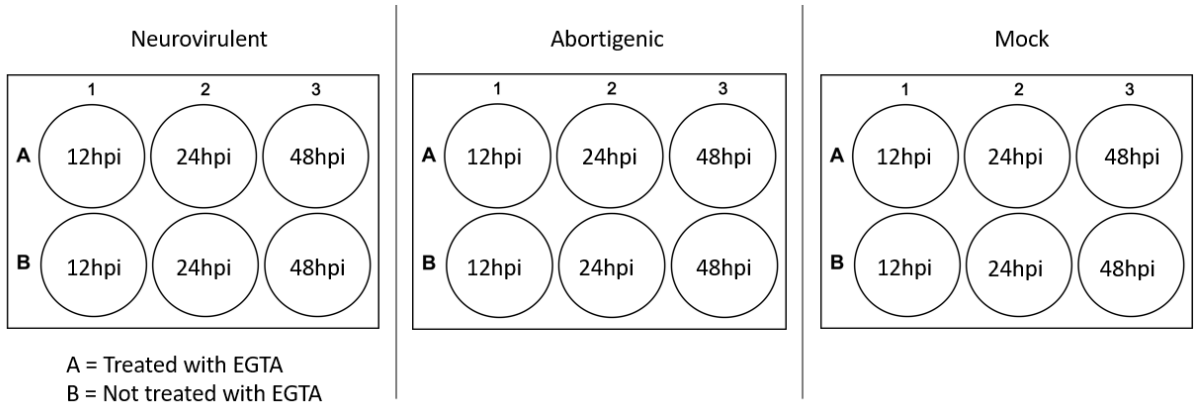

Figure 29. Schematic overview of inoculated explants

Explants were transferred into a 24-well plate and rinsed (10 times) with DPBS (Gibco) supplemented with calcium and magnesium, to remove mucus. This makes the epithelial cells more accessible to virus. These were then transferred to a second well for an additional rinse (5 times), after which they were transferred back to the original 6-well plates. EGTA (Sigma-Aldrich) was added and DPBS was used as a control, before incubation for 1 hour at 37°C and 5% CO_2. Hereafter, explants were transferred into a 24-well plate for washing with DPBS supplemented with calcium and magnesium (3 times for 5 minutes). Virus inoculum ($10^{6.5}$ $TCID_{50}$/ml) of both strains, prepared with culture medium, was added to the explants which were subsequently incubated for 1 hour at 37°C and 5% CO_2. Following incubation, the explants were transferred into another 24-well plate and washed with DPBS supplemented with calcium and magnesium (2 times for 5 minutes), to remove excess of virus that did not infect any cells. Ultimately, explants were transferred back into 6-well plates with culture medium and placed inside the incubator at 37°C and 5% CO_2 for 12, 24 and 48 hours, until fixation.

Supernatant of all explants was removed and stored in eppendorf tubes at -70°C for virus titration. Explants were placed vertically into tubes with methylcellulose (Methocel MC, Sigma-Aldrich), which were subsequently placed into a box with dry ice (solid form of CO_2) and ethanol (Disolol, laboscientific, Ede, Netherlands) for 10 minutes, after which they were stored at -70°C (see Figure 30). The objective is to freeze the tissues rapidly so that water does not have time to form crystals. Consequently, water enters a phase called 'vitreous ice'. An alternative fixation method is the use of paraffin, though freeze-drying with methylcellulose gives superior and finer explant cuts ([10]Favoreel, 2018).

[10] Favoreel, H., Celbiologische en Moleculaire Technieken voor Biomedich Onderzoek, Ugent, p 41, 2018.

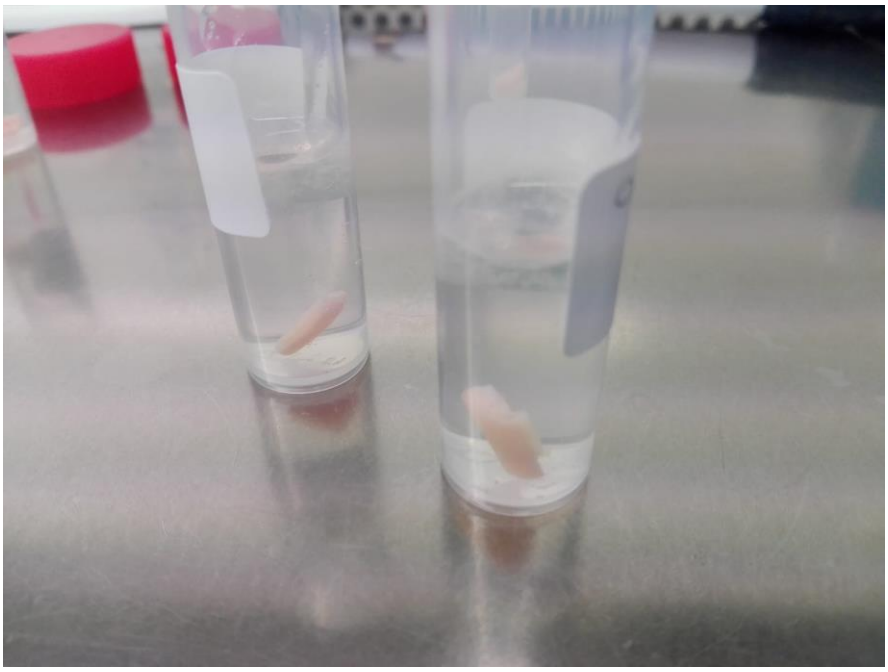

Figure 30. Explants in methylcellulose

4.3. Cryosections and fixation of explants

Explants were trimmed at 50 µm and cryosections were cut at a thickness of 16 µm (see Figure 31). Between the cuts, the explants were trimmed, in order to reach different sections of the explants. Cryosections from explants that had not been treated with EGTA (Sigma-Aldrich) were placed alternatingly onto different slides, allowing for detection of virus replication with single labeling prior to doing a double labeling for MHC-1 molecules. Slides were coated with 3-aminopropyltriethoxysilane (Sigma-Aldrich). After having dried, the explants were immersed in 4% paraformaldehyde (BDH chemicals VWR) for 15 minutes at 4°C. Finally, the explants were washed 3 times in PBS (for 5 minutes, at room temperature) and stored at 4°C.

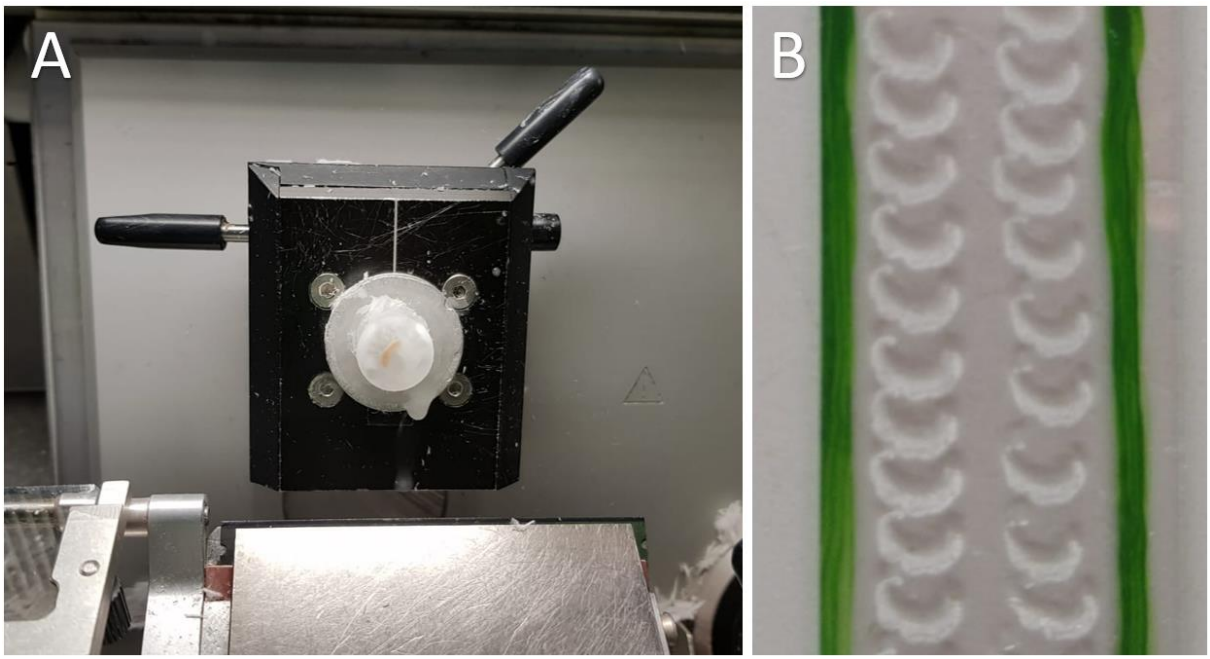

Figure 31. (A) Cryotome (B) Cryosections of mucosa explants with thickness of 16 µm

4.4. Indirect double immunofluorescence staining of explants

The fixed cryosections were permeabilized by immersion in Triton X-100 (0.1%, Sigma) for 10 minutes. This detergent removes lipids and cholesterol from the cell membrane (Hobro and Smith, 2017). Late viral proteins were stained with biotinylated equine polyclonal anti-EHV1 IgG antibody (1:20 in PBS, van der Meulen et al., 2003a), followed by streptavidin TR (1:100 in PBS, Invitrogen). Negative goat serum (Invitrogen) was used at a concentration of 1:10 in PBS.

MHC-1 molecules were stained with monoclonal antibodies made in mice against bovine MHC-1 (1:100 in PBS, Kingfisher Biotech), and subsequently with goat anti-mouse IgG FITC (1:100 in PBS, Molecular Probes) (see Figure 32). Primary antibody incubation time was 1 hour and incubation time for secondary antibodies was 50 minutes at 37°C in a humidified chamber. Ultimately, nuclei were stained with Hoechst 33342 (with a final dilution of 1:100 in PBS, Invitrogen) for 10 minutes at 37°C by adding it to the secondary antibodies. Following staining, explants were washed twice in DPBS for 5 minutes at room temperature. Subsequently, these were submerged in ultra-purified water (Gibco) before adding glycerol (VWR Chemicals)-DABCO (Acros Organics) and covering the slides with a coverslip.

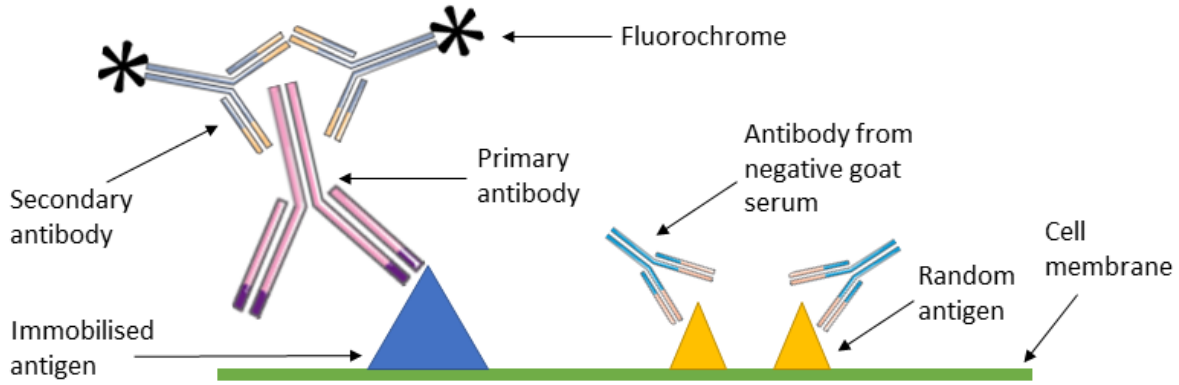

Figure 32. Schematic drawing of indirect immunofluorescence staining. (i) Primary antibody (monoclonal anti-bovine MHC-1) directed against antigen (MHC-1 molecule), (ii) secondary antibody (goat anti-mouse IgG) attached to fluorochrome (FITC) and (iii) antibodies from negative goat serum preventing non-specific binding.

4.5. Virus Titration

The extracellular viral titer was determined in supernatant from explants. Supernatant was collected at 24 hpi and stored at -70°C until titration. Virus titers were conducted on RK-13 cells and assessed by the $TCID_{50}$ according to the method of Reed and Muench (1938).

5. Confocal microscopy

Immunofluorescence of cryosections and EREC was analysed by confocal microscopy (Leica TCS SP2 Laser Scanning Spectral Confocal System; Leica Microsystems). A Gre-Ne 561 nm laser was used to excite Texas Red-fluorochromes, an Argon 488 nm laser excited FITC-fluorochromes and a Xenon 405 nm laser was used to excite Hoechst fluorochromes. The total magnification was x200 in both explants and EREC. Various pictures were also taken with total magnification of x630 for a detailed image of MHC-1 expression. Images were taken with Leica Application Suite Advanced Fluorescence (LAS AF) Software from Leica Microsystems.

6. ROI and Statistical analysis

ImageJ software was used to calculate the percentage of pixels positive for MHC-1 in explants and EREC (ImageJ, U.S. National Institutes of Health, Bethesda, MD, USA). A distinction in EREC was made between two zones, namely zone A which entailed the infected area, and zone B which included the non-infected area of approximately 1.5 cm around the viral plaque (see Figure 33A). In explants (see Figure 33B), zone A, the infected area was compared with zone B, the non-infected area that reached approximately 1 cm next to the plaque.

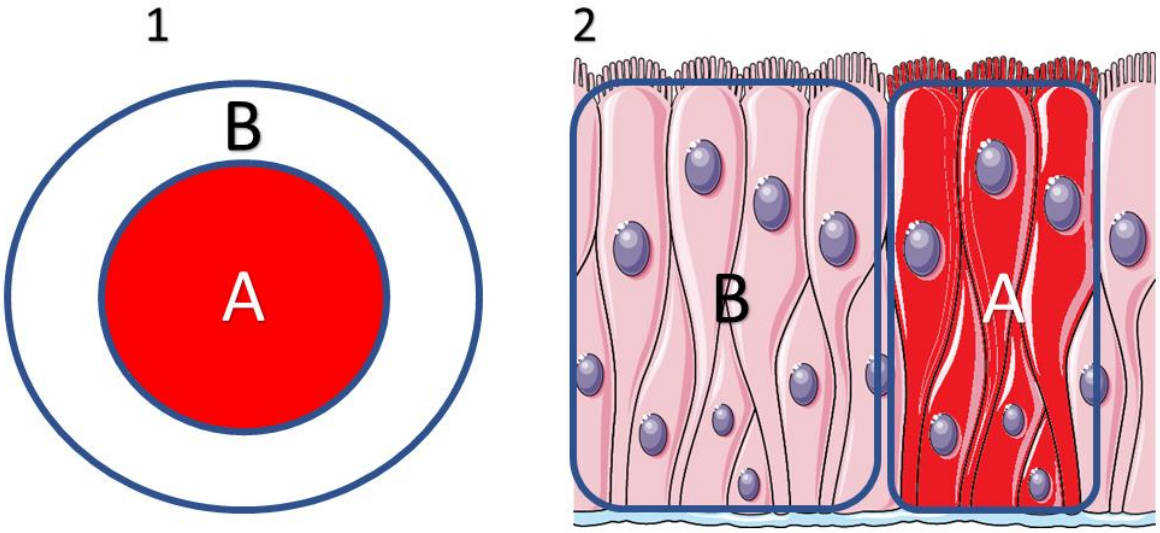

Figure 33. (1) EREC: Red zone A represents the plaque and is the first ROI, and zone B represents the region around the plaque and is the second ROI. (2) Explant: ciliated pseudostratified columnar epithelium with the plaque in red which represents the first ROI, and the neighboring area B is the second ROI.

Following ROI calculation, data from the EREC model was analyzed for statistical significance with SPSS, in which results with a P-value ≤0.05 were considered statistically significant. Normality of the residuals was verified with the Shapiro-Wilk test, in which residuals were log-transformed if they did not follow a normal distribution. In the cases that Levene F test of homogeneity could not be calculated, a nonparametric Kruskall-Wallis test was used for the analysis.

VI Results

1. In vitro cell culture model (EREC)

1.1. TEER test

Transepithelial electrical resistance test was performed, in which a resistance over 800 Ω acted as a confirmation of the barrier integrity, thus indicating a reliable *in vitro* model (the TEER test results are included in Table 2, and a representative light microscopy picture of the respiratory epithelial monolayer can be seen in Figure 34). This resistance takes into consideration the background measurement of 150-200 Ω. The integrity of tight junctions was confirmed in all cell cultures, with the exception of a single well in horse 1 (697 Ω), and a single well in horse two (585 Ω). Areas with cells growing on top of each other were observed in both these wells when observed with light microscopy, which could provide a potential explanation for the lower resistance.

Table 2. TEER test results

Horse and virus strain to be inoculated	**Resistance in Ohm Ω**
Horse 1	
Neurovirulent	1175
Neurovirulent	1090
Abortigenic	1028
Abortigenic	697
Mock	1107
Horse 2	
Neurovirulent	1080
Neurovirulent	585
Abortigenic	890
Abortigenic	865
Mock	1002
Horse 3	
Neurovirulent	848
Neurovirulent	1024
Abortigenic	1053
Abortigenic	1010
Mock	853

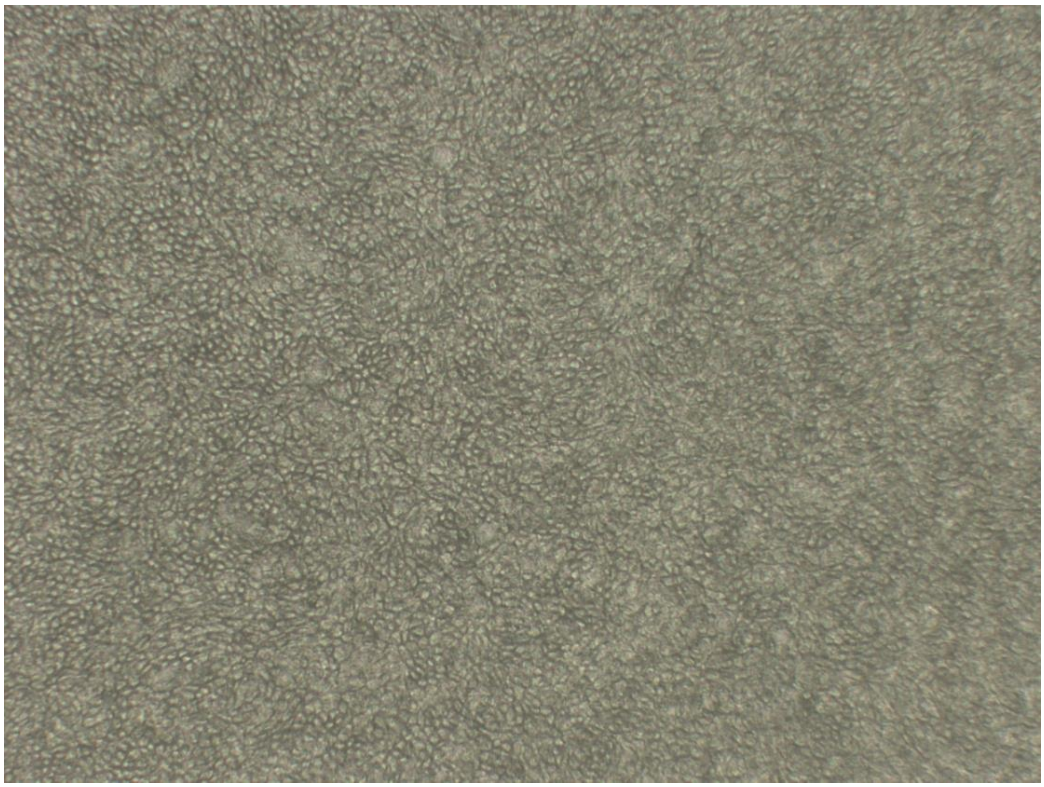

Figure 34. Representative light microscopy picture of the EREC monolayer (taken by: Van Cleemput, 2019).

1.2. Visual analysis of MHC-1 expression

The general observation is that (i) MHC-1 expression is clearly reduced in the infected areas (zone A), and (ii) there is a general upregulation of MHC-1 in EHV1 inoculated EREC, particularly in the non-infected areas directly around the plaques (zone B) (see Figures 36 and 37 for representative images of EREC inoculated with the abortigenic and neurovirulent strain, respectively).

A second observation made in EREC was the general MHC-1 expression, however with a lot of variation within a well (see Figure 35 for representative images of mock inoculated EREC, in which a relatively normal expression of MHC-1 was present). Variation between wells could also be seen, with more prominent MHC-1 expression in certain wells than others. A general difference between the abortigenic and neurovirulent strain was not noticeable. Furthermore, a general trend in MHC-1 expression when comparing surface MHC-1 with cytoplasmic and surface MHC-1 (total MHC-1) was not evident.

A final observation made in EREC, was the clear fusion of cells with the formation of large syncytia, which is consistent with general features of herpesvirus cytopathogenicity. In the positive control performed on RK-13 cells, this cytopathic effect (CPE) was more profound in cells inoculated with the abortigenic strain than cells inoculated with the neurovirulent strain.

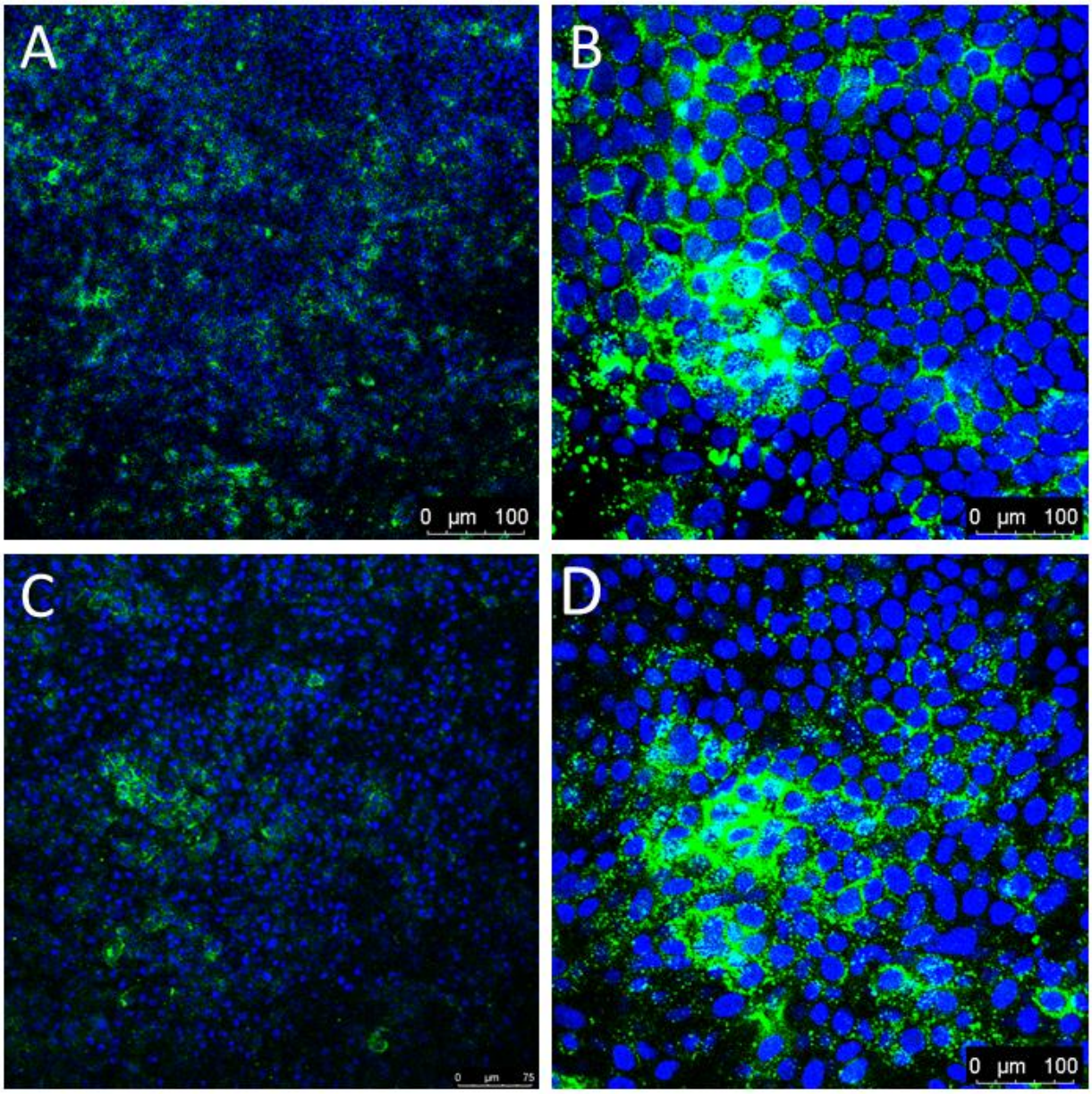

Figure 35. Representative confocal images of EREC at 18 hours after mock inoculation, in which there was a relatively normal amount of MHC-1 expression. Nuclei were labeled with the molecular probe Hoechst (blue) and MHC-1 was labeled with FITC (green). (A) EREC in which surface and cytoplasmic MHC-1 was labeled (magnification x200). (B) EREC in which surface and cytoplasmic MHC-1 (total MHC-1) was labeled (magnification x630). (C) EREC in which surface MHC-1 was labeled (magnification x200). (D) EREC in which surface MHC-1 was labeled (magnification x630).

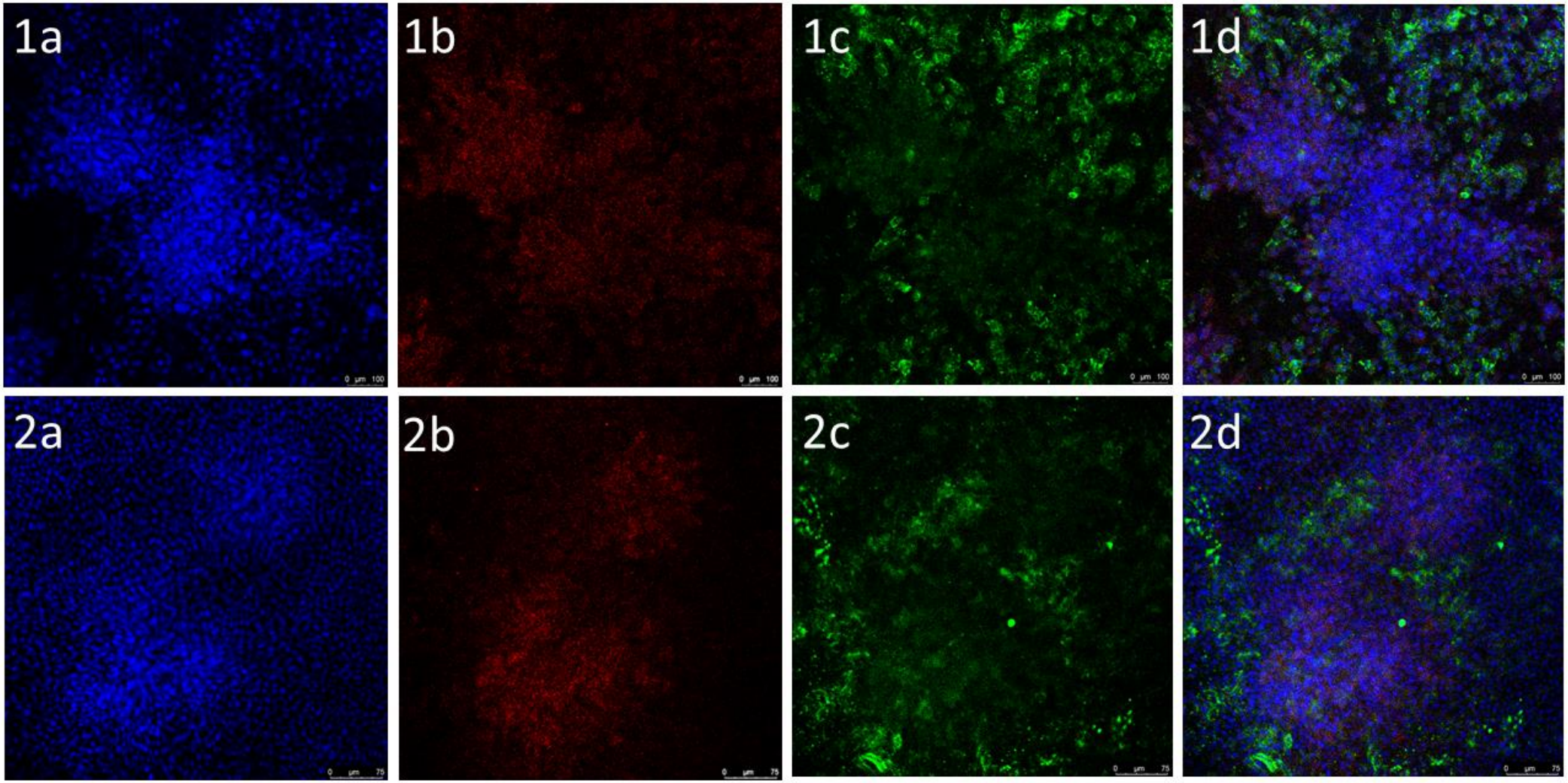

Figure 36. Representative confocal images of EREC at 18 hours after inoculation with the abortigenic strain, in which there was a general high MHC-1 expression in the non-infected areas but a reduced expression in the infected areas. Nuclei were labeled with the molecular probe Hoechst (blue), MHC-1 was labeled with FITC (green) and immediate early viral proteins were labeled with Texas Red (red). (1) EREC in which surface and cytoplasmic MHC-1 (total MHC-1) was labeled. (2) EREC in which surface MHC-1 was labeled. Figures (1d) and (2d) are merged images of (1a,b,c) and (2a,b,c), respectively.

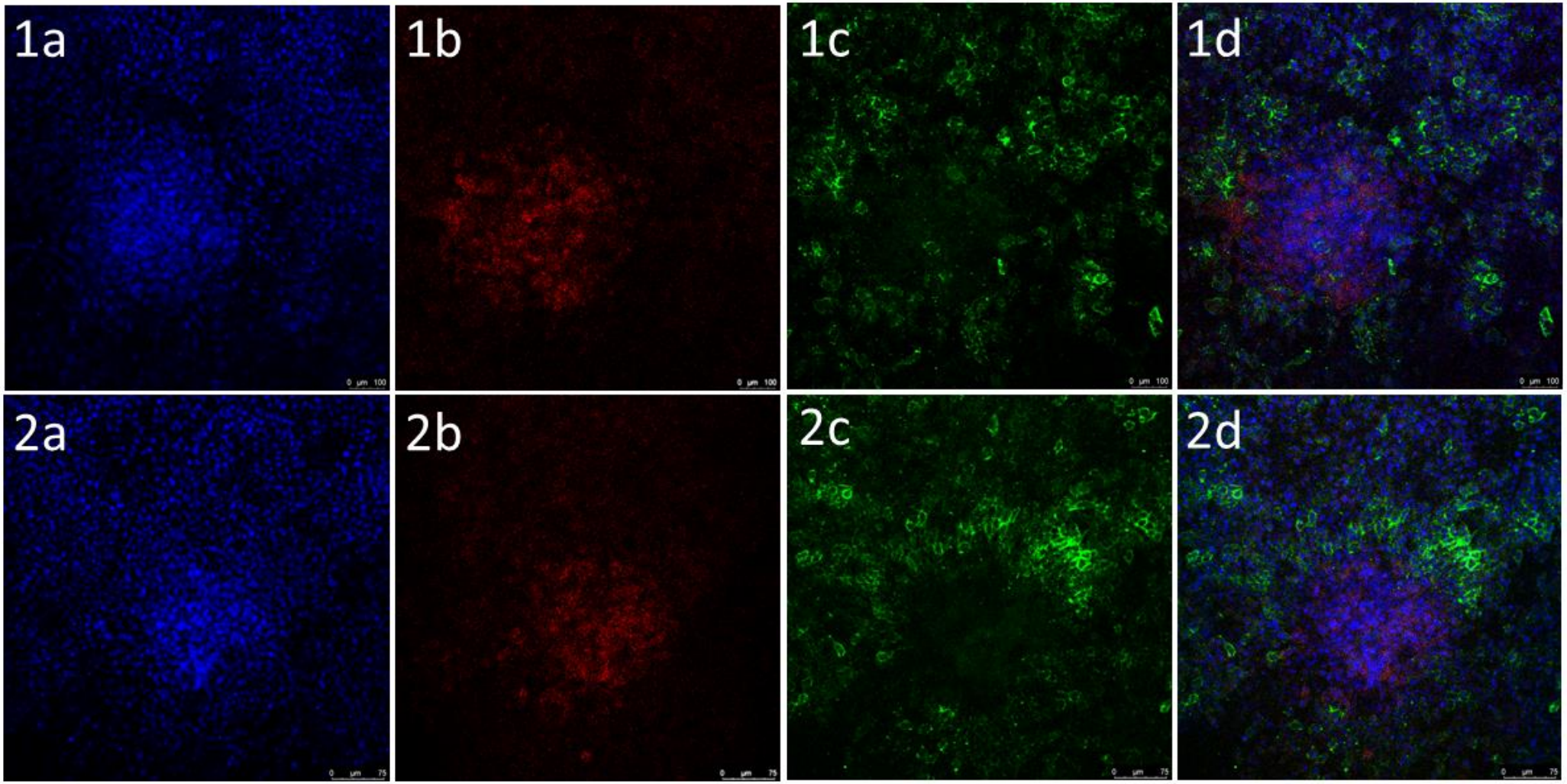

Figure 37. Representative confocal images of EREC at 18 hours after inoculation with the neurovirulent strain, in which there was a general high MHC-1 expression in the non-infected areas but a reduced expression in the infected areas. Nuclei were labeled with the molecular probe Hoechst (blue), MHC-1 was labeled with FITC (green) and immediate early viral proteins were labeled with Texas Red (red). (1) EREC in which surface and cytoplasmic (total MHC-1) was labeled. (2) EREC in which surface MHC-1 was labeled. Figures (1d) and (2d) are merged images of (1a,b,c) and (2a,b,c), respectively.

1.3. ROI analysis

The ROI analysis confirms what was seen in the visual analysis. Namely that the MHC-1 expression is reduced in infected areas (zone A), in comparison to the non-infected areas (zone B). This trend was observed for both the abortigenic as well as the neurovirulent strain, which is depicted in Figures 38 and 39. Furthermore, Figure 38 demonstrates that surface MHC-1 expression in mock inoculated EREC is higher than expression in infected areas (zone A), and lower than expression in non-infected areas (zone B) of EHV1 inoculated EREC.

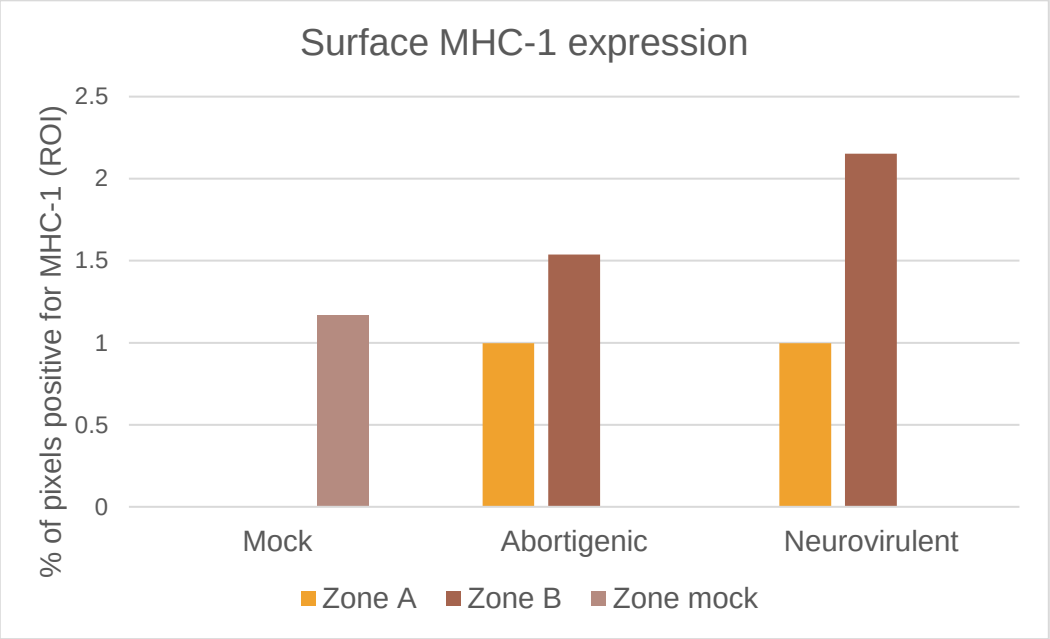

Figure 38. Surface MHC-1 expression in (i) mock inoculated EREC (zone mock), (ii) infected areas (zone A) and (iii) non-infected areas (zone B) of EREC at 18 hours after inoculation with the abortigenic and neurovirulent strain.

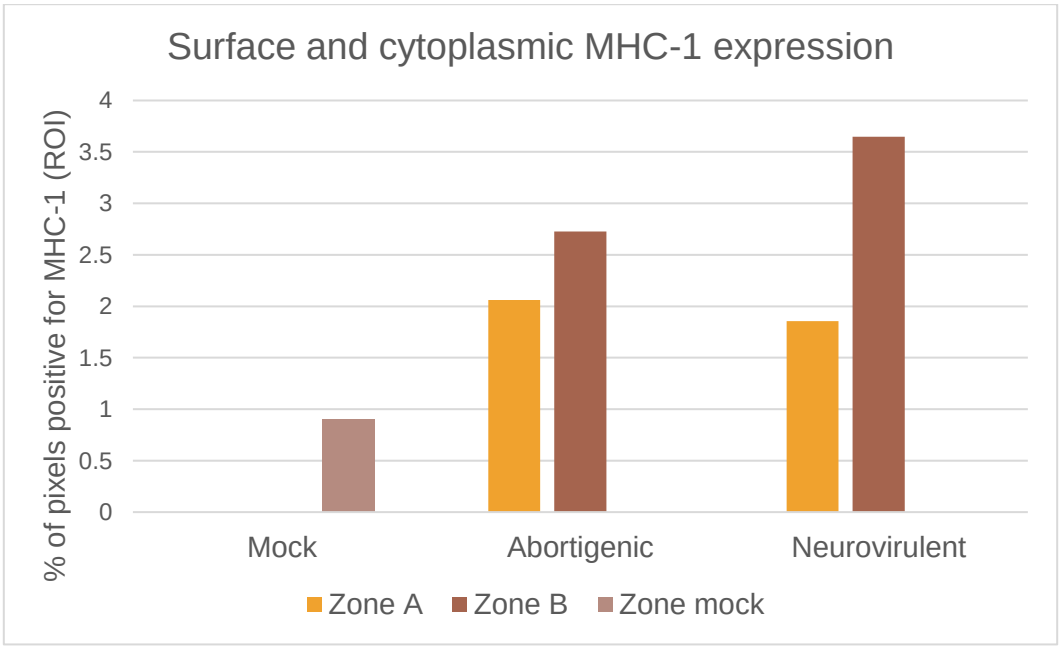

Figure 39. Surface and cytoplasmic MHC-1 (total MHC-1) expression in (i) mock inoculated EREC (zone mock), (ii) infected areas (zone A) and (iii) non-infected areas (zone B) of EREC at 18 hours after inoculation with the abortigenic and neurovirulent strain.

Surface and cytoplasmic MHC-1 (total MHC-1) expression in mock inoculated EREC is lower than expression in both zones of EHV1 inoculated EREC (see Figure 39). Finally, there is no apparent difference in MHC1 expression between the abortigenic strain and neurovirulent strain in infected areas (zone A), whereas in non-infected areas (zone B), there is a higher MHC-1 expression in the EREC inoculated with the neurovirulent strain than in EREC inoculated with the abortigenic strain.

1.4. Statistical analysis of MHC-1 expression

The data were analyzed with SPSS in which results with a P-value ≤0.05 were considered statistically significant. The independent Kruskal-Wallis test was used to analyze the difference in total MHC-1 expression between both virus strains, per zone (zone A: P=0.561, zone B: P=0.202); and the difference in surface expression, per zone (zone A: P=0.561; zone B: P=0.875). Furthermore, there was no significant difference in total MHC-1 expression between zone A and B within each virus strain (abortigenic: P=0.513, neurovirulent: P=0.513); nor was there a significant difference in surface MHC-1 expression (abortigenic: P=0.827; neurovirulent: P=0.275).

There was no statistically significant difference in total and surface MHC-1 expression in zone A, between the mock inoculated EREC, abortigenic and neurovirulent inoculated EREC (total MHC-1: P=0.561, surface MHC-1: P=0.561); or in zone B (total MHC-1: P=0.202, surface MHC-1: P=0.875). Finally, the difference in total and surface MHC-1 expression in zone A was compared within the mock inoculated EREC, abortigenic and neurovirulent inoculated EREC (mock: P=0.275, abortigenic: P=0.827, neurovirulent: P=0.275); and in zone B (mock: P=0.275, abortigenic: P=0.513, neurovirulent: P=0.827). In conclusion, the differences in MHC-1 expression were not statistically significant in this thesis.

2. Ex vivo explant model

2.1. Visual analysis of MHC-1 expression

The main observation is consistent with that made in EREC. There is a prominent downregulation of MHC-1 expression in the infected area (zone A), and simultaneously a general upregulation of MHC-1 in EHV1 inoculated explants in comparison to mock inoculated explants and explants that were fixed immediately after isolation.

MHC-1 expression was random, irrespective of the occurrence of viral plaques and not continuously present throughout the explants. MHC-1 expression patterns varied in length and intensity, and was absent in many cases. Intensities ranged from nearly absent to hyperexpression of MHC-1. In certain locations, there was a polarity in MHC-1 expression in which MHC-1 molecules mainly accumulated on the apical side of the respiratory epithelium rather than basally. However, there were also areas in which the MHC-1 molecules were present throughout the whole width of epithelium, as well as areas in which MHC-1 molecules accumulate more basally.

There was no apparent difference in MHC-1 expression between (i) EGTA pre-treated and not pre-treated explants, (ii) different time points post-inoculation and (iii) the abortigenic and virulent strain. For this reason, representative images were chosen to demonstrate the down- and upregulation of MHC-1, and not all time points or EGTA pre-treated/not pre-treated explants were included (see Figures 40 and 41).

It was noticeable that the epithelia of explants that were not pre-treated with EGTA were in better condition than those of explants pre-treated with EGTA. Additionally, the viral plaque size was larger in explants pre-treated with EGTA than in explants that were not pre-treated with EGTA.

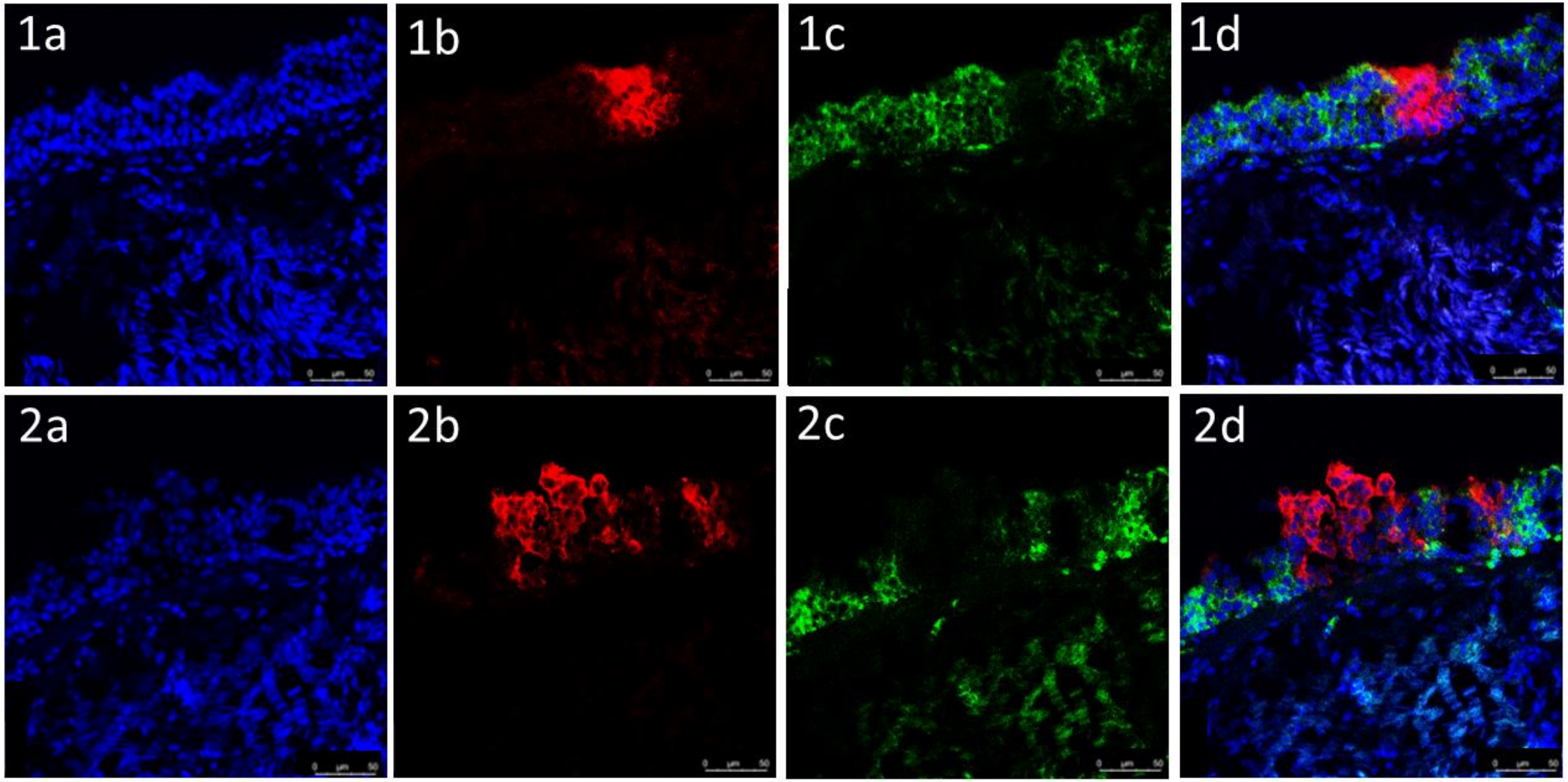

Figure 40. Representative confocal images of explants inoculated with the abortigenic strain with a decreased MHC-1 expression in the viral plaques and an increased MHC-1 expression in the direct environment of the plaques. Nuclei were labeled with the molecular probe Hoechst (blue), MHC-1 was labeled with FITC (green) and late viral proteins were labeled with Texas Red (red). (1) At 24 hpi. (2) At 48 hpi. Figures (1d) and (2d) are merged images of (1a,b,c) and (2a,b,c), respectively (bar scale is 50 µm).

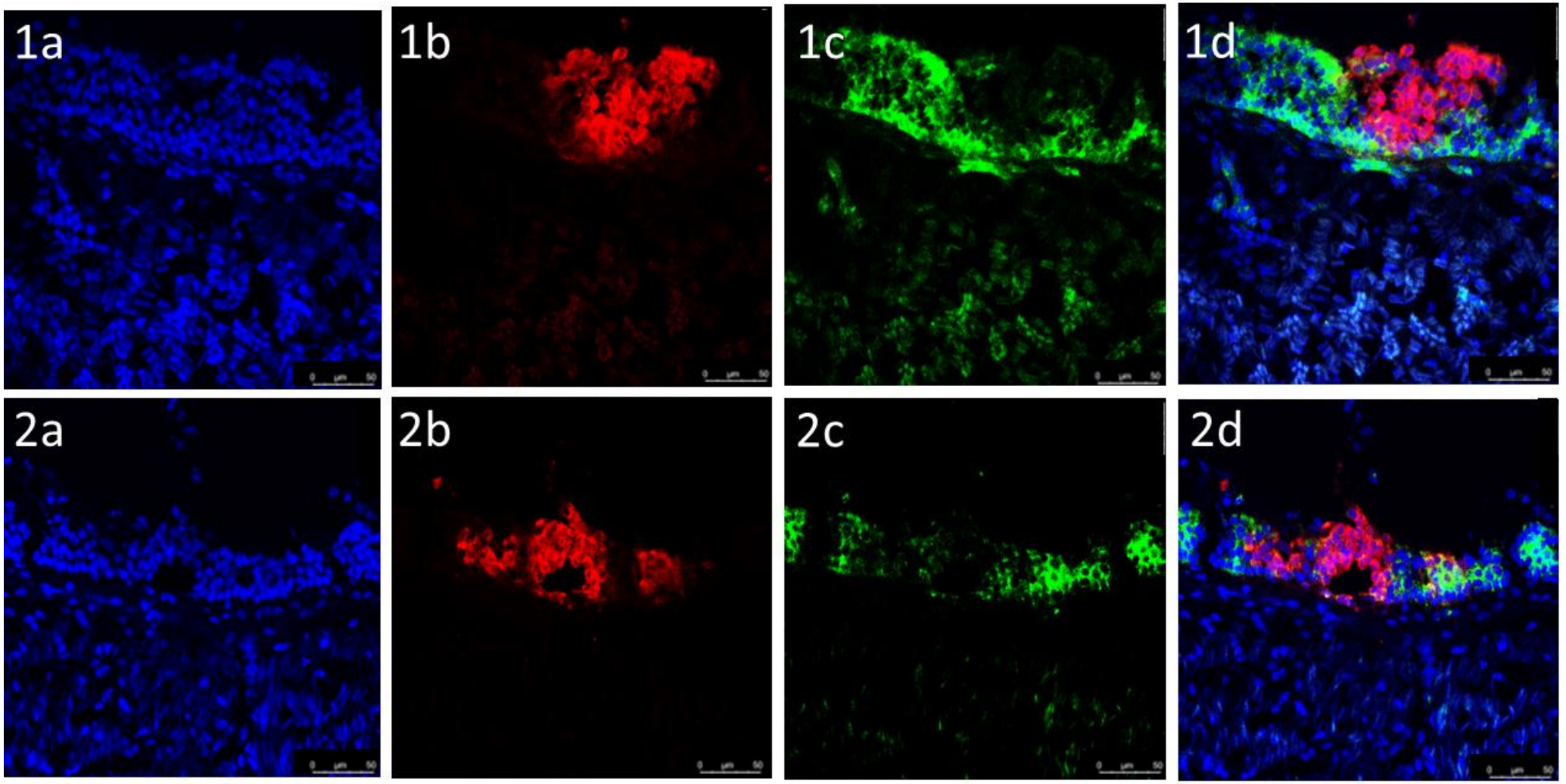

Figure 41. Representative confocal images of explants inoculated with the neurovirulent strain with a decreased MHC-1 expression in the viral plaques and an increased MHC-1 expression in the direct environment of the plaques. Nuclei were labeled with the molecular probe Hoechst (blue), MHC-1 was labeled with FITC (green) and late viral proteins were labeled with Texas Red (red). (1) At 24 hpi. (2) At 48 hpi. Figures (1d) and (2d) are merged images of (1a,b,c) and (2a,b,c), respectively (bar scale is 50 µm).

2.2. ROI analysis

The ROI analysis corresponds with what was observed in the EREC model and in the visual analysis of the explants. It confirms a prominent difference between MHC-1 expression in a plaque (zone A) and the area adjacent to the plaque (zone B), namely, decreased MHC-1 expression in zone A and increased MHC-1 expression in zone B (see Figure 42). Furthermore, there is no evident difference in MHC-1 expression between the strains, though there is a slight increase in MHC-1 expression in both zones in the explants inoculated with the abortigenic strain, which is in contrast to the slight decrease in MHC-1 expression in zone B in EREC inoculated with the abortigenic strain.

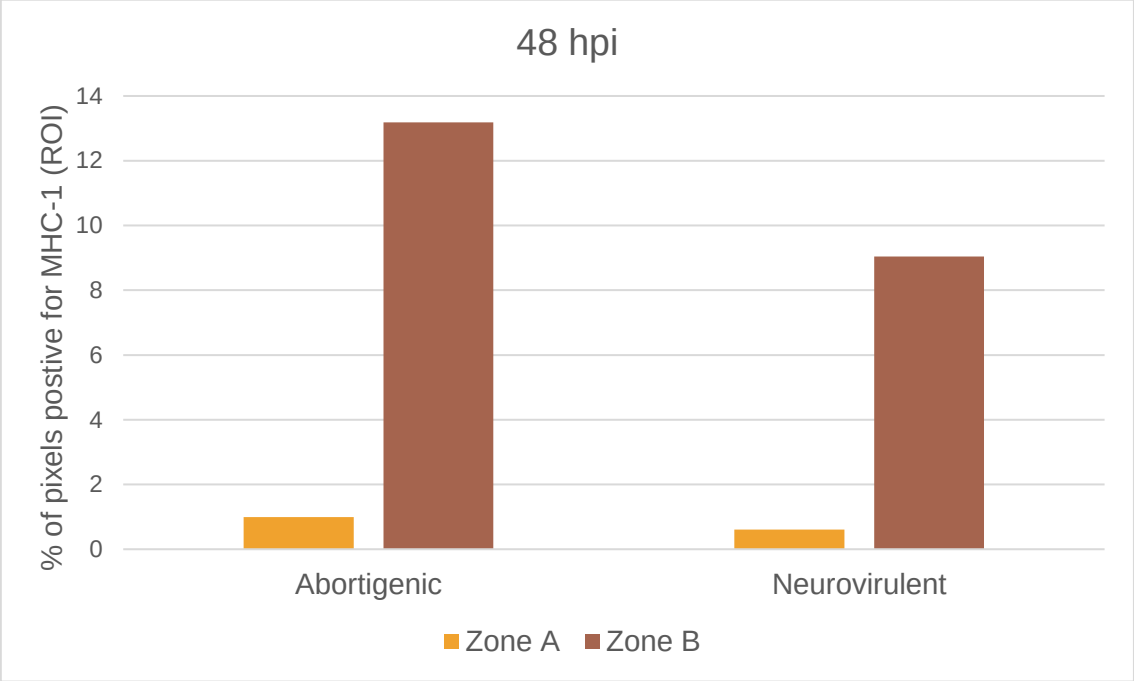

Figure 42. Comparison of MHC-1 expression between the viral plaque area (zone A) and the area adjacent to the plaque (zone B) in explants 48 hours after inoculation with the abortigenic and neurovirulent strain.

Due to the highly variable MHC-1 expression, and the fact that there was no apparent correlation in MHC-1 expression between EGTA pre-treated and explants not pre-treated with EGTA in the visual analysis (results not shown), both explants pre-treated with EGTA and not pre-treated with EGTA were included in this analysis. Furthermore, no correlation in MHC-1 expression was seen between the different time points post-inoculation in the visual analysis (results not shown), therefore the ROI analysis was done for explants at 48 hpi. This highly variable MHC-1 expression inhibited the conduction of a statistical analysis in the explant model.

2.3. Virus titration

Extracellular virus titer was measured in the supernatant of the explants at 24 hpi (see Figure 43). Average titers were higher in explants pre-treated with EGTA for both the abortigenic ($10^{4.52}$ $TCID_{50}$/ml) as well as the neurovirulent ($10^{4.3}$ $TCID_{50}$/ml) strain than in explants that were not pre-treated with EGTA, in which an average virus titer of $10^{3.19}$ and $10^{4.08}$ $TCID_{50}$/ml was present for the abortigenic and neurovirulent strain respectively.

In explants that were not pre-treated with EGTA, the neurovirulent strain induced higher virus titers ($10^{3.30}$, $10^{4.63}$, $10^{4.30}$ $TCID_{50}$/100) than the abortigenic strains ($10^{2.96}$, $10^{3.30}$, $10^{3.30}$ $TCID_{50}$/100) in horse one, two and three respectively.

In the explants pre-treated with EGTA, the abortigenic strains induced higher virus titers ($10^{4.80}$ and $10^{4.80}$ $TCID_{50}$/ml) than the neurovirulent strains ($10^{3.96}$ and $10^{4.3}$ $TCID_{50}$/ml) in supernatant of explants derived from horse one and horse two respectively. The neurovirulent strain induced a higher virus titer ($10^{4.63}$ $TCID_{50}$/100) than the abortigenic strain ($10^{3.96}$ $TCID_{50}$/100) in the supernatant of the explants derived from horse three.

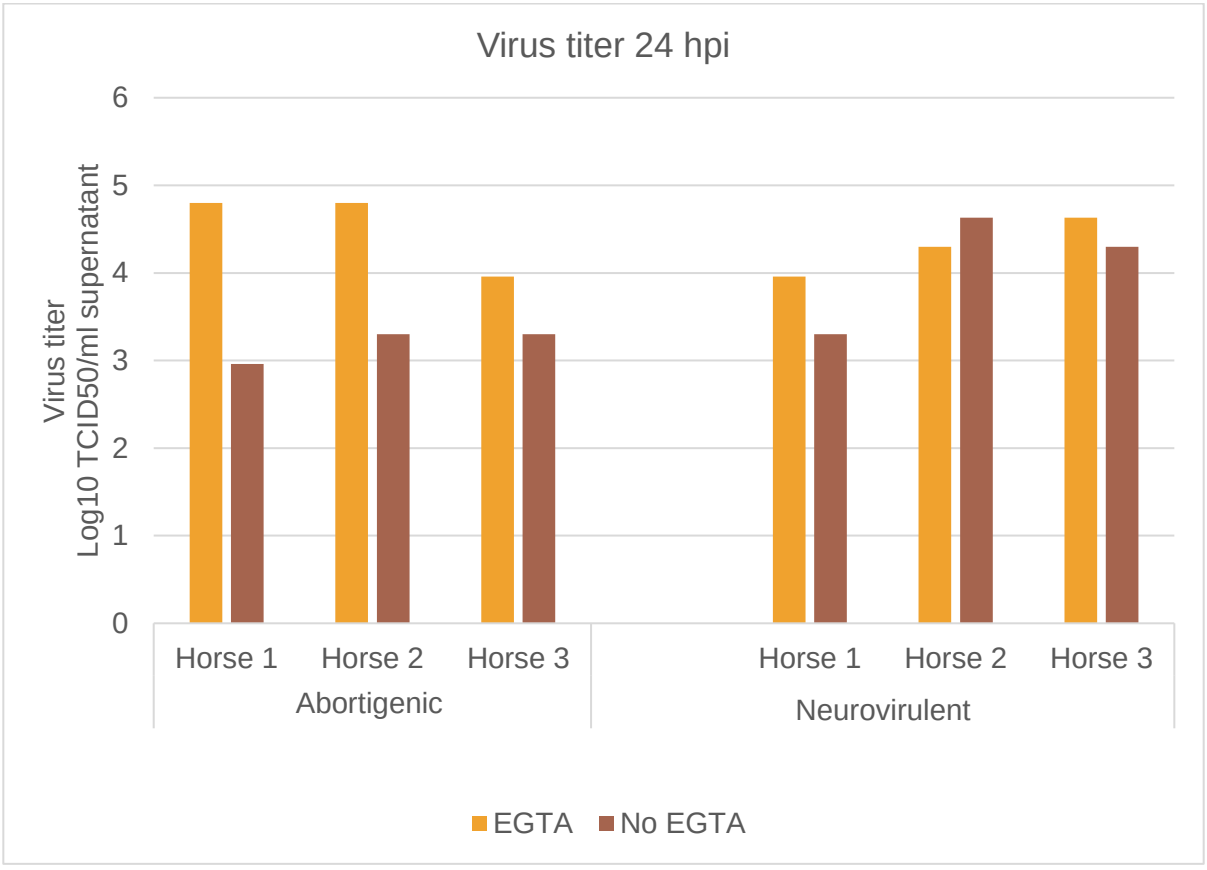

Figure 43. Extracellular virus titer measured in explants that were pre-treated and not pre-treated with EGTA, at 24 hours after inoculation with the abortigenic and neurovirulent strain.

VII Discussion

EHV1 infection causes abortions and neurological symptoms worldwide, with a majority resulting in life-long infections. EHV1's ability to overcome certain recognition systems by the immune response is related to its immune evasion strategies, which is why the production of a vaccine that is able to prevent cell-associated viremia has been difficult. To make progress in vaccine development, it is necessary to unravel these immune evasion strategies further and increase our understanding on host-pathogen interaction in relation to immunity.

The CTL mediated response is essential in eliminating intracellular virus, and studies have shown that various members of the genus *Varicellovirus* interfere with the MHC-1 antigen presenting pathway (Früh et al., 1995; Ahn et al., 1997; Favoreel et al., 1999; Hinkley et al., 2000; Koppers-Lalic et al., 2001; Koppers-Lalic et al., 2005; Eisfeld et al., 2007). EHV1 induces downregulation of MHC-1 through increased dynamin-mediated endocytosis of MHC-1 by pUL56 and pUL43 (Ma et al., 2012: Hussey et al., 2014; Huang et al., 2015). Additionally, MHC-1 downregulation is induced by inhibition of TAP activity by UL49.5 (gN) (Ambagala et al., 2004; Koppers-Lalic et al., 2008). This MHC-1 downregulation has always been demonstrated using flow cytometry with non-target cells and EREC. Although flow cytometry is an excellent quantitative tool, it cannot depict regional MHC-1 expression patterns. Therefore, in this thesis, we aimed to demonstrate the MHC-1 expression pattern during infection through confocal microscopy. Initially an EREC culture model was used, followed by a complementary respiratory explant model, in which the *in vivo* situation was mimicked more closely.

Briefly, In the EREC culture model, a distinction was made between total (cytoplasmic and surface) and surface MHC-1 expression, and between the viral plaque zone (zone A) and the zone surrounding the plaque (zone B). In the explant model, zone A and zone B were also determined as the ROI in the comparison of MHC-1 expression at the site of the viral plaque and the adjacent area respectively. Half the explants were pre-treated with EGTA to ensure viral replication by disrupting the intercellular junctions, which did not seem to have an effect on the MHC-1 expression (Van Cleemput et al., 2017). The higher virus titers in supernatant from explants pre-treated with EGTA suggest that this did indeed allow for increased virus replication.

MHC-1 downregulation was observed in the visual and ROI analysis in viral plaques (zone A) in both models, which coincides with the previous studies. Moreover, a general upregulation of MHC-1 expression was observed in the visual analysis in non-infected epithelium of EHV1 infected explants and in EREC compared to mock inoculated EREC/explants or explants fixed directly after isolation. This was also confirmed by a prominently higher MHC-1 expression in zone B than in zone A in the ROI analysis of both models.

It is clear from our research conducted in EREC and explants and other studies, that MHC-1 expression is downregulated in EHV1 infected cells (to suppress CTL activity), which makes these cells less visible for cytotoxic $CD8^+$ T lymphocytes. However, they become more susceptible to NK cells. It is not yet known whether EHV1 infected cells indeed show increased susceptibility to NK cell-mediated lysis, or if EHV1 has cleverly developed strategies to simultaneously prevent CTL mediated and NK mediated cell lysis. This could be studied by performing NK cytotoxicity assays using as target cells, cells that were inoculated with wild-type EHV1 strain and with a mutant strain lacking pUL56 and UL49.5 (and therefore will show a reduced ability to downregulate MHC-1). A potential obstacle faced conducting this kind of study is that, there is no literature with a description of techniques to isolate equine NK cells from PBMC. Unpurified PBMC could be used in the cytotoxicity assay, possibly from which the CTL have been removed by negative MACS followed by positive FACS selection of $CD3^+$ cells. This could be achieved by using antibodies that recognize equine CD3, considering T cells are $CD3^+$ and NK cells are

$CD3^-$. Porcine NK cells have previously been isolated from PBMC with this method, in which they were purity sorted based on $CD3^-$, $CD172a^-$and $CD8a^+$ expression (Grauwet et al., 2014; De Pelsmaeker, 2019).

Other herpesviruses, including alphaherpesviruses, have been described to display different NK cell evasion strategies. So far, it is known that certain alpha- beta- and gammaherpesviruses induce expression of a non-functional MHC-1 decoy receptor, selectively down-regulate MHC-1 alleles that do not send out inhibitory signals to NK cells, down-regulate ligands that are stimulatory and increase ligands that are inhibitory for NK cell cytotoxicity (Grauwet et al., 2014; Grauwet et al., 2016; De Pelsmaeker et al., 2018). Rappocciolo et al. (2003) used different monoclonal antibodies which recognized different MHC-1 epitopes, suggesting that the effect of MHC-1 downregulation may be allele- or locus-specific.

As previously mentioned, studies have already demonstrated causes for EHV1-specific downregulation of MHC-1, though research needs to be conducted on the potential causes for the general upregulation of MHC-1 in non-infected cells caused by EHV1 infection. Possible explanations can be derived from literature for the impact of certain signals on MHC-1 expression. MHC-1 expression is controlled by several regulators of which three can be linked to viral infections and induce upregulation of MHC-1, namely (i) nuclear factor-kappa B (NF-κB) and (ii) IFN Regulatory Factor 1 (IRF1) that bind to NF-κB binding Enhancer A region and IFN-sensitive response element (ISRE), respectively, in the MHC-1 promotor region (Lorenzi et al., 2012), and (iii) the PRR NLRC5, which is a regulator of MHC-1. NLRC5 is known to be upregulated during viral infection mainly as a result of increased type 1 IFN and IFN-γ (type 2 IFN) secretion (Staehli et al., 2012; Jongsma et al., 2017). IRF1 is upregulated in response to IFN-γ stimulation (Chang et al., 1992). Furthermore, ISRE is stimulated by engagement of the NF-κB pathway. Several signalling cascades activate the NF-κB pathway, such as stimulation of TLR3 during virus infection, which can then induce an increased production of type 1 IFN, resulting in the activation of the NF-κB pathway and consequently MHC-1 expression (Pfeffer, 2011).

These MHC-1 regulators are influenced by interferons, and it is possible that the early antiviral type 1 IFN that is secreted in a paracrine manner by virus infected cells, induces enhanced MHC-1 expression in surrounding uninfected cells. Poelaert et al. (2018) have already indicated the importance of the early antiviral defense in EHV1 infections with both phenotype variants, by demonstrating a suppressed replication after treatment with recombinant equine type 1 IFN treatment. Hussey et al. (2014b) showed an increase in type 1 IFN mRNA in EREC at 24 hpi, and in type 1 IFN secreted in supernatant of the wells collected at 72 hpi. Furthermore, an example of virus induced upregulation of MHC-1 due to increased type 1 IFN was seen in Reovirus (Atta et al., 1995).

Finally, a study conducted by Kurtz et al. (2010) has identified MHC-1 as a cellular entry-receptor for EHV1. Therefore, it could be postulated that an increase in MHC-1 in neighbouring, uninfected cells could be beneficial for the entry of virus. However, Van Cleemput et al. (2017) demonstrated that the blocking of this receptor does not significantly affect the infectivity in EREC.

In EREC, a distinction was made between MHC-1 expressed on the surface of the cells and total MHC-1 including the intracellular MHC-1 molecules. In both staining methods, MHC-1 expression was higher in non-infected areas (zone B) than in infected areas (zone A). Furthermore, surface and total MHC-1 expression in non-infected areas (zone B) of EREC inoculated with the abortigenic and neurovirulent strain was higher than expression in mock inoculated EREC, which is a confirmation of upregulation. Surface MHC-1 expression was reduced in viral plaques (zone A) induced by both strains in comparison to mock inoculated EREC, which correlates with results in literature regarding downregulation of MHC-1. Moreover, total MHC-1 expression was higher in viral plaques than in mock inoculated EREC. This

suggests that infected respiratory epithelial cells react to viral infection by an increased translation of MHC-1 molecules, but that EHV1 blocks the surface expression, hence resulting in a decreased surface expression of MHC-1 and simultaneously an increased total MHC-1 expression.

Reverse transcription quantitative polymerase chain reaction (RT-qPCR) could be performed to quantify mRNA production coding for MHC-1, consequently clarifying whether there is indeed an increased translation of MHC-1 molecules during EHV1 infections. Considering the highly variable MHC-1 expression, cells showing increased expression of MHC-1 would have to be isolated through microdissection with a UV or infrared laser, prior to RT-qPCR.

Finally, despite similar MHC-1 expression in EREC induced with the abortigenic and neurovirulent strain in zone A, a slightly increased MHC-1 expression was observed in EREC inoculated with the neurovirulent strain in zone B. Poelaert et al. (2018) demonstrated that the neurovirulent strain induces an increased upregulation of two T cell chemokines (CXCL9 and CXCL10), but that both phenotypes equally induce type 1 IFN secretion in the upper respiratory tract, suggesting this difference in MHC-1 expression is not likely linked to type 1 IFN secretion. In addition, a slightly increased MHC-1 expression was observed in the explants inoculated with the abortigenic strain in zone B, suggesting that there is no significant trend present between both strains in this thesis.

Curiously, surface MHC-1 expression was slightly higher than total MHC-1 expression in mock inoculated EREC. This could be explained by the variability in MHC-1 expression, or due to the effect that the detergent Triton X-100 (to permeabilize the plasma membrane to allow intracellular antibody staining) may have had on the cell membrane proteins prior to labeling of MHC-1. Indeed, studies have shown that Triton X-100 is a more aggressive detergent and can cause loss of detection of some membrane proteins (Goldenthal et al., 1985). Huang et al., (2014) had encouraging results in labeling surface and total MHC-1 expression, using 0.1% saponin as permeabilizing agent, which could perhaps be used in future studies.

Our research has also shown that there was an epithelial polarity of MHC-1 expression in explants. Although variation was observed in this once again, with MHC-1 molecules being either mostly present apically, basally, or throughout the whole thickness of the epithelium; remarkably, the general tendency of MHC-1 expression seemed to be apically. Basal cells are in close proximity to underlying blood vessels and submucosa with patrolling immune cells such as lymphocytes, DC, monocytes and plasma cells; which could suggest that these basal cells are potentially more important in presenting MHC-1 antigen complex to immune cells rather than epithelial cells that are in contact with the respiratory lumen. Furthermore, this proximity means that basal cells are more in contact with NK cells than the apical epithelial cells, and therefore require the inhibitory signal of MHC-1. Basal cells differ from the overlying epithelial cells in that they are multipotent and act as stem/progenitor cells capable of self-renewal and differentiation into the overlying epithelial cells (Rock et al., 2010). A possible explanation for this contradictory lack of MHC-1 expression basally, is that in a non-activated state, these undifferentiated cells are relatively quiescent, perhaps making them less active in expressing membrane proteins such as MHC-1, though they must have some form of inhibitory signal for NK cells.

Despite a plaque-specific downregulation and general upregulation of MHC-1, there was a lot of variability in MHC-1 expression patterns in both models. Although expression seemed to be homogeneous within the wells of EREC, which was confirmed in the ROI analysis; this homogeneous pattern consisted of alternating MHC-1 expression. Variation in explants was even more prominent. There are several possible explanations for this variable instead of ubiquitous expression, which would seem more likely as MHC-1 molecules are expressed on all nucleated cell types to prevent destruction by NK cells. Firstly, we do not know what the effects were on MHC-1 expression of manipulation,

cultivation, inoculation and permeabilization procedures applied during the entire protocol. In an attempt to eliminate these effects, we fixed explants immediately after isolation, and even though this variability still seemed to be present, it could be useful to once again fix explants immediately after isolation to determine the effects of cultivation on MHC-1 expression.

Secondly, inter-horse variability was clearly present. In the *ex vivo* explant model, the properties and MHC-1 expression signals are dependent on the biopsied tissue, which is determined by factors such as age, sex, environmental and living patterns of the horse (Poelaert, 2019).The EREC model allows for more controlled conditions, though is still dependent on the horse from which cells are isolated. Future research should perhaps be conducted on EREC and explants derived from the same horse, thus eliminating this inter-horse variability.

Finally, it is not clear whether this variable expression is associated with less or no expression in certain areas, or whether we simply were not able to show the particular MHC-1 molecules that were expressed with our immunofluorescent labeling. It is known that MHC-1 genes show allelic variation, for example, the human MHC-1 gene family is the most polymorphic gene in the human genome (Tallmadge et al., 2010). Therefore, it is possible that MHC-1 alleles and therefore amino acid sequences, were expressed that are not recognized by the antibody, considering that we used a monoclonal antibody that targets a specific epitope with a specific amino acid sequence. In the case that lack of MHC-1 detection indeed would be indicative for lack of MHC-1 expression, even in non-infected cells, one has to assume that these cells then probably need to express other inhibitory signals equally as important as MHC-1 to avoid destruction by NK cells (for which MHC-1 typically serves as a powerful inhibitory signal).

Following ROI calculation, SPSS was used to analyze the differences in MHC-1 expression between zone A and zone B in EREC, which were not significant. This was in contrast to prominent results from the visual and ROI analysis, and there are possible explanations and adaptations that can be made in future research to potentially translate this visually significant outcome to a statistically significant outcome. Firstly, variability in MHC-1 expression seemed to be a major issue. Future studies should be performed within horses, to eliminate inter-horse variability. Another important element within the EREC model, was the influence of background signals. Despite the use of an isotype antibody control to verify lack of background signal, background immunofluorescence seemed to be present particularly in the area of viral plaques; perhaps because of the clustering of cells, formation of syncytia in the plaques and the occurrence of death/dying cells. The software we used could not distinguish between these interfering signals and MHC-1 expression, therefore resulting in insignificant differences.

To eliminate this issue of background interference, future research should focus on optimizing signal-to-noise ratio. This could be done by testing different antibody dilutions and using anti-horse MHC-1 instead of anti-bovine MHC-1 antibodies, which relies on cross-reactivity and therefore could be a contributing factor in signal-to-noise ratio. Additional improvements of the protocol should be made, that could optimize the fluorescence signal. These include the comparison of appropriate fixation and permeabilization methods; and which concentration, exposure time and temperature should be taken into account. Finally, alternative image analysis software packages could be used to analyze differences.

A statistical analysis was not performed in the respiratory explant model due to the highly variable MHC-1 expression between horses and within explants. Despite the possibility for an excellent visual analysis of MHC-1 expression patterns in *ex vivo* conditions, the explant model does not seem suitable for statistical analysis.

Previous studies have always used flow cytometry to quantify MHC-1 downregulation, and in this thesis confocal microscopy was used to asses MHC-1 expression in two models that mimicked the *in vivo* situation more closely than flow cytometry. It could be interesting to perform a (semi-quantitative) Western blot to confirm the results, allowing for the use of several techniques in parallel which maximizes reliability.

In conclusion, this research demonstrated the MHC-1 expression patterns in an *in vitro* EREC model and in an equine *ex vivo* respiratory explant system, closely mimicking *in vivo* conditions, for the first time to our knowledge. An EHV1 induced downregulation of MHC-1 was seen in infected areas, whilst a general upregulation of MHC-1 was present in non-infected areas, both in explants and EREC. This research also demonstrated that, in both systems, there was very substantial variability in MHC-1 expression/detection using the monoclonal antibody from this study. Further research should focus on investigating the mechanism underlying virus-induced MHC-1 upregulation in non-infected cells and whether MHC-1 downregulation by EHV1 in infected cells effectively renders these cells more susceptible to NK mediated cell lysis. A better understanding of EHV1's effect on MHC-1 can contribute to the development of vaccines that will elicit an effective cellular immune response, which could lead to a drastic reduction in economic and emotional losses.

VIII References

Agrawal, P., Nawadkar, R., Ojha, H., Kumar, J., Sahu, A., 2017. Complement Evasion Strategies of Viruses: An Overview. Frontiers in microbiology 8, 1117.

Allen, G., Yeargan, M., Costa, L.R., Cross, R., 1995. Major histocompatibility complex class I restricted cytotoxic T-lymphocyte responses in horses infected with equine herpesvirus 1. Journal of Virology 69, 606-612.

Ahn, K., Gruhler, A., Galocha, B., Jones, T.R., Wiertz, E.J., Ploegh, H.L., Peterson, P.A., Yang, Y., Früh, K., 1997. The ER-luminal domain of the HCMV glycoprotein US6 inhibits peptide translocation by TAP. Immunity 6, 613-621.

Ambagala, A.P., Hinkley, S., Srikumaran, S., 2000. An early pseudorabies virus protein down-regulates porcine MHC class I expression by inhibition of transporter associated with antigen processing (TAP). Journal of Immunology 164, 93-99.

Ambagala, A.P.N., Gopinath, R.S., Srikumaran, S., 2004. Peptide transport activity of the transporter associated with antigen processing (TAP) is inhibited by an early protein of equine herpesvirus-1. Journal of General Virology 85, 349-353.

Atta, M.S., Irving, W.L., Powell, R.J., Todd, I., 1995. Enhanced expression of MHC class I molecules on cultured human thyroid follicular cells infected with reovirus through induction of type 1 interferons. Clinical and Experimental Immunology 101, 121-126.

Baker, T.S., Newcomb, W.W., Booy, F.P., Brown, J.C., Steven, A.C., 1990. Three-Dimensional Structures of Maturable and Abortive Capsids of Equine Herpesvirus 1 from Cryoelectron Microscopy. Journal of Virology 64, 563-573.

Bayly-Jones, C., Bubeck, D., Dunstone, M.A., 2017. The mystery behind membrane insertion: a review of the complement membrane attack complex. Royal Society 372, 1726.

Breathnach, C.C., Yeargan, M.R., Sheoran, A.S., and Allen, G.P., 2001. The mucosal humoral immune response of the horse to infective challenge and vaccination with equine herpesvirus-1 antigens. Equine Veterinary Journal 33, 651-657.

Breathnach, C.C., Hussey, G.S., Suresh, M., Lunn, D.P., 2005. Equine herpesvirus-1 infection induces IFN-γ production by equine T lymphocyte subsets. Veterinary Immunology and Immunopathology 103, 207-2015.

Brosnahan, M.M., Damiani, A., van de Walle, G., Erb, H., Perkins, G.A. Osterrieder, N., 2009. The effect of siRNA treatment on experimental equine herpesvirus type 1 (EHV-1) infection in horses. Virus research 147, 176-81.

Bryant, N.A., Davis-Poynter, N., Vanderplasschen, A., Alcami, A., 2003. Glycoprotein G isoforms from some alphaherpesviruses function as broad-spectrum chemokine binding proteins. EMBO Journal 22, 833-846.

Burrows, R., Goodridge, D., Denyer, M.S., 1984. Trials of an inactivated equid herpesvirus 1 vaccine: challenge with a subtype 1 virus. The Veterinary Record 114, 369-374.

Chang, C.H., Hammer, J., Loh, J.E., Fodor, W.L., Flavell, R.A., 1992. The activation of major histocompatibility complex class I genes by interferon regulatory factor-1 (IRF-1). Immunogenetics 35, 378-384.

Chavakis, E., Choi, E.Y., Chavakis, T., 2009. Novel aspects in the regulation of the leukocyte adhesion cascade. Thrombosis and Haemostasis 102, 191-197.

Chesters, P.M., Allsop, R., Purewal, A., Edington, N., 1997. Detection of Latency-Associated Transcripts of Equid Herpesvirus 1 in Equine Leukocytes but Not in Trigeminal Ganglia. Journal of Virology 71, 3437-43.

Coller, K.E., Lee, J.I., Ueda, A., Smith, G.A., 2007. The capsid and tegument of the alphaherpesviruses are linked by an interaction between the UL25 and VP1/2 proteins. Journal of Virology 1, 11790-11797.

Cook, R.F., O'Neill, T., Strachan, E., Sund quist, B., Mumford, J.A., 1990. Protection against lethal equine herpesvirus type 1 (subtype 1) infection in hamsters by immune stimulating complexes (ISCOMs) containing the major viral glycoproteins. Vaccine 8, 491-496.

Cosman, D., Fanger, N., Borges, L., 1999. Human cytomegalovirus, MHC class I and inhibitory signalling receptors: more questions than answers. Immunological Reviews 168, 177-185.

Crabb, B.S., MacPherson, C.M., Reubel, G.H., Browning, G.F., Studdert, M.J., Drummer, H.E., 1995. A type-specific serological test to distinguish antibodies to equine herpesviruses 4 and 1. Archives of Virology 140, 245-258.

Da Costa, X.J., Brockman, M.A., Alicot, E., Ma, M., Fischer, M.B., Zhou, X., Knipe, D.M., Carroll, M.C., 1999. Humoral response to herpes simplex virus is complement-dependent. Proceedings of the National Academy of Sciences of the United States of America 96, 12708-12712.

Davidson, A.J., 2007. Comparative analysis of genomes. Ln: Human Herpesviruses: Biology, Therapy, and Immunoprophylaxis, Cambridge University Press, Cambridge, UK.

Davidson, A.J., 2008. Herpesviruses: General Features. Ln: Encyclopedia of Virology, Elsevier Ltd, Glasgow, UK, pp. 430-436.

Davidson, A.J., Eberle, R., Ehlers, B., Hayward, G.S., Mcgeoch, D.J., Minson, A.C., Pellet, P.E., Roizman, B., Studdert, M.J., Thiry, E., 2009. The order Herpesvirales. Archives of Virology 154, 171-177.

Davidson, A.J., Minson, A.C., Roizman, B., Ehlers, B., Wang, F., Hayward, G.S., Studdert, M.J., Nicholas, J., Pellet, P.E., Eberle, R., Lacoste, V., 2011. Herpesvirales. King, A.M.Q., Adams, M.J., Carstens, E.B., Lefkowitz, E.J. Ln: Virus Taxonomy, Elsevier, Oxford, Mississippi, USA, 99-107.

De Pelsmaeker, S., Romero, N., Vitale, M., Favoreel, H.W., 2018. Herpesvirus Evasion of Natural Killer Cells. Journal of Virology 92.

De Pelsmaeker,S. Dierick, E., Klupp, B., Mettenleiter, T.C., Cantoni, C., Vitale, M., Favoreel, H.W., 2019. Expression of the Pseudorabies Virus gB Glycoprotein Triggers NK Cell Cytotoxicity and Increases Binding of the Activating NK Cell Receptor PILRβ. Journal of Virology 93, 7.

Dowler, K.W. Veltri, R.W., 1984. In vitro neutralization of HSV-2: inhibition by binding of normal IgG and purified Fc to virion Fc receptor (FcR). Journal of Medical Virology 13, 251-259.

Dubin, G., Frank, I., Friedman, H.M., 1990. Herpes simplex virus type 1 encodes two Fc receptors which have different binding characteristics for monomeric immunoglobulin G (IgG) and IgG complexes. Journal of Virology 64, 2725-2731.

Eisfeld, A.J., Yee, M.B., Erazo, A., Abendroth, A., Kinchington, P.R., 2007. Downregulation of class I major histocompatibility complex surface expression by varicella-zoster virus involves open reading

frame 66 protein kinase-dependent and -independent mechanisms. Journal of virology 81, 9034-9049.

Favoreel, H.W., Nauwynck, H.J., Van Oostveldt, P., Mettenleiter, T.C., Pensaert, M.B., 1997. Antibody-induced and cytoskeleton mediated redistribution and shedding of viral glycoproteins, expressed on pseudorabies virus-infected cells. Journal of Virology 71, 8254-8261.

Favoreel, H.W., Nauwynck, H.J., Halewyck, H.M., Van Oostveldt, P., Mettenleiter, T.C., Pensaert, M.B., 1999. Antibody-induced endocytosis of viral glycoproteins and major histocompatibility complex class I on pseudorabies virus-infected monocytes. Journal of General Virology 80, 1283-1291.

Favoreel, H.W., Van de Walle, G.R., Nauwynck, H.J., Pensaert, M.B., 2003. Virus Complement Evasion Strategies. Journal of General Virology 84, 1-15.

Feng, X., Thompson, Y. G., Lewis, J. B., Caughman, G. B., 1996. Expression and function of the equine herpesvirus 1 virion-associated host shutoff homolog. Journal of Virology 70, 8710-8718.

Fensterl, V., Sen, G.C., 2009. Interferons and Viral Infections. Biotechnology and Applied Biochemistry 35, 14-20.

Foote, C.E., Love, D.N., Gilkerson, J.R., Whalley, J.M., 2002. Serological responses of mares and weanlings following vaccination with an inactivated whole virus equine herpesvirus 1 and equine herpesvirus 4 vaccine. Veterinary Microbiology 88, 13-25.

Foote, C.E., Raidal, S.L., Pecenpetelovska, G., Wellington, J.E., Whalley, J.M., 2006. Inoculation of mares and very young foals with EHV-1 glycoproteins D and B reduces virus shedding following respiratory challenge with EHV-1. Veterinary Immunology and Immunopathology 111, 97-108.

Frampton, A.R., Goins, W.F., Cohen, J.B., von Einem, J., Osterrieder, N., O'Callaghan, D.J., Glorioso, J.C., 2005. Equine Herpesvirus 1 Utilizes a Novel Herpesvirus Entry Receptor. Journal of Virology 79, 3169-3173.

Frank, I., Friedman, H.M., 1989. A novel function of the herpes simplex virus type I Fc receptor: participation in bipolar bridging of antiviral immunoglobulin G. Journal of Virology 63, 4479-4488.

Fulton, A., Peters, S.T., Perkins, G.A., Jarosinski, K.W., Damiani, A., Brosnahan, M., Buckles, E.L., Osterrieder, N. Van de Walle, G.R., 2009. Effective treatment of respiratory alphaherpesvirus infection using RNA interference. PLOS One 4, 4118.

Früh, K., Ahn, K., Djaballah, H., Sempé, P., van Endert, P.M., Tampé R, Peterson, P.A., Yang, Y., 1995. A viral inhibitor of peptide transporters for antigen presentation. Nature 375, 415-418.

Garré, B., Gryspeerdt, A., Croubels, S., De Backer, P., Nauwynck, H.J., 2009. Evaluation of orally administered valacyclovir in experimentally EHV1-infected ponies. Veterinary Microbiology 135, 214 221.

Gilkerson, J.R., Love, D.N., Whalley, J.M., 1997. Serological evidence of equine herpesvirus 1 (EHV-1) infection in Thoroughbred foals 30-120 days of age. Australian Equine Veterinarian 15, 128-134.

Gilkerson, J.R., Whalley, J.M., Drummer, H.E., Studdert, M.J., Love, D.N., 1999. Epidemiological studies of equine herpesvirus 1 (EHV-1) in Thoroughbred foals: a review of studies conducted in the Hunter Valley of New South Wales between 1995 and 1997. Veterinary Microbiology 68, 15-25.

Gleeson, L.J., Coggins, L., 1980. Response of pregnant mares to equine herpesvirus 1 (EHV1). The Cornell Veterinarian 70, 391-400.

Glorieux, S., Van den Broeck, W., van der Meulen, K.M., van Reeth, K., Favoreel, H.W., Nauwynck, H.J., 2007. In vitro culture of porcine respiratory nasal mucosa explants for studying the interaction of porcine viruses with the respiratory tract. Journal of Virological Methods 142, 105-112.

Glorieux, S., Vandekerckhove, A.P., Goris, N., Yang, X.Y., Steukers, L., Van de Walle, G.R., Croubels, S., Neyts, J., Nauwynck, H.J., 2012. Evaluation of the antiviral activity of (1'S,2'R)-9-[[1',2'-bis(hydroxymethyl)cycloprop-1'-yl]methyl]guanine (A-5021) against equine herpesvirus type 1 in cell monolayers and equine nasal mucosal explants. Antiviral Research 93, 234-238.

Goehring, L.S., Sloet van Oldruitenborgh-Oosterbaan, M.M., 2001. The mystery of equine herpes myeloencephalopathy. Equine Veterinary Education 13, 36-42.

Goehring, L.S., Wagner, B., Bigbie, R., Hussey, S.B., Rao, S., Morley, P.S., Lunn, D.P., 2010. Control of EHV-1 viremia and nasal shedding by commercial vaccines. Vaccine 28, 5203-5211.

Goldenthal, K.L., Hedman, K., Chen, J.W., August, J.T., Willingham, M.C., 1985. Postfixation detergent treatment for immunofluorescence supresses localization of some integral membrane proteins. The Journal of Histochemistry and Cytochemistry 33, 813-820.

Goodman, L.B., Wagner, B., Flaminio, M.J., Sussman, K.H., Metzger, S.M., Holland, R., Osterrieder, N., 2006. Comparison of the efficacy of inactivated combination and modified-live virus vaccines against challenge infection with neuropathogenic equine herpesvirus type 1 (EHV-1). Vaccine 24, 3636-3645.

Grauwet,K., Cantoni,C., Parodi, M., De Maria, A., Devriendt, B., Pende, D., Moretta, L., Vitale, M., Favoreel, H.W., 2014. Alphaherpesvirus gD-mediated evasion from NK cells. Proceedings of the National Academy of Sciences 111, 16118-16123.

Grauwet, K., Vitale, M., De Pelsmaeker, S., Jacob, T., Laval, K., Moretta, L., Parodi, M., Parolini, S., Cantoni, C., Favoreel, H.W., 2016. Pseudorabies Virus US3 Protein Kinase Protects Infected Cells from NK Cell-Mediated Lysis via Increased Binding of the Inhibitory NK Cell Receptor CD300a. Journal of Virology 90, 1522-1533.

Gray, W.L., Baumann, R.P., Robertson, A.T., Caughman†, G.B., O'Callaghan, D.J., Staczek, J., 1987. Regulation of equine herpesvirus type 1 gene expression: Characterization of immediate early, early, and late transcription. Virology 158, 79-87.

Gryspeerdt, A.C., Vandekerckhove, A.P., Garré, B., Barbé, F., Van de Walle, G.R., Nauwynck, H.J., 2010. Differences in replication kinetics and cell tropism between neurovirulent and non-neurovirulent EHV1 strains during the acute phase of infection in horses. Veterinary Microbiology 142, 242-253.

Gryspeerdt, A., 2011. The pathogenesis of EHV1 in horses: novel insights from experimental inoculations and field situations. PhD thesis, Doctor in Veterinary Sciences, Faculty of Veterinary Medicine, Ghent University, Belgium.

Gulati, B.R., Sharma, H., Riyesh, T., Khurana, S.K., Kapoor, S., 2015. Viral and Host Strategies for Regulaton of Latency and Reactivation in Equid Herpesviruses. Asian Journal of Animal and Veterinary Advances 10, 669-689.

Hasebe, R., Sasaki, M., Sawa, H., Wada, R., Umemura, T., Kimura T., 2009. Infectious entry of equine herpesvirus-1 into host cells through different endocytic pathways. Virology 393, 198-209.

Henninger, R.W., Reed, S.M., Saville, W.J., Allen, G.P., Hass, G.F., Kohn, C.W. Sofaly, C., 2007. Outbreak of Neurologic disease Caused by Equine Herpesvirus-1 at a University Equestrian Center. Journal of Veterinary Internal Medicine 21, 157-165.

Hannant, D., Cullinane, A.A., Prendergast, M.J., Mumford, J.A., Nelly, M., Kydd, J.H., Weststrate, M.W., van den Hoven R., 2001. Clinical and virological evaluation of the efficacy of an inactivated EHV1 and EHV4 whole virus vaccine (Duvaxyn EHV1,4). Vaccination/challenge experiments in foals and pregnant mares. Vaccine 19, 4307-4317.

Hazrati, E., Galen, B., Lu, W., Wang, W., Ouyang, Y., Keller, M.J., Lehrer, R.I., Herold, B.C., 2006. Human alpha-and beta-defensins block multiple steps in herpes simplex virus infection. Journal of Immunology 177, 8658-66.

Hewitt, E.W., 2003. The MHC class I antigen presentation pathway: strategies for viral immune evasion. Immunology 110, 163-169.

Hinkley, S., Ambagala, A.P., Jones, C.J., Srikumaran, S., 2000. A vhs-like activity of bovine herpesvirus-1. Archives of Virology 145, 2027-2046.

Hobro, A.J., Smith, N.L., 2017. An evaluation of fixation methods: Spatial and compositional cellular changes observed by Raman imaging. Vibrational Spectroscopy 91, 31-45.

Huang, T., Lehmann, M.J., Said, A., Ma, G., Osterrieder, N., 2014. Major histocompatibility Complex Class 1 Downregulation Induced by Equine Herpesvirus Type 1 pUL56 is through Dynamin-Dependent Endocytosis. Journal of Virology 88, 12802-12815.

Huang, T., Ma, G., Osterrieder, N., 2015. Equine Herpesvirus 1 Multiply Inserted Transmembrane Protein pUL43 Cooperates with pUL56 in Downregulation of Cell Surface Major Histocompatibility Complex Class 1. Journal of Virology 89, 6251-6263.

Huemer, H.P., Nowotny, N., Crabb, B.S., Meyer, H., Hubert, P.H., 1995. gp13 (EHV-gC): a complement receptor induced by equine herpesviruses. Virus Research 37, 113-126.

Hussey, S.G., Whalley, J.M., Allen, G.P., Koen, M.T., Santucci, N., Fraser, D.G., Macklin, M.D., Swain, W.F., Lunn, D.P., 2006. Antibody and cellular immune responses following DNA vaccination and EHV-1 infection of ponies. Veterinary Immunology and Immunopathology 111, 81-95.

Hussey, G.S., Goehring, L.S., Lunn, D P., Hussey, S.B., Huang, T., Osterrieder, N., Powell, C., Hand, J., Holz, C., Slater, J., 2013. Experimental infection with equine herpesvirus type 1 (EHV-1) induces chorioretinal lesions. Veterinary research, 44, 118.

Hussey, S.G., Ashton, L.V., Quintana, A.M., Lunn, D.P., Goehring, L.S., Annis, K., Landolt, G., 2014a. Innate immune responses of airway epithelial cells to infection with equine herpesvirus-1. Veterinary Microbiology 170, 28-38.

Hussey, S.G., Ashton, L.V., Quintana, A.M., Van de Walle, G.R., Osterrieder, N., Lunn, D.P., 2014b. Equine herpesvirus type 1 UL56 modulates innate responses of airway epithelial cells. Virology 464, 76-86.

Iwasaki, A., 2007. Mucosal dentritic cells. Annual Review of Immunology 25, 381-418.

Jongsma, M.L.M., Guarda, G., Spaapen, R.M., 2017. The regulatory network behind MHC class I expression. Molecular Immunology.

Kawai, T., Akira, S., 2007. Signaling to NF-kappaB by Toll-like receptors. Trends in Molecular Medicine 13, 460-469.

Koppers-Lalic, D., Rijsewijk, F.A., Verschuren, S.B., van Gaans-Van den Brink, J.A., Neisig, A., Ressing, M.E., Neefjes, J., Wiertz, E.J., 2001. The UL41-encoded virion host shutoff (vhs) protein and vhs-independent mechanisms are responsible for down-regulation of MHC class I molecules by bovine herpes virus 1. Journal of General Virology 82, 2071-2081.

Koppers-Lalic, D., Reits, E.A., Ressing, M.E., Lipinska, A.D., Abele, R., Koch, J., Marcondes Rezende, M., Admiraal, P.,van Leeuwen, D., Bienkowska-Szewczyk, et al., 2005. Varicelloviruses avoid T cell recognition by UL49.5-mediated inactivation of the transporter associated with antigen processing. Proceedings of the National Academy of Sciences of the United States of America 102, 5144-5149.

Koppers-Lalic, D., Verweij, M.C., Lipińska, A.D., Wang, Y., Quinten, E., Reits, E.A., Koch, J., Loch, S., Marcondes, Rezende, M., et al., 2008. Varicellovirus UL49.5 proteins differentially affect the function of the transporter associated with antigen processing, TAP. PLOS Pathogens 4, 5.

Kurtz, B.M., Singletary, L.B., Kelly, S.D., Framptom, A.R., 2010. *Equus caballus* Major Histocompatibility Complex Class I Is an Entry Receptor for Equine Herpesvirus Type 1. Journal of Virology 84, 9027-9034.

Kydd, J.H., Smith, K.C., Hannant, D., Livesay, G.J., Mumford, J.A., 1994. Distribution of Equid herpesvirus-1 (EHV-1) in respiratory tract associated lymphoid tissue: implications for cellular immunity. Equine Veterinary Journal 26, 470-473.

Kydd, J.H., Townsend, H.G.G., Hannant, D., 2006. The equine immune response to equine herpesvirus-1: The virus and its vaccines. Veterinary Immunology and Immunopathology 111, 15-30.

Lara, F.J., Aguiar, D.A., Cássia, C.R., Aloísio, D.S., Martinez, R.S., Fernandes, S.M., Zugaib, M., Paulo B.S., 2012. Evaluation of Distinct Freezing Methods and Cryoprotectants for Human Amniotic Fluid Stem Cells Cryopreservation. Journal of Biomedicine and Biotechnology 4.

Laval, K., Favoreel, H. W., Poelaert, K.C., Van Cleemput, J., Brown, I.K., Nauwynck, H. J., 2015a. EHV-1 enhances viral replication in CD172a+ monocytic cells upon adhesion to endothelial cells. Journal of Virology 89, 10912-10923.

Laval, K., Favoreel, H.W., Nauwynck, H.J., 2015b. Equine herpesvirus type 1 replication is delayed in CD172a+ monocytic cells and controlled by histone deacetylases. Journal of General Virology 96, 118-130.

Laval, K., 2016. Equine CD172a+ monocytic cells, the 'Trojan Horse' for equine herpesvirus type 1 (EHV-1) dissemination in the horse. PhD thesis, Doctor in Veterinary Sciences, Faculty of Veterinary Medicine, Ghent University, Belgium.

Leoni, V., Gianni, T., Salvioli, S., Campadelli-Fiume, G., 2012. Herpes simplex virus glycoproteins gH/gL and gB bind Toll-like receptor 2, and soluble gH/gL is sufficient to activate NF-kappaB. Journal of Virology 86, 6555-62.

Lorenzi, S., Forloni, M., Cifaldi, L., Antonucci, C., Citti, A., Boldrini, R., Pezzullo, M., Castellano, A., Russo, V., van der Bruggen, P., 2012. IRF1 and NF-kB restore MHC class I-restricted tumor antigen processing and presentation to cytotoxic T cells in aggressive neuroblastoma. PLOS One 7, 10.

Lund, J., Sato, A., Akira, S., Medzhitov, R., Iwasaki, A., 2003. Toll-like receptor 9-mediated recognition of herpes simplex virus-2 by plasmocytoid dendritic cells. Journal of Experimental Medicine 198, 513-520.

Lunn, D.P., Davis-Pointer, N., Flaminio, M.J., Horohov, D.W., Osterrieder, K., Pusterla, N., Townsend, H.G., 2009. Equine Herpesvirus-1 Consensus Statement. Journal of Veterinary Internal Medicine 23, 450-461.

Ma, G., Feineis S., Osterrieder, N., Van de walle, G.R., 2012. Identification and Characterization of Equine Herpesvirus Type 1 pUL56 and its Role in Virus-Induced Downregulation of Major Histocompatibility Complex Class 1. Journal of Virology 86, 3554-3563.

Ma, G., Azab, W., Osterrieder, N., 2013. Equine herpesviruses type 1 (EHV-1) and 4 (EHV-4)-Masters of co-evolution and a constant threat to equids and beyond. Veterinary Microbiology 167, 123-134.

Mahmoud, H.Y., Andoh, K., Hattori, S., Terada, Y., Noguchi, K., Shimoda, H., Maeda, K., 2013. Characterization of glycoproteins in equine herpesvirus-1. The Journal of Veterinary Medical Science 75, 1317–1321.

McAuliffe, S.B., 2013. Ln: Knottenbelt and Pascoe's Color Atlas of Diseases and Disorders of the Horse, Second Edition, Saunders Ltd, Nottingham, UK, pp. 400-442.

Mettenleiter, T.C., 2002. Herpesvirus Assembly and Egress. Journal of Virology 76, 1537-1547.

Mettenleiter, T.C., 2004. Budding events in herpesvirus morphogenesis. Virus Research 106, 167-180.

Mettenleiter, T.C., Klupp, B.G., Granzow, H., 2006. Herpesvirus assembly: a tale of two membranes. Current Opinion in Microbiology 9, 423-429.

Mettenleiter, T.C. and Sobrino F., 2008. Ln: Animal Viruses: Molecular biology, Caister Academic Press, Norfolk, UK.

Mettenleiter, T.C., Klupp, B.G., Granzow, H., 2009. Herpesvirus assembly: An update. Virus Research 143, 222-234.

Mettenleiter, T.C., Müller, F., Granzow, H., Klupp, B.G., 2013. The way out: What we know and what we don't know about herpesvirus nuclear egress. Cellular Microbiology 15, 170-178.

Minke, J.M., Fischer, L., Baudu, P., Guigal, P.M., Sindle, T., Mumford, J.A. Audonnet, J.C., 2006. Use of DNA and recombinant canarypox viral (ALVAC) vectors for equine herpes virus vaccination. Veterinary Immunology and Immunopathology 111, 47-57.

Mumford, J.A., Hannant, D.A., Jesset, D.M., O'Neill, T., Smith, K.C., Ostlund, E.N., 1994. Abortigenic and neurological disease caused by experimental infection with equine herpesvirus 1. Proceedings of the 7th International Conference of Equine Infectious diseases, Newmarket, UK 261-275.

Murphy, K., 2008. Ln: Janeway’s Immunobiology, Seventh edition, Garland Science, Taylor & Francis Group, LLC, New York, USA, figure 1-26.

Murphy, K., 2012a. Ln: Janeway’s Immunobiology, Eighth edition, Garland Science, Taylor & Francis Group, LLC, New York, USA, Part 1.

Murphy, K., 2012b. Ln: Janeway’s Immunobiology, Eighth edition, Garland Science, Taylor & Francis Group, LLC, New York, USA, Part 4.

Nugent, J., Birch-Machin, I., Smith, K.C., Mumford, J.A., Swann, Z., Newton, J.R., Bowden, R.J., Allen, G.P., Davis-Poynter, N., 2006. Analysis of Equid Herpesvirus 1 Strain Variation Reveals a Point Mutation of the DNA Polymerase Strongly Associated with Neuropathogenic versus Nonneuropathogenic Disease Outbreaks. Journal of Virology 80, 4047-4060.

O'Neill, T., Kydd, J.H., Allen, G.P., Wattrang, E., Mumford, J.A. & Hannant, D., 1999. Determination of equid herpesvirus 1-specific, CD8+, cytotoxic T lymphocyte precursor frequencies in ponies. Veterinary Immunology and Immunopathology 70, 43-54.

Osterrieder, N., 1999. Construction and characterization of an equine herpesvirus 1 glycoprotein C negative mutant. Virus Research 59, 165-177.

Owen, D.J., Crump, C.M., Graham, S.C., 2015. Tegument Assembly and Secondary Envelopment of Alphaherpesviruses. Viruses 7, 5084–114.

Parham, P., 2009. Ln: The Immune System, Third Edition, Garland Science, New York, USA.

Parham, P., 2015. Ln: The Immune System, Fourth Edition, Garland Science, New York, USA, Figure 13.18.

Patel, J.R., Heldens, J., 2005. Equine herpesviruses 1 (EHV-1) and 4 (EHV-4)-epidemiology, disease and immunoprophylaxis: A brief review. The Veterinary Journal 170, 14-23.

Petersen, J.L., Morris, C.R., Solheim, J.C., 2003. Virus evasion of MHC class I molecule presentation. Journal of Immunology 171, 4473-4478.

Pfeffer, L.M., 2011. The role of nuclear factor κB in the interferon response. Journal of interferon & cytokine research 31, 553-559.

Poelaert, K., Van Cleemput, J., Laval, K., Favoreel, H.W., Soboll Hussey, G., Maes, R.K., Nauwynck, H.J., 2018. Abortigenic but Not Neurotropic Equine Herpes Virus 1 Modulates the Interferon Antiviral Defense. Frontiers in cellular and infection microbiology 8, 312.

Poelaert, K.C.K., Van Cleemput, J., Laval, K., Favoreel, H.W., Couck, L., Van den Broeck, W., Azab, W., Nauwynck, H.J., 2019a. Equine herpesvirus 1 bridles T-lymphocytes to reach its target organs. Journal of Virology 93, 7.

Poelaert, K.C.K., 2019b. Immune-metabolic factors mediate the pathogenesis of equine herpesvirus 1: an evolutionary *pas-de-deux*. PhD thesis, Doctor in Veterinary Sciences, Faculty of Veterinary Medicine, Ghent University, Belgium.

Poelaert, K.C.K., Van Cleemput, J., Laval, K., Descamps, S., Favoreel, H.W., Nauwynck, H.J., 2019c. Beyond instinct: gut short-metabolic chain fatty acids moderate the pathogenesis of equine herpesvirus 1. Frontiers in Microbiology 10, 723.

Pusterla, N., Wilson, W.D., Mapes, S., Finno, C., Isbell, D., Arthur, R.M., Ferraro, G.L., 2009. Characterization of viral loads, strain and state of equine herpesvirus-1 using real-time PCR in horses following natural exposure at a racetrack in California. Veterinary Journal 179, 230-239.

Powell, D.G., 1991. Viral respiratory disease of the horse. Veterinary Clinic North American Equine Practice 7, 27-52.

Pusterla, N., Wilson, W.D., Mapes, S., Finno, C., Isbell, D., Arthur, R.M., Ferraro, G.L., 2009. Characterization of viral loads, strain and state of equine herpesvirus-1 using real-time PCR in horses following natural exposure at a racetrack in California. Veterinary Journal 179, 230-239.

Quintana, A.M., Sandlot, G.A., Annis, K.M., Sobole Hussey, G., 2011. Immunological Characterization of the Equine Airway Epithelium and of a Primary Equine Airway Epithelial Cell Culture Model. Veterinary Immunology and Immunopathology 140, 226–36.

Rappocciolo, G., Birch, J., Ellis, S.A., 2003. Downregulation of MHC class 1 expression by equine herpesvirus-1. Journal of General Virology 84, 293-300.

Raulet, D.H. and Vance, R.E., 2006. Self-tolerance of Natural Killer cells. Nature Reviews Immunology 6, 520-531.

Rock, J.R., Randell, S.H., Hogan, B.L., 2010. Airway basal stem cells: a perspective on their roles in epithelial homeostasis and remodeling. Disease models & mechanisms 3, 545-556.

Roizman, B. and Pellett, P.E., 2001. Ln: The Family Herpesviridae: A Brief Introduction, Lippincott Williams and Wilkins, Philadelphia, Pennsylvania, USA.

Sand, J.M.B., Genovese, F., Karsdal, M.A., 2016. Ln: Biochemistry of Collagens, Laminins and Elastin. Academic Press, Cambridge, Massachusetts, USA, 31-41.

Scott, J.C., Dutta, S.K. Myrup, A.C., 1983. In vivo harboring of equine herpesvirus-1 in leukocyte populations and subpopulations and their quantitation from experimentally infected ponies. American Journal of Veterinary Research 44, 1344-1348.

Slater, J.D., Gibson, J.S., Field, H.J., 1993. Pathogenicity of a thymidine kinase-deficient mutant of equine herpesvirus 1 in mice and specific pathogen-free foals. Journal of General Virology 74, 819-828.

Smith, K.C., Whitwell, K.E., Binns, M.M., Dolby, C.A., Hannant, D. Mumford, J.A., 1992. Abortion of virologically negative foetuses following experimental challenge of pregnant pony mares with equid herpesvirus 1. Equine Veterinary Journal 24, 256-259.

Smith, K.C., Whitwell, K.E., Mumford, J.A., Gower, S.M., Hannant, D., Tearle, J.P., 1993. An immunohistological study of the uterus of mares following experimental infection by equid herpesvirus 1. Equine Veterinary Journal 25, 36-40.

Smith, K.C., Mumford, J.A., Lakhani, K., 1996. A comparison of equid herpesvirus-1 (EHV-1) vascular lesions in the early versus late pregnant equine uterus. Journal of Comparative Pathology 114, 231-247.

Smith, D., Hamblin, A., Edington, N., 2002. Equid herpesvirus 1 infection of endothelial cells requires activation of putative adhesion molecules: an in vitro model. Clinical and Experimental Immunology 129, 281-287.

Spear, P.G., Longnecker, R., 2003. Herpesvirus entry: An update. Journal of Virology 77, 10179-10185.

Staehli, F., Ludigs, K., Heinz, L.X., Seguín-Estévez, Q., Ferrero, I., Braun, M., Schroder, K., Rebsamen, M., Tardivel, A., Mattmann, C., et al., 2012. NLRC5 Deficiency Selectively Impairs MHC Class I- Dependent Lymphocyte Killing by Cytotoxic T Cells. The Journal of Immunology 188, 3820-3828.

Srinivasan, B., Kolli, A.R. Esch, M.B., Abaci, H.E., Shuler, M.L., Hickman, J.J., 2015. TEER measurement techniques for in vitro barrier model systems. Journal of Laboratory Automation 20, 107-126.

Stierstorfer, B., Eichhorn, W., Schmahl, W., Brandmuller, C., Kaaden, O.R. Neubauer, A., 2002. Equine herpesvirus type 1 (EHV-1) myeloencephalopathy: a case report. Journal of Veterinary Medicine B. Infectious Diseases and Veterinary Public Health 49, 37-41.

Takeuchi, O., Akira, S., 2010. Pattern recognition receptors and inflammation. Cell 140, 805-20.

Tallmadge, R.L., Campbell, J.A., Miller, D.C., Antczak, D.F., 2010. Analysis of MHC class I genes across horse MHC haplotypes. Immunogenetics 62, 159-172.

Telford, E., Watson, M., McBride, K., Davidson, A., 1992. The DNA sequence of equine herpesvirus-1. Virology 189, 304-313.

Tsujimura, K., Shiose, T., Yamanaka, T., Nemoto, M., Kondo, T. Matsumura, T., 2009. Equine herpesvirus type 1 mutant defective in glycoprotein E gene as candidate vaccine strain. Journal of Veterinary Medicine and Science 71, 1439-1448.

Turtinen, L.W., Allen, G.P., 1982. Identification of the Envelope Surface Glycoproteins of Equine Herpesvirus Type 1. Journal of General Virology 63, 481-485.

Van Cleemput, J., Poelaert, K.C.K., Laval, K., Maes, R., Hussey, G.S., Van den Broeck, W., Nauwynck, H.J., 2017. Access to a main alphaherpesvirus receptor, located basolaterally in the respiratory epithelium, is masked by intercellular junctions. Scientific Reports 7, 16656.

Van Cleemput, J., Laval, K., Favoreel, H.W., Hussey, G.S., Maes, R.K., Nauwynck, H.J., 2018. Abortigenic but Not Neurotropic Equine Herpes Virus 1 Modulates the Interferon Antiviral Defense. Frontiers in Cellular and Infection Microbiology 8, 312.

Van Cleemput, J., 2018. The horse's respiratory mucosa, airborne pathogens and respirable hazards: the archetypical trifecta of co-evolution. PhD. thesis, Doctor in Veterinary Sciences, Faculty of Veterinary Medicine, Ghent University, Belgium.

Van Cleemput, J., Poelaert, C.K., Laval, K., Impens, F., Van den Broeck, W., Gevaert, K., Nauwynck, H.J., 2019. Pollens destroy respiratory epithelial cell anchors and drive alphaherpesvirus infection. Scientific Reports 9, 4787.

van der Strate, B.W, Beljaars, L., Molema, G., Harmsen, M.C., and Meijer, D.K., 2001. Antiviral activities of lactoferrin. Antiviral Research 52, 225-39.

Vandekerckhove, A., Glorieux, S., Van den Broeck, W., Gryspeerdt, A., van der Meulen, K.M., Nauwynck, H.J., 2009. In vitro culture of equine respiratory mucosa explants. The Veterinary Journal 181, 280-287.

Vandekerckhove, A.P., Glorieux, S., Gryspeerdt, A.C., Steukers, L., Duchateau, L., Osterrieder, N., Van de Walle, G.R., Nauwynck, H.J., 2010. Replication kinetics of neurovirulent versus non-neurovirulent equine herpesvirus type 1 strains in equine nasal mucosal explants. Journal of General Virology 91, 2019-2028.

van der Meulen, K., Nauwynck, H., Buddaert, W., Pensaert, M., 2000. replication of equine herpes virus type 1 in freshly isolated equine peripheral blood mononuclear cells and changes in susceptibility following mitogen stimulation. Journal of General Virology 81, 21-25.

van der Meulen, K., Vercauteren, G., Nauwynck, H., Pensaert, M., 2003a. A local epidemic of equine herpesvirus 1-induced neurological disorders in Belgium. Vlaams Diergeneeskundig Tijdschrift 72, 366-372.

van der Meulen, K.M., Nauwynck, H.J., Pensaert, M.B., 2003b. Absence of viral antigens on the surface of equine herpesvirus-1-infected peripheral blood mononuclear cells: a strategy to avoid complement-mediated lysis. Journal of General Virology 84, 93-97

van der Meulen, K.M., 2003c. The interaction of equine herpesvirus with equine peripheral blood mononuclear cells. PhD thesis, Doctor in Veterinary Sciences, Faculty of Veterinary Medicine, Ghent University, Belgium.

van der Meulen, K.M., Favoreel, H.W., Pensaert, M.B., Nauwynck, H.J, 2006a. Immune escape of equine herpes virus 1 and other herpesviruses of veterinary importance. Veterinary Immunology and Immunopathology 111, 31-40.

van der Meulen, K.M., Caij, B., Nauwynck, H.J., 2006b. Absence of viral envelope proteins in equine herpesvirus 1-infected blood mononuclear cells during cell-associated viremia. Veterinary Microbiology 113, 265-273.

Van De walle, G.R., Peters, S.T., Vanderven, B.C., O'Callaghan, D.J., Osterrieder, N., 2008. Equine Herpesvirus 1 Entry via Endocytosis Is Facilitated by V Integrins and an RSD Motif in Glycoprotein D. Journal of Virology 82, 11859-11868.

Van de Walle, G.R., May, M.A., Peters, S.T., Metzger, S.M., Rosas, C.T. Osterrieder, N., 2010. A vectored equine herpesvirus type 1 (EHV-1) vaccine elicits protective immune responses against EHV-1 and H3N8 equine influenza virus. Vaccine 28, 1048-1055.

van Maanen, C., Sloet van Oldruitenborgh-Oosterbaan, M.M., Damen, E.A. Derksen, A. G., 2001. Neurological disease associated with EHV-1-infection in a riding school: clinical and virological characteristics. Equine Veterinary Journal 33, 191-196.

van Maanen C., 2002. Equine herpesvirus 1 and 4 infections: an update. Veterinary Quarterly 24, 58-78.

Voyles, B.A., 2002. Ln: Smith, J. M. The Biology of Viruses, Second Edition, McGraw-Hill Companies, New York, USA.

Wang, L., Raidal, S.L., Pizzirani, A., Wilcox, G.E., 2007. Detection of respiratory herpesviruses in foals and adult horses determined by nested multiplex PCR. Veterinary Microbiology 121, 18-28.

Williams, A., Peh, C.A., Elliott, T., 2002. The cell biology of MHC class I antigen presentation. Tissue Antigens 59, 3-17.

Wilson, W.D., 1997. Equine herpesvirus 1 myeloencephalopathy. Veterinary Clinic North American Equine Practice 13, 53-72.

Wilsterman, S., Hussey, S.G., Lunn, D.P., Ashton, L.V., Callan, R.J., Rao, S. Goehring, L.S., 2011. Equine herpesvirus-1 infected peripheral blood Mononuclear cell subpopulations during viremia. Veterinary Microbiology 149, 40-70.

Zhang, S.Y., Jouanguy, E., Ugolini, S., Smahi, A., Elain, G., Romero, P., Segal, D., Sancho-Shimizu, V., Lorenzo, L., Puel, A., et al., 2007. TLR3 deficiency in patients with herpes simplex encephalitis. Science 317, 1522-1527.

Ziemann, K., Mettenleiter, T.C., Fuchs, W., 1998. Infectious laryngotracheitis herpesvirus expresses a related pair of unique nuclear proteins which are encoded by split genes located at the right end of the U_L genome region. Journal of Virology 72, 6867-6874.